Analysis of protein-protein interactions in base excision repair (BER) complexes

A thesis
Submitted to the University of Manchester
for the degree of Doctor of Philosophy
in the Faculty of
Medicine, Dentistry, Nursing and Pharmacy

2001

by

Steven J. Pearson BSc.

Cancer Research UK Carcinogenesis group,
Paterson Institute for Cancer Research,
Christie Hospital,
Wilmslow Road,
Manchester,
M20 4BX

ProQuest LLC.
789 East Eisenhower Parkway
P.O. Box 1346
Ann Arbor, MI 48106 – 1346

CONTENTS

CONTENTS **2**
ABSTRACT **8**
DECLARATION **9**
COPYRIGHT **9**
ABBREVIATIONS **10**
ACKNOWLEDGEMENTS **12**

CHAPTER 1 ..... **13**
1.0 Introduction **13**
1.1 Genetic causes of cancer **13**
1.2 Generation of DNA damage **14**
1.3 Reactive oxygen species **15**
1.4 Oxidative DNA damage **17**
1.4.1 Sugar damage 17
1.4.2 Strand breaks 17
1.4.3 Cross-links 18
1.4.4 Pyrimidine base damage 19
1.4.5 Oxidation of guanine 20
1.4.6 Biological significance of 8-oxodG 23
1.4.7 Oxidation of adenine 24
1.5 Steady-state levels of DNA lesions **24**
1.6 Repair of oxidative DNA damage **27**
1.6.1 ROS scavenging enzymes 27
1.6.2 The regulation of cellular stress 28
1.7 DNA repair mechanisms **30**
1.7.1 Base excision repair 31
1.7.2 Nucleotide excision repair 33
1.7.3 Mismatch repair 35
1.7.4 Biological consequences of lack of repair 37
1.8 BER DNA glycosylases **39**
1.8.1 8-oxoguanine-DNA-glycosylase (OGG1) 42

1.8.2 The GO-system 45
1.8.3 Endonuclease III (NTH1) 47
1.8.4 Alkylpurine-DNA-N-glycosylase (APNG) 48
1.9 Aims of project 49

CHAPTER 2 51
2.0 Materials and Methods 51
2.1 Molecular biology 51
2.1.1 Enzymes 51
2.1.2 Molecular biology kits 51
2.1.3 Vectors 51
2.1.4 Buffers and reagents 52
2.1.5 Oligonucleotides 54
2.2 DNA Protocols 55
2.2.1 PCR amplification of DNA 55
2.2.2 Agarose gel electrophoresis 55
2.2.3 Isolation of DNA fragments 55
2.2.4 Ligation reactions 55
2.2.5 Plasmid purification (mini and maxi-preps) 56
2.2.6 DNA sequencing 56
2.3 Bacterial work 57
2.3.1 Bacterial strains 57
2.3.2 Bacterial culture media 57
2.3.3 Preparation of competent bacteria 58
2.3.4 Transformation of bacteria 58
2.3.5 Preparation of bacterial cell extracts 58
2.3.6 Bradford assay for total protein estimation 59
2.3.7 Overexpression of recombinant proteins 59
2.4 Protein Protocols 60
2.4.1 Purification of His-mOGG1 60
2.4.2 Purification of GST-mOGG1 60
2.4.3 SDS-Polyacrylamide gel electrophoresis 61
2.4.4 Western blot analysis 62

2.4.5 *In vitro* transcription/translation (IVTT) reaction 63
2.4.6 *In vitro* transcription/translation (IVTT) pull-down experiment 63
2.4.7 OGG1 glycosylase activity assay 64
2.4.7.1 5' end-labelling of oligonucleotides using [γ-^{32}P]-ATP 64
2.4.7.2 Annealing of [^{32}P]-labelled oligo to complementary oligo 64
2.4.7.3 Oligonucleotide cleavage assay 65
2.5 RNA protocols 66
2.5.1 RNA extraction and purification 66
2.5.2 DNase treatment of total RNA 66
2.5.3 Reverse-transcription PCR 67
2.6 Yeast work 68
2.6.1 Yeast strains 68
2.6.2 Yeast culture media 68
2.6.3 Small-scale yeast transformation procedure 69
2.6.4 Yeast two-hybrid experiment 70
2.6.4.1 Library screens 70
2.6.4.2 Identification of library inserts 71
2.6.5 Yeast mutation analysis 72
2.6.5.1 Mutation analysis using SD-Trp liquid medium 72
2.6.5.2 Mutation analysis using SD-Trp agar medium 72
2.6.5.3 Mutation analysis after treatment with chemical agents 73
2.7 Cell culture work 74
2.7.1 Tissue culture cell lines 74
2.7.2 Maintenance and subculture of cell lines 74
2.7.3 Mammalian two-hybrid experiment 75

CHAPTER 3 76
3.0 Results: Yeast two-hybrid screens 76
3.1 Introduction 76
3.2 The principle of the yeast two-hybrid system 76
3.3 Amplification of the mouse testes cDNA library 79
3.4 Production of the yeast two-hybrid constructs 81
3.5 Viability of the yeast containing the two-hybrid constructs 84

3.6 Clone specific two-hybrid experiments **86**
3.7 Yeast two-hybrid library analysis **88**
3.7.1 Summary of the mAPNG two-hybrid analysis 89
3.7.2 Summary of the mOGG1 two-hybrid analysis 90
3.7.2.1 Dnaja1 91
3.7.2.2 mRanBP9 92
3.7.2.3 mDnaja3 93
3.7.2.4 Library clone 7 93
3.7.2.5 Unidentified or novel sequences 94
3.8 Summary **98**

CHAPTER 4 ..... **99**
4.0 Results: Purification of mOGG1 ..... **99**
4.1 Introduction **99**
4.2 The His-tag purification system **99**
4.2.1 Production of the pTrcHisA-mOGG1 construct **100**
4.2.2 Expression of recombinant His-mOGG1 protein 102
4.2.3 Increasing the expression levels of His-mOGG1 104
4.2.4 Purification of His-mOGG1 105
4.3 The GST-tag purification system **107**
4.3.1 Production of the GST-mOGG1 construct 108
4.3.2 Expression and purification of GST-mOGG1 109
4.3.3 Expression and purification of GST-hOGG1a 110
4.3.4 Functional activity of purified GST-mOGG1 111
4.3.5 Thrombin cleavage of GST-tag 114
4.4 Summary **116**

CHAPTER 5 ..... **117**
5.0 Results: *In vitro* transcription/translation pull-down experiments **117**
5.1 Introduction **117**
5.2 The principle of the IVTT pull-down system **117**
5.3 Production of the IVTT constructs **118**
5.4 IVTT pull-down experiments **119**

5.4.1 mDnaja1 119
5.4.2 mRanBP9 123
5.4.3 mDnaja3 124
5.4.4 Library clone 7 125
5.4.5 Library clone 18 127
5.4.6 Library clone 4 130
5.4.7 Remaining library clones 131
5.5 Summary 131

CHAPTER 6 133
6.0 Results: Investigation of protein interactions between DNA glycosylases and molecular chaperones 133
6.1 Introduction 133
6.2 The principle of the mammalian two-hybrid experiment 134
6.3 Production of the mammalian two-hybrid constructs 136
6.4 Mammalian two-hybrid experiments 138
6.5 Confirmation of mammalian two-hybrid results 141
6.6 Summary 145

CHAPTER 7 147
7.0 Results: Analysis of mDnaja1 function in genome maintenance 147
7.1 Introduction 147
7.2 Principle of the yeast mutation analysis 148
7.3 Mutation analysis results 151
7.4 Effect of oxidative DNA damage on mutation rates 154
7.5 Analysis of OGG1 activity 156
7.6 Summary 158

CHAPTER 8 159
8.0 Discussion 159
8.1 Introduction 159
8.2 Summary of protein-protein interaction experiments 159
8.3 DNA repair and Heat-shock proteins 164

8.4 Protein interactions with BER DNA glycosylases..... 165

8.5 Future perspective 167

REFERENCES..... 170

ABSTRACT

The exposure of cellular DNA to reactive oxygen species (ROS) generates the highly promutagenic lesion 7,8-dihydro-8-oxoguanine (8-oxodG) in abundant amounts. If not repaired efficiently the presence of this lesion generates G:C to T:A transversion mutations during subsequent rounds of DNA replication. Similarly, numerous alkylating agents produce a multitude of both cytotoxic and mutagenic base damage in cellular DNA. To combat the deleterious effects of these lesions, cells have developed a complex and efficient range of DNA repair systems to protect both the mitochondrial and nuclear genomes from DNA damage. One of these, base excision repair (BER), relies on a series of DNA N-glycosylases to excise modified bases from DNA. Thus, 8-oxodG is excised from DNA by 8-oxoguanine DNA glycosylase (OGG1), while a range of modified purines are removed by alkylpurine-DNA-*N*-glycosylase (APNG). However, while the mode of action of these glycosylases is well documented, little is known about their regulation and co-ordination with downstream components of the BER pathway. Therefore, the aim of this work was to obtain evidence for novel protein partners that may facilitate or regulate the activities of OGG1 and APNG. To investigate this, yeast two-hybrid analyses were carried out using the cDNAs encoding murine OGG1 and APNG to screen a mouse testes cDNA library. Interestingly, the co-expression of a library protein with APNG in yeast proved to be cytotoxic and consequently no two-hybrid interactions were observed. In contrast, co-expression with mOGG1 did not result in the same toxicity and 24 two-hybrid interacting clones were obtained. Six clones were found to contain the cDNA for a novel molecular chaperone, mDnaja1. Intriguingly, mDnaja1 is a member of the heat shock (HSP40) family of proteins, whose activities have been reported to protect the cell under conditions of severe oxidative stress. Although, the yeast two-hybrid interaction between mOGG1 and mDnaja1 was confirmed *in vitro*, to date, the subsequent detection of this interaction *in vivo* has proved more elusive. However, there is an increasing amount of evidence to suggest that molecular chaperones play an important role in the repair of DNA damage and further evidence is presented in this study.

DECLARATION

No portion of the work referred to in this thesis has been submitted in support of an application for another degree or qualification of this or any other university or other institute of learning.

COPYRIGHT

ABBREVIATIONS

3-meA	3-methyladenine
5-OHC	5-hydroxycytosine
5-OHT	5-hydroxythymine
7-meG	7-methylguanine
εA	$1,N^6$-ethenoadenine
8-oxodG	8-oxo-7,8-dihydro-2′-deoxyguanosine
8-oxoG	8-oxo-7,8-dihydro-guanosine
AD	Activating domain
APS	Ammonium persulfate
Amp	Ampicillin
APE	AP-endonuclease
APNG	Alkylpurine-DNA-N-glycosylase
ATCC	American Tissue Culture Collection
BER	Base excision repair
BD	Binding domain
bp	Base pair
CS	Cockayne syndrome
Da	Dalton
dA	deoxyadenosine
dC	deoxycytodine
dG	deoxyguanosine
dT	deoxythymidine
DMSO	Dimethyl sulphoxide
DNA	Deoxyribonucleic acid
DSB	Double-strand breaks
E. coli	*Esherichia coli*
ECL	Enhanced chemiluminescence
EDTA	Ethylenediamine tetra acetic acid
ERK	Extracellular signal-regulated kinases
FaPy	2,6-diamino-5-formamido-4-hydroxypyrimidine
Fpg	Formamidopyrimidine DNA glycosylase
GG-NER	Global genome- nucleotide excision repair
GST	Glutathione-S-transferase
HAP1	Human AP-endonuclease
H_2O_2	Hydrogen peroxide
HhH	Helix-hairpin-Helix
His	Histidine
HSP	Heat shock protein
HSR	Heat shock response
Hx	Hypoxanthine
IDL	Insertion/deletion loop
IPTG	Isopropyl-β,δ-1-thiogalactopyranoside
IVTT	*In vitro* transcription translation
JNK	c-Jun amino-terminal kinase cascade
Kan	Kanamycin
kb	Kilobase
kDa	Kilo Dalton

ko	Knockout
LB	Luria-Bertani
Leu	Leucine
MAPK	Mitogen activated protein kinase
MCS	Multiple cloning site
MMR	Mismatch repair
MSH	MutS homolog
NER	Nucleotide excision repair
NHEJ	Non-homologous end joining
NF-kB	Nuclear factor-κB
$^{\cdot}NO$	Nitric oxide radical
$^{\cdot}NO_2$	Nitrogen dioxide radical
NTH	Mammalian endonuclease III homolog
$^{\cdot}O_2^-$	Superoxide
OD	Optical density
OGG1	8-oxoguanine DNA glycosylase
$^{\cdot}OH$	Hydroxyl radical
ORF	Open reading frame
PAGE	Polyacrylamide gel electrophoresis
PARP	Poly(ADP-ribose) polymerase
PBS	Phosphate buffered saline
PCNA	Proliferating cell nuclear antigen
PCR	Polymerase chain reaction
PI(3)K	Phosphoinositide 3-kinase
PMSF	Phenylmethanesulfonyl floride
Pol	Polymerase
PNK	Polynucleotide kinase
RAR	Replication associated repair
RNA	Ribonucleic acid
ROS	Reactive oxygen species
$ROO^{\cdot}$	Peroxyl
$RO^{\cdot}$	Alkoxyl
RPA	Replication protein A
RT-PCR	Reverse transcription polymerase chain reaction
UV	Ultra violet
S. cerevisiae	*Saccharomyces cerevisiae*
SDS	Sodium dodecylsulphate
SOD	Superoxide dismutase
SSB	Single-strand breaks
TBS	Tris-buffered saline
TCR	Transcription coupled repair
TEMED	N,N,N′,N′-tetramethylethylenediamine
TEMPO	2,2,6,6-tetramethyl-1-piperidinyloxy, free radical
TFIIH	Transcription factor-IIH
Trp	Tryptophan
wt	Wild-type
X-gal	5-Bromo-4-chloro-3-indolyl-β-D-galactosidase
XP	Xeroderma pigmentosum

ACKNOWLEDGEMENTS

I would like to thank my supervisors Dr. Rhod Elder and Dr. Geoff Margison for all their help, advice and support throughout the past three years. A further special thanks goes to Dr. Lene Juel Rasmussen for her unwavering support and enthusiasm, and to the members of her laboratory (Dr. Merete Rasmussen, Lene Markussen and Gerda Olsen) who were extremely warm and welcoming and provided unending technical support.

CHAPTER 1

1.0 Introduction

1.1 Genetic causes of cancer

Cancer is a general term used to describe a variety of conditions characterised by an unscheduled and uncontrolled proliferation of cells. As the average age of the population in most western countries is rising, so are the incidences of cancers (de Rijke et al., 2000) making it one of the most common causes of death in the 21st century (Kennedy, 1998). Finding a cure for cancer has been complicated by the many and varied causes of the disease (Doll and Peto, 1981), and by its ability to occur in almost every mammalian organ and cell type (Pisani et al., 1999), producing a vast array of different clinical outcomes.

Several factors can aid the initiation of cancer, including genetic predisposition (Houlston and Peto, 1996), environmental influences (Olden and Wilson, 2000), infectious agents (Pisani et al., 1997) and ageing (Peto et al., 1986; Jones and Laird, 1999; Hastie et al., 1990). These processes are able to transform normal cells into cancerous cells by disrupting a wide range of regulatory pathways. With few exceptions, cancers are derived from single somatic cells and their progeny. Cells emerging in the neoplastic clone accumulate a series of genetic and epigenetic changes that lead to alterations in gene activity, usually imparting a growth advantage. Ultimately a population of cells evolves that can escape the normal controls of proliferation and territory and become a cancer (Nowell, 1976). Hanahan and Weinberg,. (2000) have identified six 'hallmark features' of the cancer phenotype that include disregard of signals to stop proliferation and differentiation; capacity for sustained proliferation; evasion of apoptosis; invasion; and angiogenesis (Figure 1.1).

One of the main advances in understanding the molecular mechanisms of cancer has been the elucidation of the genetic changes that activate proto-oncogenes (Bishop, 1991) and inactivate tumour suppressor genes (Fowlis and Balmain, 1993), thereby initiating many of the aberrant phenotypes described by Hanahan and Weinberg. The predominant forms of genetic change observed in these genes are DNA mutations. These mutations are defined as any alteration to the normal coding sequence of the DNA and include point mutations, DNA insertions and deletions, including chromosomal translocations, and mutagenic and cytotoxic base modifications.

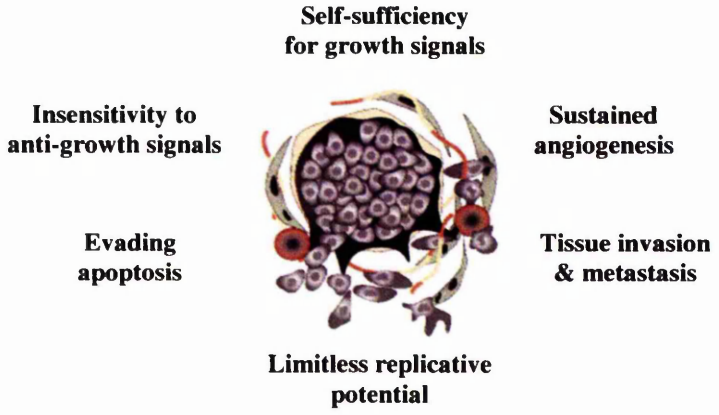

Figure 1.1. Acquired features of metastatic cancer cells (Hanahan and Weinberg, 2000).

1.2 Generation of DNA damage

As previously described, cancer is a disease of genes (Bishop, 1991). The molecular constitution of the DNA molecule is under constant attack from endogenously and exogenously generated carcinogens and mutagens that cause a wide range of DNA lesions (Singer and Hang, 1997). This DNA damage occurs from two general sources. The direct attack from environmental agents such as UV light, ionising radiation and numerous genotoxic chemicals cause alterations in the structure of DNA, which if left unrepaired, may lead to mutations. A specific example is exposure to the genotoxic compounds found in cigarette smoke, (specifically, Benzo(a)pyrene diol-epoxides; Wei et al., 1996), which are responsible for approximately 35% of all 'avoidable' cancers (Doll and Peto, 1981). Alternatively, reactive oxygen species (ROS) generated by a variety of environmental agents and endogenous processes, most importantly from the mitochondrial respiratory chain. These ROS cause a wide range of DNA damage and constitute a permanent threat to DNA integrity from within the cell.

1.3 Reactive oxygen species

Oxidative cellular damage is thought to play an important role in the aetiology of cancer. Reactive oxygen species can react with most of the major macromolecules of the cell including lipids, protein and DNA, disrupting normal biological processes and leading to mutagenesis, carcinogenesis and ageing. Examples of ROS include hydrogen peroxide (H_2O_2) (Hydrogen peroxide is not strictly a ROS but is widely accepted to be part of this group of molecules), singlet oxygen ($^1O_2$), superoxide ($^{\cdot}O_2^-$), and hydroxyl radicals ($^{\cdot}OH$), generated mainly by the aerobic respiration of mitochondria (Boveris, 1977; Ku et al., 1993) and peroxyl ($ROO^{\cdot}$), and alkoxyl ($RO^{\cdot}$) radicals, formed as products of lipid peroxidation. Reactive nitrogen species also have the ability to cause numerous DNA lesions and add to the generation of $^{\cdot}OH$ radicals. Examples of these species include nitric oxide ($^{\cdot}NO$), nitrogen dioxide ($^{\cdot}NO_2$), and peroxynitrite (ONO_2-), generated by activated phagocytes (Inoue and Kawanishi, 1995).

Hydrogen peroxide and $^{\cdot}O_2^-$ are amongst the most abundant ROS generated in the cell. Superoxide can be converted to H_2O_2 by spontaneous and/or superoxide dismutase (SOD)-catalysed dismutation of $^{\cdot}O_2^-$. However, neither H_2O_2 nor $^{\cdot}O_2^-$ cause significant damage to DNA under normal physiological conditions (Lesko et al., 1980; Aruoma et al., 1989; Blakely et al., 1990). Therefore, the toxicity of these molecules has been largely attributed to $^{\cdot}OH$ radicals, generated by metal ion-catalysed Fenton reactions of H_2O_2 (Cadet et al., 1999; Henle and Linn, 1997) (Eq.1.1) Hydroxyl radicals are relatively abundant and extremely reactive and therefore only diffuse short distances (~15Å) before reacting with a cellular component. This high reactivity suggests they are unlikely to be able to diffuse from the mitochondria into the nucleus to cause DNA damage. Therefore, H_2O_2 may serve as a latent form of $^{\cdot}OH$, diffusing throughout the cell and releasing the oxidant radical when it comes into contact with a metal ion (Marnett, 2000).

$$Metal^{n+} + H_2O_2 \xrightarrow{\text{Fenton reaction}} Metal^{n+1} + 2^{\cdot}OH \quad (1.1)$$

A second important source of $^{\cdot}OH$ formation comes from ionising radiation (hν). Ionisation of a water molecule produces an electron (e^-) and $H_2O^{\cdot+}$ (Eq. 2.1), which rapidly loses a proton to give rise to $^{\cdot}OH$ (Eq. 2.2). Alternatively, ionising radiation can excite a water molecule initiating homolysis, and generating a proton (H^+) and $^{\cdot}OH$ (Eq. 2.3) (Breen and Murphy, 1995).

$$H_2O \xrightarrow{h\nu} H_2O^{\cdot+} + e^- \quad (2.1)$$

$$H_2O^{\cdot+} + H_2O \longrightarrow H_3O^+ + {}^{\cdot}OH \quad (2.2)$$

$$H_2O \xrightarrow{h\nu} H_2O^* \longrightarrow H^+ + {}^{\cdot}OH \quad (2.3)$$

Hydroxyl radicals are now considered to be the main ROS contributing to the oxidation of cellular DNA. However, some of the other oxidants mentioned also induce similar damage. These include singlet oxygen ($^1O_2$) (Schulz et al., 2000), one electron oxidants (as generated by the ionisation of water – Eq 2.1) and peroxynitrite (ONO_2^-) (Koppenol et al., 1992). Peroxynitrite is the reaction product of $^{\cdot}NO$ and $^{\cdot}O_2^-$ (Eq 3.1). Although ONO_2^- does generate small quantities of $^{\cdot}OH$ (Eq 3.2), the protonated form of ONO_2^- (peroxynitrous acid, ONO_2H) is also capable of oxidising DNA directly. The pattern of oxidised bases produced by ONO_2^- is similar to those observed from $^{\cdot}OH$ attack (Burney et al., 1999; Inoue and Kawanishi, 1995).

$$^{\cdot}O_2^- + {}^{\cdot}NO \rightarrow ONO_2^- + H^+ \rightleftharpoons ONO_2H \quad (3.1)$$

$$ONO_2H \rightarrow {}^{\cdot}OH + {}^{\cdot}NO_2 \rightarrow NO_3^- + H^+ \quad (3.2)$$

1.4 Oxidative DNA damage

So far, more than 100 oxidised DNA lesions have been identified, encompassing damage to all four DNA bases and the phosphodiester backbone. These are derived from ROS attack on both base and sugar moieties generating, oxidised bases, abasic sites, DNA-DNA cross-links, strand breaks and DNA-protein cross-links. All of these DNA modifications have the potential to compromise genomic integrity and lead to carcinogenesis.

1.4.1 Sugar damage

Reactive oxygen species are able to attack deoxyribose at a variety of positions with the exception of C2′ (Figure 1.2). The majority of this damage results in DNA strand breaks, but may also release purine or pyrimidine bases to produce an abasic site. Abasic sites can be cytotoxic because they block the activities of replicative DNA polymerases. The most common sites of oxidative attack are at C1′, which generally results in an abasic site with the phosphate backbone left intact, and C4′, which may result in both base loss and strand incision (Breen and Murphy, 1995).

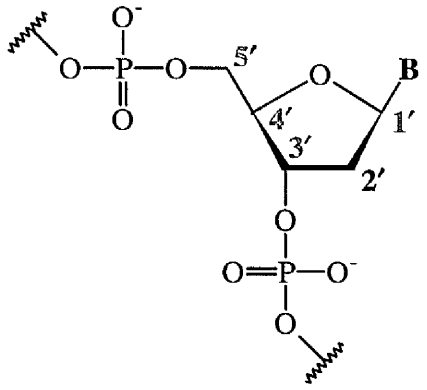

Figure 1.2. Carbon positions on the sugar phosphate DNA backbone available to oxidative attack. **B** = purine or pyrimidine base. .

1.4.2 Strand breaks

Strand breaks, and in particular double-strand breaks (DSB) have important biological consequences, as they can lead to potentially lethal chromosomal aberrations and therefore a loss of genetic information. While still potentially damaging, single-strand breaks (SSB) have limited effects because the adjacent strand can be used to maintain the integrity of the DNA molecule during the repair of the break.

1.4.3 Cross-links

Reactive oxygen species can also modify DNA and proteins such that a covalent linkage is formed between the two molecules. Furthermore, DNA-DNA cross-links may occur between bases in the same strand (intrastrand) or in different strands (interstrand), resulting in both cytotoxic and mutagenic damage following attempted repair or DNA replication processes.

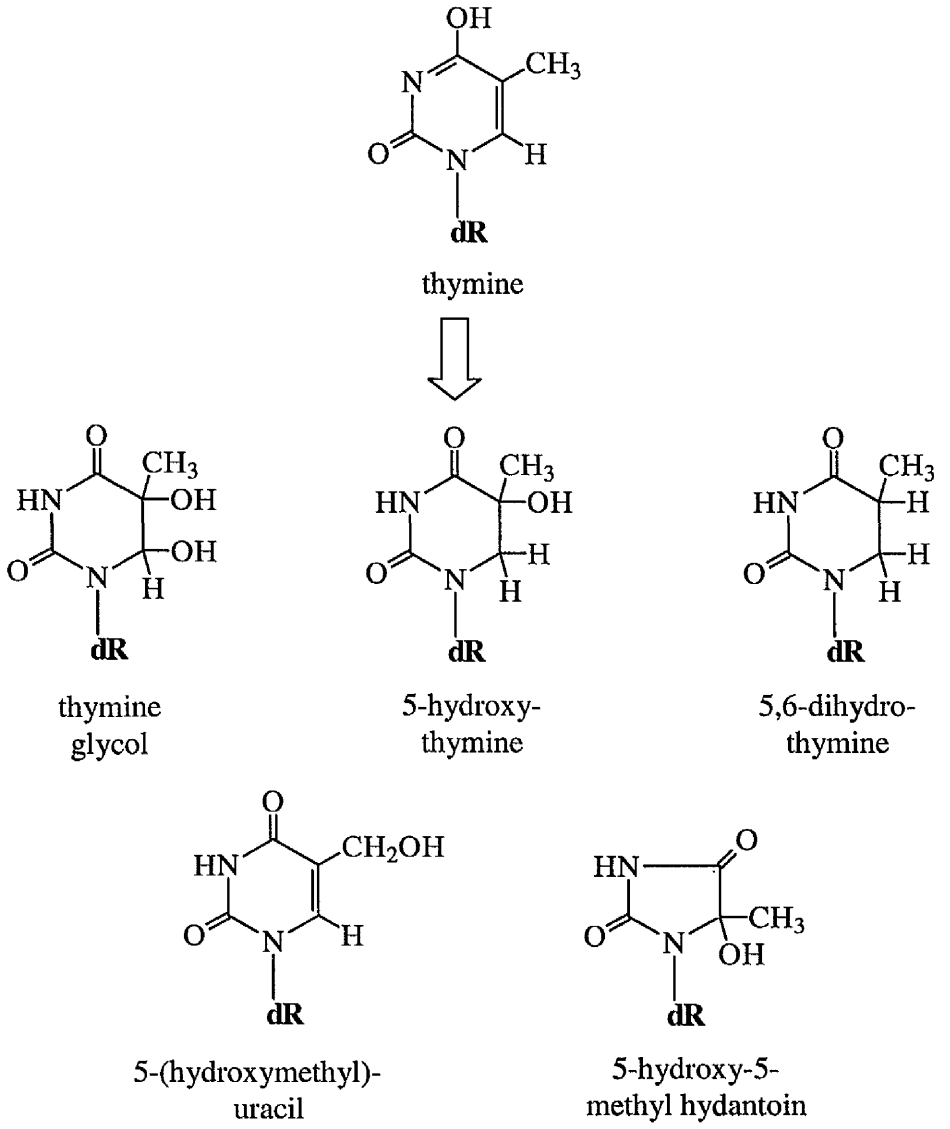

Figure 1.3. Structures of oxidised thymidine bases and their derivatives.

1.4.4 Pyrimidine base damage

A number of products result from oxidative attack on the pyrimidine bases, thymine and cytosine. These occur primarily by the addition of ·OH to the π bonds of the bases. Thymine glycol is the most predominant thymine oxidation product generated after the oxidation of DNA (Breimer and Lindahl, 1985; Teoule et al., 1977). However, many other oxidation products are also produced (Figure 1.3). The oxidation products of cytosine are similar in nature to those observed from the oxidation of thymine. However, unlike thymine glycol, cytosine glycol is an unstable oxidation product and does not generally persist in DNA. Figure 1.4 illustrates the generation of various cytosine oxidation products. The formation of both pyrimidine hydrates and pyrimidine glycols abolishes the planar structure of the parent molecules, allowing the bases to become non-coding, and block DNA polymerases. In addition, saturation of the C5-C6 double bond increases the rate of hydrolytic deamination producing uracil products. These uracil derivatives base pair preferentially with adenine, not guanine, and hence may cause G:C to A:T transition mutations.

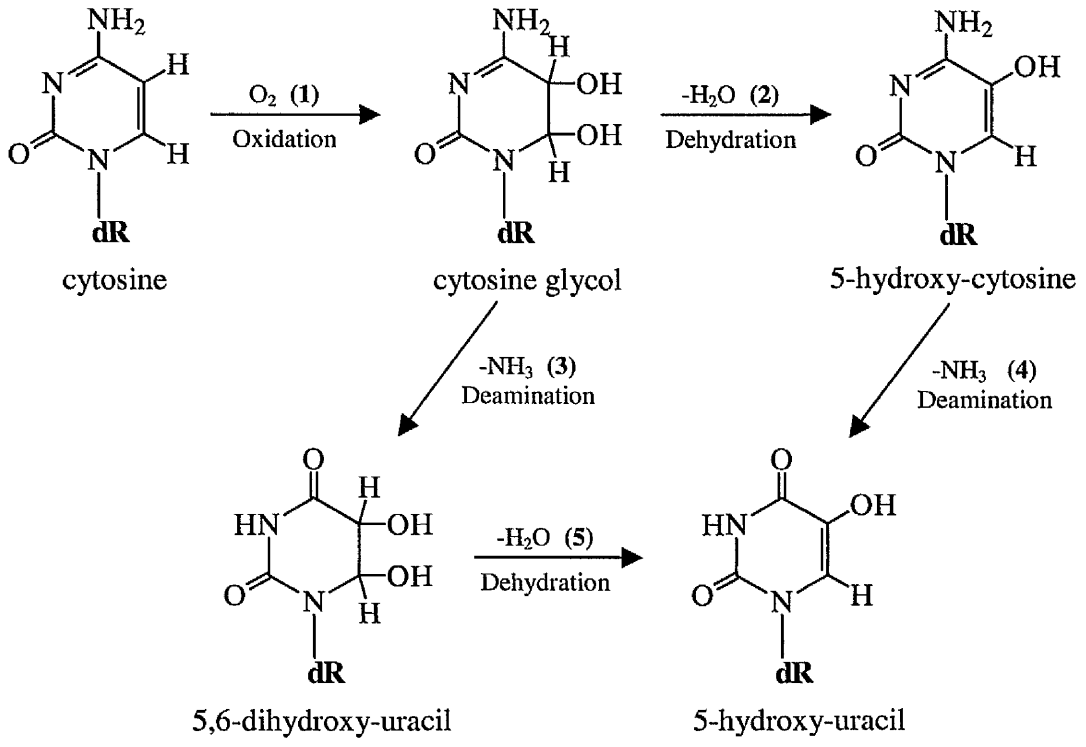

Figure 1.4. Mechanism for the oxidation of cytosine. (1) Initial oxidation of cytosine can form the relatively unstable species, cytosine glycol, that can either dehydrate (2), deaminate (3), or undergo both reactions (4,5) to form 5-hydroxy-cytosine, 5,6-dihydroxy-uracil, or 5-hydroxy-uracil, respectively.

1.4.5 Oxidation of guanine

Guanine is the most susceptible base target for oxidative damage in DNA (Steenken, 1997) and is readily oxidised by $^{\cdot}OH$, $^{1}O_2$, e^{-} and $^{\cdot}ONO_2^{-}$. Hydroxyl radical attack at the C8′ position of guanine produces the most abundant type of oxidative damage, 8-oxo-7,8-dihydro-2'-deoxyguanine (8-oxodG), and also 2,6-diamino-5-formamido-4-hydroxypyrimidine (FaPy-dG) (Figure 1.5) (Aruoma et al., 1989). Ring opened FaPy-dG lesions are predominantly cytotoxic and block the action of DNA polymerases as shown by the inhibition of *E. coli* DNA Pol I and phage T4 DNA polymerase (O'Connor et al., 1988). This lesion also posseses marginal pro-mutagenic potential, increasing the G:C to C:G and G:C to T:A transversion rate 3-fold in FaPy-dG containing phage DNA transfected into *E. coli* (Tudek et al., 1992).

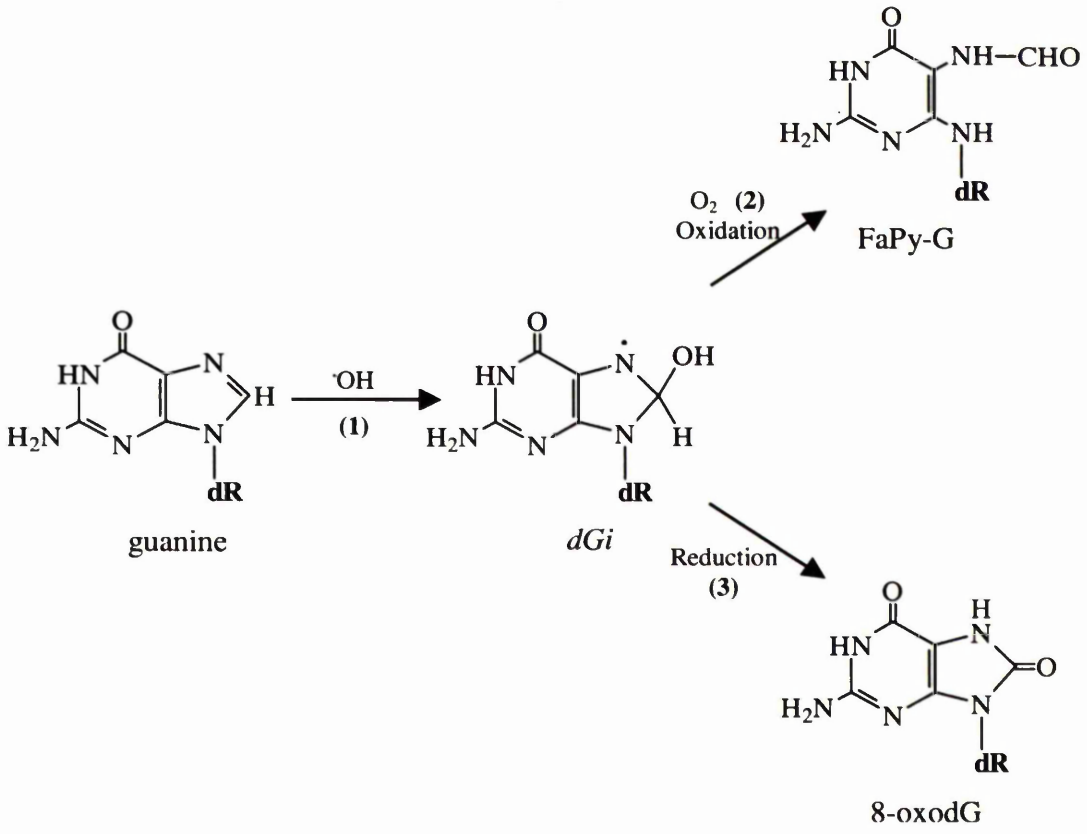

Figure 1.5. Mechanism for the oxidation of guanine. (1) Initial oxidation of guanine forms the unstable radical intermediate *dGi* (8-hydroxy-7,8-dihydro-guanyl radical intermediate), that can either be oxidised to FaPy-dG (2,6-diamino-5-formamido-4-hydroxypyrimidine) (2), or reduced to form 8-oxodG (8-oxo-7,8-dihydro-2'-deoxyguanine (8-oxodG) (3). Key . = uncoupled electron.

Although 8-oxodG lesions do not block DNA replication, they are highly pro-mutagenic. Shibutani et al., (1991), confirmed the pro-mutagenic nature of this lesion *in vitro* with the observation that several DNA polymerases efficiently mis-incorporate dA opposite 8-oxodG in DNA templates. The ratios of insertion of dC and dA was dependent on the DNA polymerase used, with polymerases associated with repair (DNA Pol I and DNA Pol β) favouring the incorporation of dC, while the polymerases associated with replication (DNA Pol α and DNA Pol δ) favoured the incorporation of dA. These results were confirmed in bacteria using a phage *lacZ* colony reversion assay, whereby 1% of *LacZ* revertants were found to contain G:C to T:A transversion mutations at the specific location of 8-oxodG incorporation (Cheng et al., 1992). Cheng et al., (1992) also conducted experiments with 8-oxodGTP which demonstrated that incorporation of the nucleotide generated A:T to C:G transversion mutations. The mutagenic potential of 8-oxodG was assessed *in vivo* by the ability of mammalian cells to replicate the adduct when incorporated into single stranded shuttle vectors. Moriya et al., (1993), and Le Page et al., (1995), both demonstrated mutation events in approximately 4% of the progeny in these experiments.

The mutagenic nature of 8-oxodG has also been investigated using NMR spectroscopy. While free 8-oxodG in solution adopts a *syn* conformation about the glycosidic bond, in duplex DNA the conformation adopted depends upon the identity of its base pair partner. Thus, when paired opposite dC, 8-oxodG resides in an *anti*-orientation and is capable of forming a stable Watson–Crick pair. However, when 8-oxodG assumes a *syn* conformation, it can form a stable Hoogsteen mispair with dA (Figure 1.6). The mutagenicity of 8-oxodG has been attributed to this ability to undergo a conformational switch from *anti* to *syn* relative to the deoxyribose sugar (Wang et al., 1998).

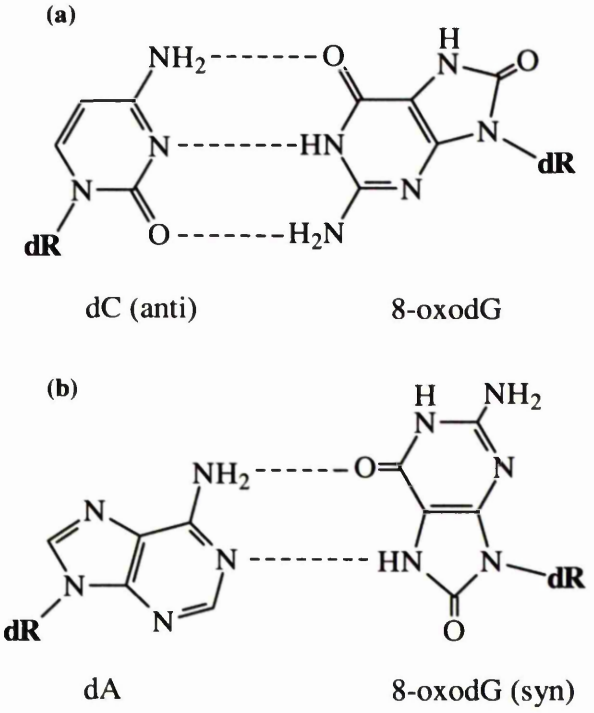

Figure 1.6. Differential base pairing properties of 8-oxodG. (a) 8-oxodG orientated in the *anti* configuration about the glycosidic bond allowing base pairing with dC (cytosine). (b) 8-oxodG orientated in the *syn* configuration about the glycosidic bond allowing pro-mutagenic base pairing with dA (adenine).

The base sequence surrounding 8-oxodG has also been shown to effect the ability of the lesion to cause mutations. Hatahet et al., (1998) demonstrated sequence contexts that both decrease the efficiency of the enzymatic removal of the lesion, and simultaneously increase the efficiency of mis-incorporation opposite the lesion by DNA polymerases. Furthermore, these sequences correlate strongly with G:C to T:A transversion mutation 'hotspots' observed in spontaneous mutational spectra reported for the *E. coli LacI* gene and the human p53 and factor IX genes. The presence of 8-oxodG lesions in regulatory promoter regions has also been shown to cause a decrease in gene expression levels, including alterations in DNA methylation surrounding the lesion, and the production of truncated translation products (Viswanathan and Doetsch, 1998; Weitzman et al., 1994). Each of these events has the potential to disrupt other cellular pathways.

1.4.6 Biological significance of 8-oxodG

The mutagenic potential of 8-oxodG has been demonstrated in several model systems. However, a proven link between the levels of 8-oxodG and tumour formation has been more difficult to establish. While studies of human tumours have shown elevated levels of 8-oxodG when compared to the surrounding tissue and these increases may aid tumour progression, they are unlikely to be the cause of the tumour formation (Olinski et al., 1992). The most promising evidence linking the levels of 8-oxoG to cancer has been obtained from cigarette smokers. Asami et al., (1996) observed a significant increase in the 8-oxodG levels found in the leukocytes of smokers compared to a control group. Furthermore, a significant proportion of smoking related tumours have been found to contain higher levels of G:C to T:A transition mutations in major regulatory genes (*p53*, *K-ras*) than those seen in non-smokers (Suzuki et al., 1992; Chiba et al., 1990). As lung cancer rates are known to be higher in smokers, it is of significance that both the levels of 8-oxodG lesions and G:C to T:A transition mutations are increased in these patients.

Two of the most convincing studies that associate the presence of 8-oxodG lesions to tumour formation have been carried out in rats. Nagashima et al., (1995) exposed rats to diesel exhaust particles, which produce tumours in the respiratory tract, and found these animals had high levels of 8-oxodG in lung tissue, as well as a lower 8-oxoguanine-DNA-glycosylase activity (Tsurudome et al., 1999). Furthermore, rats exposed to quartz were found to develop lung tumours and contain significantly increased levels of 8-oxodG in lung tissue compared to a control group (Seiler et al., 2001). The levels of 8-oxodG have also been measured after treatment with environmental carcinogens and mutagens in various cell types. For example, asbestos treatment has been found to increase 8-oxodG levels in human mesothelial cells (Chen et al., 1996), while UV irradiation has been shown to increase the 8-oxodG levels in human and murine skin cells (Beehler et al., 1992; Kvam and Tyrrell, 1997). Furthermore, the renal carcinogens potassuim bromate ($KBrO_3$) and ferric nitrilotriacetate (Fe-NTA) have also been shown to increase the levels of 8-oxodG in the kidney, while levels in the liver, a non-target tissue, remained unchanged (Kasai et al., 1987; Umemura et al., 1990). These are a few representative studies of many experiments that correlate exposure to carcinogenic agents, which generate many oxidative adducts, to increased levels of 8-oxodG.

1.4.7 Oxidation of adenine

The oxidation of DNA also generates adenine derived oxidation products with the most predominant form being 8-oxo-7,8-dihydro-2'-deoxyadenine (8-oxodA), although this lesion is generated in smaller quantities than 8-oxodG (Bonicel et al., 1980). Shibutani et al., (1993) showed that 8-oxodA also has the potential to form DNA mispairs *in vitro* depending on the DNA polymerase used. However, further investigations carried out *in vivo* by Kamiya et al., (1995) indicated that mutations induced by 8-oxodA lesions occur at very low levels under physiological conditions. Therefore, 8-oxodA is not thought to play an important role in mutation formation resulting from oxidative stress. The poor mutagenic capacity of 8-oxodA is explained by earlier work by Guschlbauer et al,. (1991) who observed stable Watson and Crick base-pairing between 8-oxodA and thymine (dT) in duplex DNA. Furthermore, Leonard et al., (1992) also showed that the expected mis-pairing between 8-oxodA and guanine (dG), or cytosine (dC), involved an unstable *syn* wobble conformation. The relative stabilities of the 8-oxodA mispairs and the 8-oxodA:dT base pair, in comparison with the stabilities of 8-oxodG:dA and 8-oxodG:dC pairs, provides an explanation why 8-oxodG has a much more profound biological significance than 8-oxodA.

1.5 Steady-state levels of DNA lesions

Oxidative DNA lesions are known to persist in cellular DNA despite the presence of scavengers of ROS and DNA repair pathways. The equilibrium between the generation and repair of these lesions results in steady-state levels of oxidative DNA modifications within the nuclear and mitochondrial genomes. Though a direct correlation between DNA lesion formation and tumour incidence has been difficult to prove unambiguously (Gupta and Lutz, 1999; Otteneder and Lutz, 1999), there is evidence that links DNA adducts to the formation of DNA mutations (Wang et al., 1998), and DNA mutations to an increase in tumour incidence (Daya-Grosjean et al., 1995). Therefore, it is thought that DNA base adducts could be used as biomarkers to identify individuals or groups at increased risk of particular cancers. The close relationship between increased levels of all oxidative adducts and 8-oxodG allows the measurement of this lesion to be used as an accurate biomarker for cellular stress.

However, determination of accurate levels of 8-oxodG in nuclear DNA from human cells has proved to be more difficult than first thought. In fact, a review of the recent literature shows over a 3,000-fold variation in background levels between cell-types and detection techniques (Table 1.1) (Pflaum et al., 1997). This variation is caused by several factors including the sensitivity of the detection technique used, artifactual production of lesions during DNA preparation, specifically acid hydrolysis and laboratory specific experimental factors. Despite the current variation in measurements, the value of steady-state 8-oxodG lesions in human lymphocytes is thought to be about one 8-oxodG per 10^6 bp.

Technique	Cell-type	Sites detected per 10^6 bp[a]
HPLC/ECD	Human Lymphocytes	30 ± 2
HPLC/ECD	Human Lymphocytes	24 ± 3
HPLC/ECD	Human Lymphocytes	5 ± 2
HPLC/ECD	Human Lymphocytes	1.9 ± 1.4
HPLC/ECD	Human Lymphocytes	1.1 ± 0.6
HPLC/ECD	Human Lymphocytes	0.83 ± 0.6
HPLC/ECD	HeLa	5 ± 2
GC/MS	Human Lymphocytes	102-218[b]
GC/MS	K562	154 ± 24
GC/MS	Human epithelial	282 ± 60
SCGE	Human Lymphocytes	0.13 ± 0.05
Alkaline unwinding	V79	0.17
Alkaline unwinding	HeLa	0.38 ± 0.1
Alkaline elution	L1210	0.3
Nick translation	Fibroblasts	0.08

Table 1.1. Reported steady-state levels of 8-oxoG and Fpg-sensitive modifications in nuclear DNA of human cells (Table ref. (Pflaum et al., 1997), contains original study citations). [a]8-oxoG residues only in the case of HPLC/ECD and GC/MS. [b]Interindividual variations. Abbreviations: HPLC/ECD, High performance liquid chromatography/electrochemical detection; GC/MS, Gas chromatography coupled with mass spectrometry; SCGE, single cell gel electrophoresis (comet assay).

1.6 Repair of oxidative DNA damage

To protect the genome from the toxic and mutagenic effects of oxidative DNA damage, cells have developed complex DNA caretaking systems, consisting of a variety of ROS scavenging mechanisms and a battery of DNA repair pathways.

1.6.1 ROS scavenging enzymes

The burden of ROS production is largely counteracted by an intricate antioxidant defence system composed of enzymatic scavengers such as SOD (superoxide dismutase), catalase and glutathione peroxidase. SOD catalyses the conversion of superoxide to hydrogen peroxide (Tainer et al., 1983), whereas catalase and glutathione peroxidase convert hydrogen peroxide to water (Quan et al., 1986; Chada et al., 1990). While the activities of both catalase and glutathione peroxidase are restricted to the peroxisome, a new family of peroxide scavengers termed peroxiredoxins has recently been discovered that acts throughout the cytoplasm (Park et al., 2000). A variety of other non-enzymatic, low molecular mass molecules are also important in scavenging ROS. These include ascorbate, pyruvate, flavonoids, carotenoids and most importantly glutathione. An imbalance between ROS production and antioxidant defences can increase the spontaneous levels of DNA mutations. Indeed, studies have shown that mammalian cells that have a diminished antioxidant defence accumulate increased levels of oxidative lesions in nuclear DNA (Beckman and Ames, 1998). Furthermore, SOD ko mice were found to have a reduced ability to deal with ROS generated in the mitochondrion, which subsequently led to a significant increase in the level of mitochondrial DNA rearrangements (Melov et al., 1999).

1.6.2 The regulation of cellular stress

If the amount of ROS generated in a cell rises to a level that alters the normal redox balance, the cell shifts into a state of oxidative stress. When the stress is severe, the survival of the cell is dependent on its ability to adapt or resist the stress by the repair or replacement of damaged molecules. If the damage is too great the cell may respond by undergoing apoptosis. A number of stress response pathways have evolved that act in co-ordination to determine this outcome. Among the main stress signalling pathways are the nuclear factor (NF)-κB signaling system, the heat shock response (HSR), and the mitogen activated protein kinase (MAPK) signaling cascades, which include, the p38 pathway, the extracellular signal-regulated kinases (ERK), and the c-Jun amino-terminal kinase (JNK) cascade. In addition, several pathways are activated specifically in response to oxidative DNA damage. These include, the phosphoinositide 3-kinase-like (PI(3)K-like) pathways and p53 activation.

The heat shock response (HSR) is the main defence mechanism used by cells to counteract the detrimental effects of cellular stress on protein structure. Cells counteract the effects of stress by increasing their stabilising forces; among others they strongly increase the synthesis of heat shock proteins (HSP). Many of the stress-induced HSP's such as HSP90, HSP70, HSP40 and the small HSP's are isoforms of constitutive chaperones and fulfil similar or identical functions. However, with these increased amounts of HSP's many cellular functions become stress-tolerant, as shown by the ability of cells to initiate a controlled cell-cycle arrest under conditions of high stress (Helmbrecht et al., 2000; Jolly and Morimoto, 2000).

The MAPK-stress response pathways (ERK, JNK and p38) are activated by a variety of stress signalling molecules including mitogens, cytokines, growth factors, ROS and environmental molecules (Waskiewicz and Cooper, 1995). Once initiated, these pathways activate a cascade of serine/threonine protein kinases resulting in the activation of downstream transcription factors. Recent studies have started to show that each of the pathways results in the activation of a similar set of AP-1-like transcription factors (Jun proteins, c-Myc, ATF-2 and Elk-1). While the gene targets of these transcription factors are not yet known, the cellular responses to MAPK activation suggest it is likely that they act in combination with other factors to upregulate check-point control enzymes, and a range of HSP and DNA repair enzymes (Davis, 2000; Nebreda and Porras, 2000).

In mammalian cells the PI(3)K pathways consist of three independent pathways initiated by the enzymes, ATM, ATR and DNA-PK (Durocher and Jackson, 2001). Each of these proteins belongs to a family of PI(3)K-kinases that is conserved from yeast to humans. While there are subtle differences in both the activation signals and downstream targets of these proteins, in general, they are all activated by the presence of single and double-strand DNA breaks, and initiate separate phosphorylation cascades that regulate cell-cycle check-points and DNA repair and recombination (Kastan and Lim, 2000; Shiloh, 2001).

The NF-κB family of proteins (p50/p105 (NF-κB1), p52/p100 (NF-κB2), p65 (RelA), RelB and c-Rel) has been associated with both pro- and anti-apoptotic roles (Karin and Lin, 2002). While NF-κB is well established as a regulator of the immune and inflammatory responses (Baldwin, 2001), more recently, it has been shown to be activated in response to DNA damage and is thought to be regulated, at least in part, by ATM (Piret et al., 1999).

As multiple stress response pathways may be activated at any one time, the process by which the MAPK, NF-κB and PI(3)K-like signalling pathways co-ordinate their responses is not fully understood. However, it is clear that despite a wide range of stress factors, initiating a variety of cascade events, the outcome generally results in cell-cycle arrest, and the upregulation of HSP and DNA repair proteins, or apoptosis. The p53 protein is thought to be a critical factor in mediating the cellular response directed from these pathways. Indeed, p53 has been characterized as a transcription factor, DNA damage sensor, and has sites for phosphorylation, acetylation, and numerous protein interaction domains. It is also known to be an essential determinant for either cell-cycle arrest or apoptosis.

In response to DNA damage, p53 is phosphorylated at its amino-terminus and becomes stabilised upon disruption of an interaction with its negative inhibitor, MDM2. Subsequent phosphorylation and acetylation of p53 promote different interactions with other proteins and with target regulatory elements to facilitate cell-cycle arrest, apoptosis, or adaptation. The PI(3)K-like, NF-κB and MAPK signalling cascades have all been found to have associations with the activation of p53, either by direct phosphorylation or by downstream effectors (Colman et al., 2000; Wahl and Carr, 2001).

1.7 DNA repair mechanisms

There are at least five main, partly overlapping damage repair pathways that operate in mammalian cells. These are base-excision repair (BER), nucleotide-excision repair (NER), mismatch repair (MMR), homologous recombination and non-homologous end joining. The following section concentrates on the BER, NER, and MMR pathways.

1.7.1 Base excision repair

Base excision repair operates as a global genome repair mechanism that deals with a variety of DNA modifications generated by ROS, alkylating agents, deamination, single-strand breaks and base loss. This pathway can be initiated by a range of DNA glycosylases that have relatively narrow substrate specificities (see Section 1.8). The following paragraph describes the mechanism by which BER deals with DNA base lesions and is illustrated in Figure 1.7 (For reviews see; Hoeijmakers, 2001; Nilsen and Krokan, 2001; Norbury and Hickson, 2001; Wood, 1996).

When a base lesion is discovered, the glycosylase places the DNA backbone under compression, which flips the damaged base out of the helix and into an internal cavity of the protein. The base is then cleaved from the sugar-phosphate backbone generating an abasic site (a). Abasic sites can also occur from direct oxidative damage or spontaneously by hydrolysis (b). If the DNA glycosylase contains an associated AP lyase activity, the sugar-phosphate backbone is also cleaved 3′ to the abasic site (AP lyase activity is not shown in Figure 1.7. See Section 1.8 for details), if not, the reaction proceeds as normal. The downstream components of BER are activated by strand incision 5′ to the abasic site by the endonuclease, APE1 (c). If the glycosylase has previously generated a 3′ incision, the baseless sugar-phosphate is released from the phosphate backbone at this stage. If a whole nucleotide has been lost from DNA by damage, a second pathway has recently been proposed whereby poly(ADP-ribose) polymerase (PARP), which binds to and is activated by DNA strand breaks, and polynucleotide kinase (PNK), protect and trim the exposed ends ready for repair (d). In mammalian cells, short-patch repair is the dominant pathway for the remainder of the reaction in which DNA polymerase β is sequestered to fill the one-nucleotide gap and its associated deoxyribose phosphatase activity removes the 5′-terminal baseless sugar, if not previously removed by the activity of the glycosylase and APE1 (e). The remaining nick is sealed by DNA ligase III, in complex with XRCC1 (f). XRCC1 is a scaffold protein that interacts with several BER components (DNA Polβ, ligase III and PNK) and is essential for the BER function. The long-patch repair pathway involves the re-synthesis of a section of DNA, extending 2-10 bases in the 3′ direction, by DNA Polδ/ε, which acts in complex with proliferating cell nuclear antigen (PCNA) (g). The

flap specific endonuclease, FEN1 is then used to excise the displaced single strand flap (h) and DNA ligase I seals the remaining nick (i).

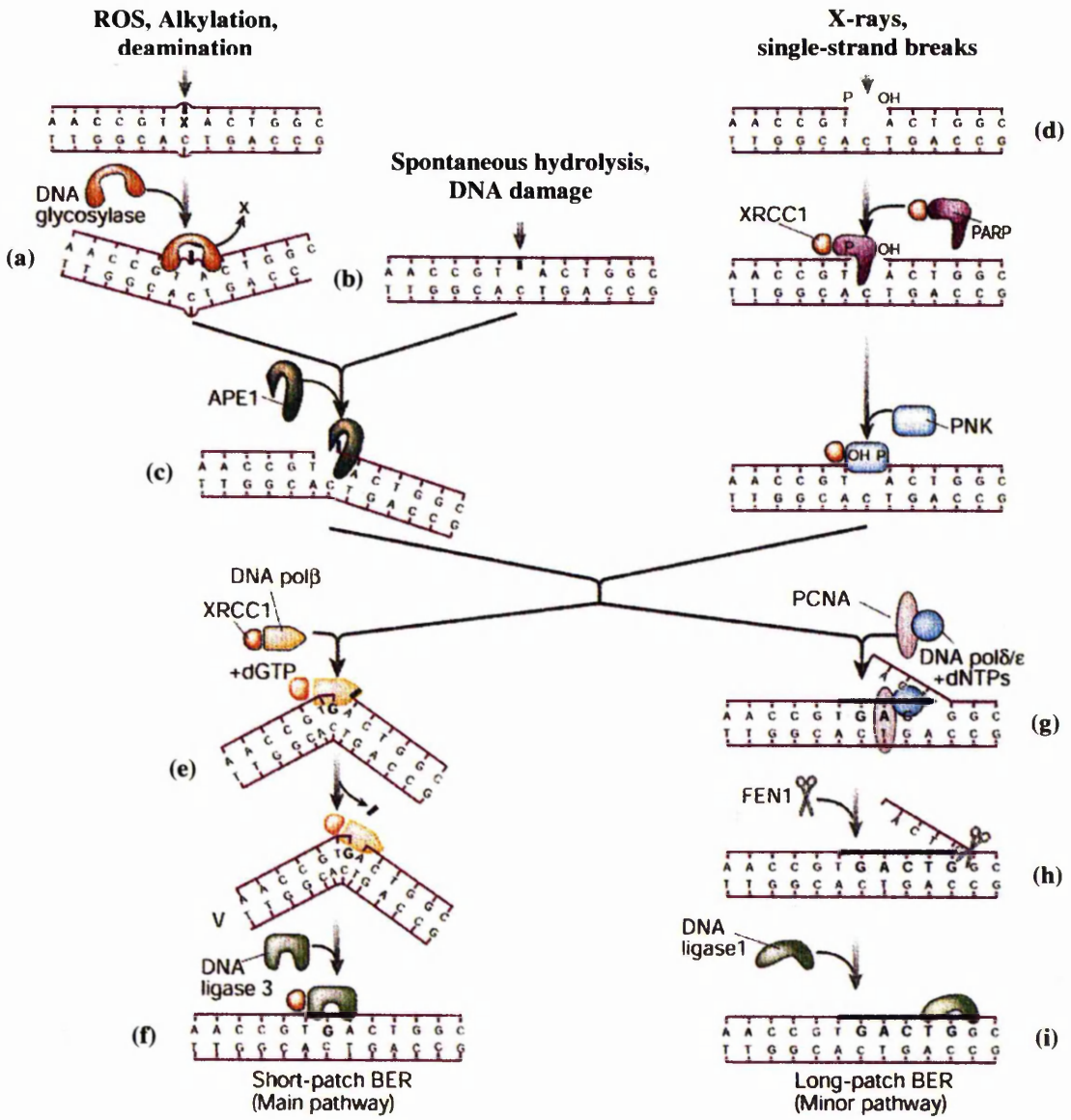

Figure 1.7. Model for the mechanism of BER Initially a DNA glycosylase binds to, and excises a damaged base from the DNA backbone, generating an abasic site (a). Bases may also be lost from DNA by hydrolysis or by direct DNA damage (b). The downstream BER components are then activated by strand incision, 5′ to the abasic site, by APE1 (c). The repair of nucleotide loss and single-strand breaks may proceed by the activities of PARP and PNK, which protect and trim the exposed DNA ends in readiness for repair (d). At this point the mechanisms converge and repair is completed by one of two pathways, short patch repair (left) or long patch (right). In short patch repair DNA Polβ is sequestered to fill the one-nucleotide gap and its associated deoxyribose phosphatase activity removes the 5′-terminal baseless sugar (e). The remaining nick is sealed by ligase III (f). In long patch repair, a strand of DNA 2-10 bases is replaced by DNA Polδ/ε in complex with PCNA (g).The resultant flap is removed by FEN1 (h) and the remaining nick is sealed by DNA ligase I (i). Diagram taken from (Hoeijmakers, 2001).

1.7.2 Nucleotide excision repair

Nucleotide excision repair is the main pathway used to remove a variety of DNA helix distorting lesions, so called "bulky" lesions, induced by UV light and chemical mutagens. If left unrepaired, these lesions interfere with DNA base pairing and may obstruct transcription and replication. Within NER, two sub-pathways have been identified with slightly different substrate specificities. These are global genome NER (GG-NER), which surveys the entire genome for helical distortions, and transcription-coupled repair (TCR), which focuses on damage that blocks elongating RNA polymerases (Figure 1.8). In total the mammalian NER system comprises of 25 or more proteins that act in succession. The following paragraph describes the mechanism by which NER is thought to repair DNA lesions (illustrated in Figure 1.8; For reviews see; Araujo and Wood, 1999; Hoeijmakers, 2001; Wood, 1999).

During global repair, the XPC-hHR23B complex is responsible for scanning the genome looking for helical distortions and base-pair disruption, rather than recognition of the lesion itself (a). In contrast, TCR is initiated by the ability of a lesion to block the progression of RNA polymerase II (b). Once stalled, the polymerase is displaced by two TCR-specific factors, CSB and CSA. In the following steps, both GG-NER and TCR are thought to follow a similar route. First, the XPB and XPD helicases of the transcription factor TFIIH complex initiate the opening of the DNA strands, approximately 30 bp surrounding the lesion, in an ATP-dependent manner (c). The damage recognition protein, XPA, is then thought to scan the opening for any base abnormalities. If a lesion is discovered the repair process is continued, otherwise XPA initiates the dissociation of the complex. The DNA opening is stabilised by the single-stranded-binding protein, RPA, which binds to the undamaged strand (d). The damaged strand is then excised by the endonuclease activities of XPG and ERCC1/XPF, which cleave both 5′ and 3′ of the opening, releasing a 24-30 bp oligonucleotide (e). The missing strand is then resynthesised by either DNA Polδ or Polε and the remaining nick sealed by DNA ligase I (f).

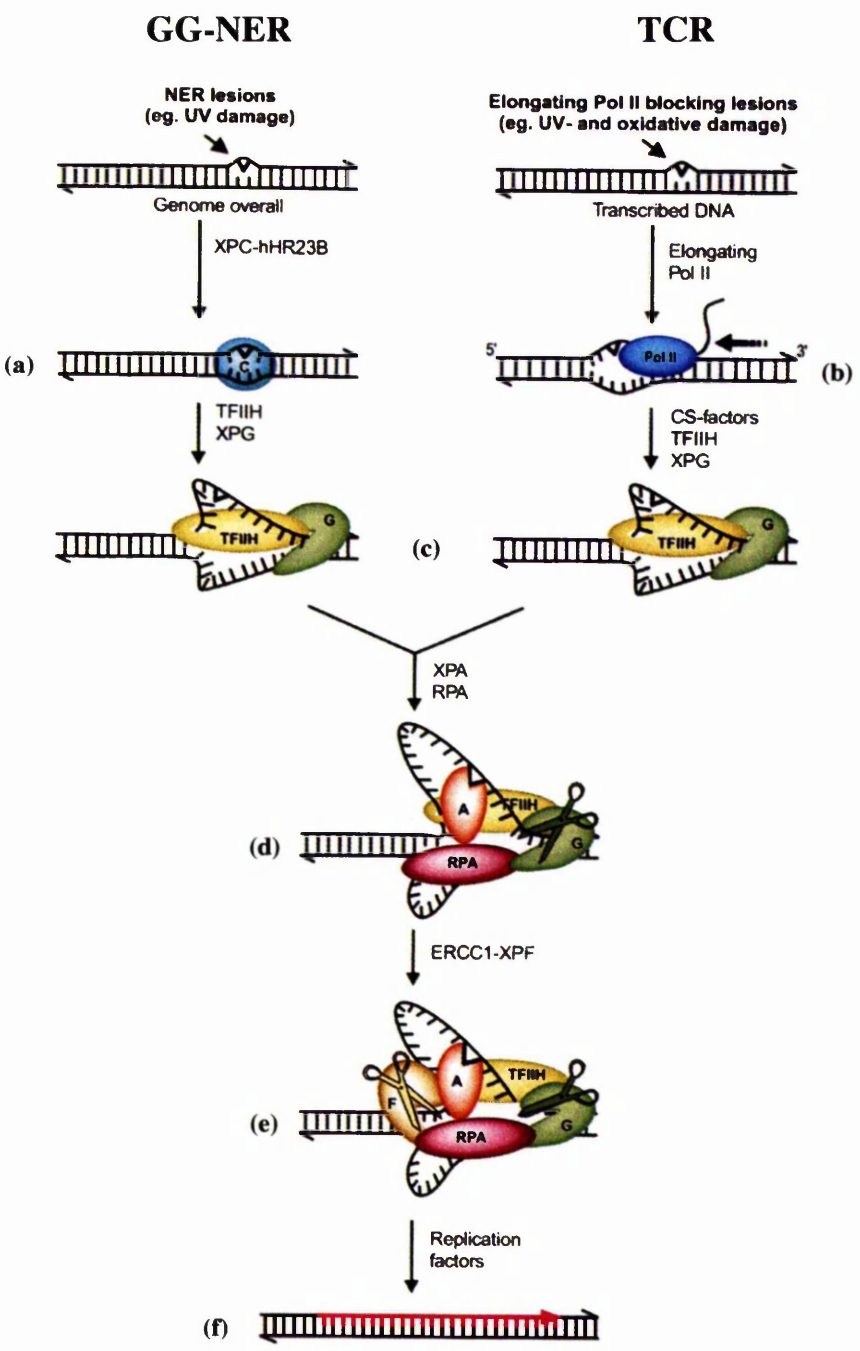

Figure 1.8. Model for the mechanism of global genome NER and transcription coupled NER. In the case of GG-NER, XPC-hHR23B detects the DNA helical distortions generated by a lesion (a), while in TC-NER the lesion is detected by the stalling of RNA pol II (b). TFIIH and XPG then bind to the opening and initiate strand separation (c). The opening is then stabilized by RPA, while XPA binds to the complex and scans for the lesion (e). XPG and ERCC1-XPF then incise the damaged SS-DNA at the 3′ and 5′ ends of the opening releasing the strand (e). The missing strand is then replaced by DNA Polδ/ε and the remaining nick is sealed by DNA ligase I (f). Diagram taken from (Hoeijmakers, 2001).

1.7.3 Mismatch repair

Mismatch repair is a replication associated repair (RAR) pathway used to identify and repair base mismatches and insertion/deletion loops (IDL). If base mismatches are not repaired efficiently subsequent rounds of DNA replication will "fix" the mutations, thereby altering the coding sequence of the DNA. Equally, IDL's generated by slippage during replication, or during recombination may produce a loss of genetic information. While a complete mechanism for MMR is still unclear, the following paragraph describes what is known so far (illustrated in Figure 1.9; For reviews see; Hoeijmakers, 2001; Hsieh, 2001; Jiricny, 1998).

Eukaryotic MMR involves multiple homologs of the prokaryotic proteins, MutS and MutL. In the first stages of MMR, hMSH2-hMSH6 heterodimers (called hMutSα; homologs of the MutS proteins) recognise and bind to both base mismatches and single-base loops in the newly synthesised strand (a). Similarly, hMSH2-hMSH3 heterodimers (called hMutSβ) recognise and bind insertion/deletion loops (b). The preferential binding of hMutSα/β to the newly synthesised strand is thought to be directed by the DNA replication machinery. Once a mutation is bound, both complexes are able to sequester the heterodimeric complexes of the hMutL-like proteins, hMLH1-hPMS2 (hMutLα) and hMLH1-hPMS1 (hMutLβ). While the role of the hMutLα/β heterodimers is unknown, each of the component proteins has been found to contain N-terminal homology to HSP90 and is therefore suggested to perform a chaperone function. The hMutLα/β complexes have also been shown to activate downstream components of the MMR pathway. These include the activities of 5′-3′ and 3′-5′ exonucleases, which act on the leading and lagging strand of DNA, respectively, and remove the newly sythesised strand from the replication fork to the site of the mutation. The strand can then be re-synthesised by DNA Polβ/δ. Several other proteins have been associated with the MMR pathway (RPA, PCNA, RFC and FEN1), although their roles in the repair mechanism has not yet been determined. It is clear, however, that BER, NER and MMR pathways share many of the same downstream proteins including polymerases, endonucleases, ligases and stabilisation proteins.

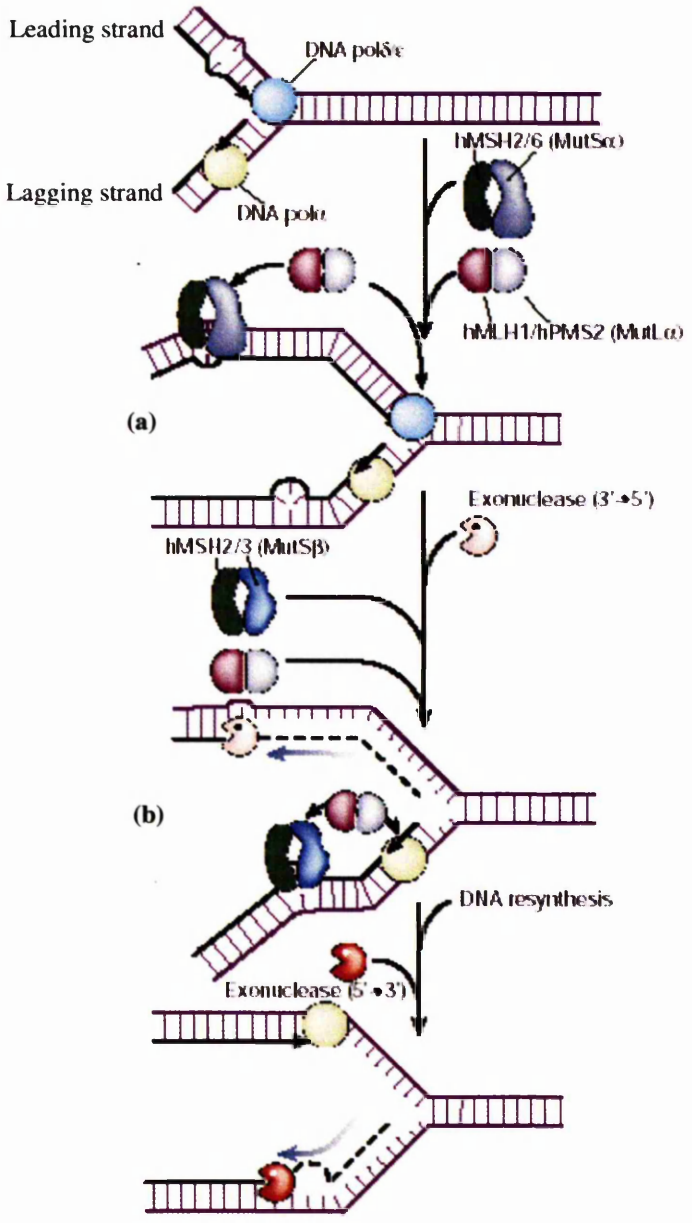

Figure 1.9. Model for the mechanism of MMR. (a) The MutSα heterodimer binds to base mismatches and single base loops, whereas (b) the MutSβ heterodimers bind to IDL regions. Both complexes are able to sequester the MutLα/β Heterodimers, which aid in stabilising the structure and activate downstream MMR components. The activities of 5′-3′ and 3′-5′ exonucleases, which act on the leading and lagging strand of DNA, respectively, remove the newly sythesised strand from the replication folk to the site of the mutation. The strand can then be re-synthesised by polβ/δ. Diagram taken from (Hoeijmakers, 2001).

1.7.4 Biological consequences of lack of repair

At present no human disorders caused by inherited BER deficiencies have been identified. These findings have been borne out in murine studies whereby the deletion of individual glycosylases does not cause an overt phenotype. The mild effects of these deletions may be explained, at least in part, by the redundancy observed between different glycosylases (see Section 1.8). In contrast, the inactivation of BER core proteins induces embryonic lethality, highlighting the vital importance of the process as a whole (Tebbs et al., 1999). However, at this time it is not known whether this lethality is induced by the accumulation of spontaneously occurring abasic sites and SSBs and/or to the generation of reaction intermediates by the glycosylases that cannot be processed further (Lindahl and Wood, 1999; Wilson and Thompson, 1997).

In contrast to BER, at least three human syndromes have been linked to defects in NER including, xeroderma pigmentosum (XP), Cockayne's syndrome (CS) and trichothiodystrophy (TTD) (Lehmann, 2001). Each of these syndromes results in extreme sensitivity to sunlight, increasing the incidence of sun-related cancers ~1000-fold. Furthermore, in XP patients the frequency of internal tumours is modestly elevated and accelerated neurodegeneration is often observed. Xeroderma pigmentosum disorders arise from mutations in one of seven genes (*XPA–XPG*), while CS is caused by mutations in the *CSA* or *CSB* genes. Cockayne syndrome is a TCR-specific disorder that is remarkably dissimilar to XP. No predisposition to cancer is observed, as these cells are particularly sensitive to lesion-induced apoptosis, although both physical and neurological development is impaired, resulting in dwarphism and dysmyelination. Trichothiodystrophy is a condition sharing many similarities to CS, except patients also experience brittle hair, nails and scaly skin. For almost all NER factors, mouse mutants have been generated. Overall, the NER defect is accurately preserved, although cancer predisposition is more pronounced and neurological complications are milder in mice. Moreover, mice exhibit features of premature ageing (de Boer and Hoeijmakers, 1999).

A functional MMR pathway is essential to prevent the formation of a variety of sporadic cancers including hereditary nonpolyposis colorectal cancer (HNPCC). These cancers arise from mutation generated by slippage during DNA replication, resulting in a loss of genetic information. Mutations in hMLH1 and hMSH2 together account for approximately half of all HNPCC patients, with hMLH1 being responsible for most (~60%) of these cases. Defects in hMSH6 cause late-onset atypical HNPCC. No hMSH3mutations have been reported. This is consistent with the notion that loss of hMLH1 and hMSH2 is associated with complete inactivation of MMR, whereas defects in the other proteins cause only a partial MMR deficiency. Mutations in hPMS2 and hPMS1 have been reported only in very few cases, implying that other factors have still to be identified (Jiricny and Nystrom-Lahti, 2000).

1.8 BER DNA glycosylases

The majority of base lesions generated by oxidative and alkylating agents are bound and excised from DNA by a variety of DNA glycosylases in the first step of the BER pathway. While the substrate specificity of each glycosylase is relatively narrow, the number and diversity of glycosylase enzymes (approximately 10 have been identified so far) allows a broad range of lesions to be repaired. DNA glycosylases can be separated into two main groups. These are the monofunctional DNA glycosylases, which cleave the N-glycosyl bond releasing the damaged base from the phosphate backbone (Figure 1.10a), and the bifunctional DNA glycosylase/AP-lyases, which remove the damaged base and incise the phosphate backbone adjacent to the newly formed abasic site. DNA glycosylase/AP-lyases can also be divided into a further two classes, the *E. coli* endonuclease III (Nth)-like glycosylases and the Fpg-like glycosylases. The Nth family of glycosylases uses an internal lysine residue as the active site nucleophile and carry out a β-elimination reaction (after excising the damaged base), which cleaves the phosphate backbone generating 3′-phospho-α,β-unsaturated aldehyde and 5′-phosphate termini (Figure 1.10b). Only prokaryotic Fpg and its paralog Nei comprise the second class, and use an N-terminal proline as the active site nucleophile. The Fpg-like glycosylases are able to cleave the phosphate backbone either side of the abasic site by successive β,δ-elimination generating both 3′ and 5′ phosphate termini (Figure 1.10c) (Cunningham, 1997).

Once the damaged base has been excised, removal of the remaining abasic site and the generation of 5′ OH and 3′ phosphate termini, which allow the DNA polymerase to replace the missing base, continue the repair process. The monofunctional glycosylases sequester APE1 to generate the 5′ OH terminus, while the deoxyribophosphodiesterase (dRpase) activities of Polβ (in eukaryotes; Wilson, 1998) and probably Fpg (in prokaryotes; Graves et al., 1992) generate the 3′ phosphate termini (Figure 1.10a). The Nth-like glycosylases, which only carry out β-elimination, also require APE1 to generate the 5′ OH terminus (Figure 1.10b). However, the β,δ-elimination reactions of the Fpg-like glycosylases leave a 5′ phosphate terminus that is processed by RecJ (in prokaryotes) and probably PNK (in eukaryotes).

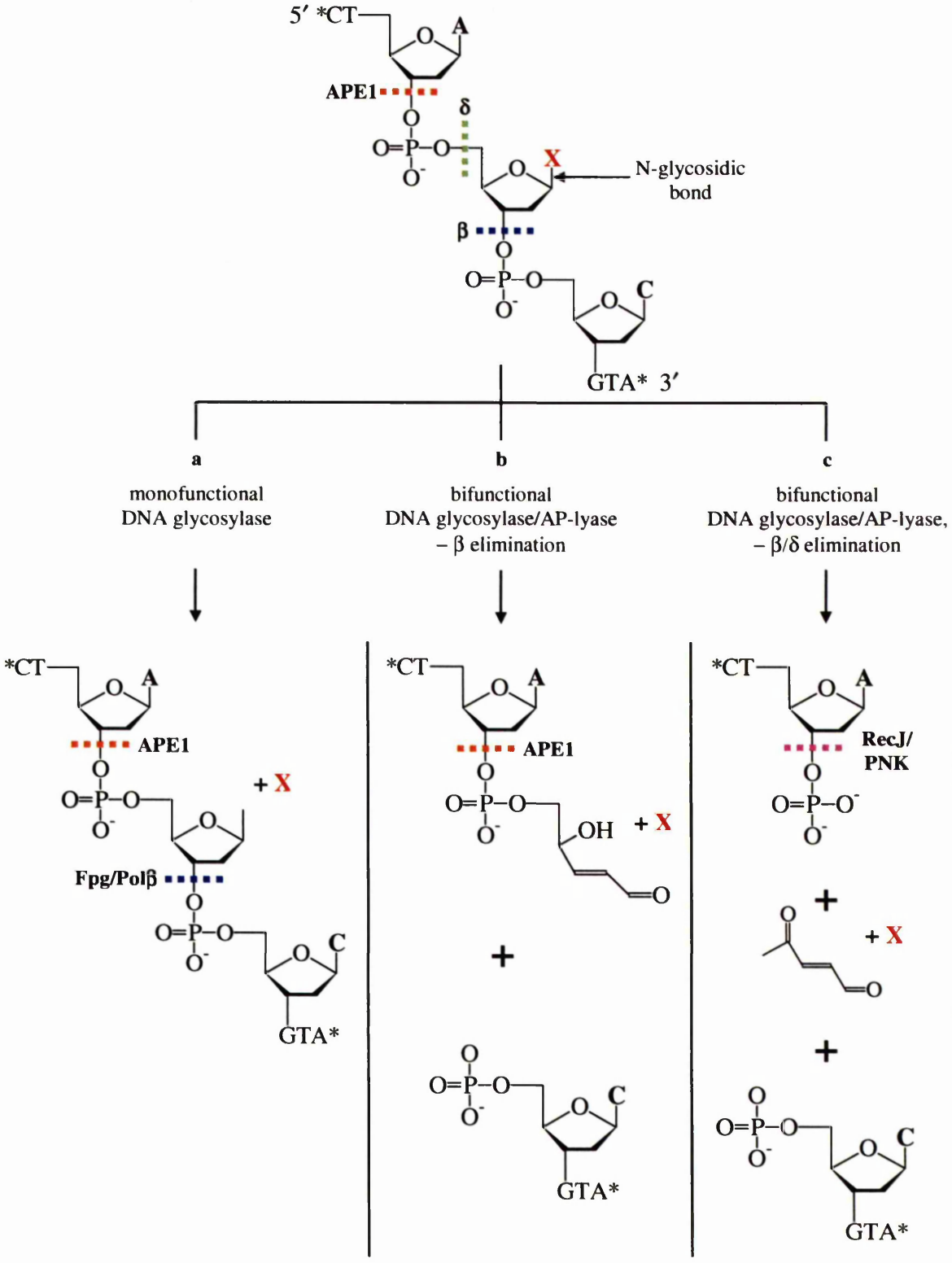

Figure 1.10. Diagram showing the cleavage products remaining after the removal of a damaged DNA base by (a) a monofunctional DNA glycosylase, (b) a bifunctional DNA glycosylase/AP-lyase, able to incise the phosphate backbone by β elimination (blue), and (c) a bifunctional DNA glycosylase/AP-lyase, able to incise the phosphate backbone via successive β- and δ-elimination (blue/green). The generation of 5′ OH termini is produced by APE1 (orange) in (a) and (b), and RecJ/PNK in (c). The dRpase activities of Fpg/Polβ are also required to generate the 3′ phosphate in (a). Key: X, represents the position of the damaged base, while *, represents a continuation of the DNA strand.

A helix-hairpin-helix (HhH) motif is common to all of the DNA glycoslyases and indeed to a wide variety of other DNA binding proteins (Doherty et al., 1996). It is suggested that this motif, of which one, two or four copies may be present, binds to the DNA in a non-sequence specific manner by the formation of hydrogen bonds between the protein and phosphate backbone. A further motif conserved in these proteins follows the HhH motif. This second motif is comprised of a glycine- and/or proline rich loop and an aspartate residue and with the HhH element is termed the HhH-GPD motif (Nash et al., 1996). The aspartate residue is conserved in all BER glycosylases that possess the HhH motif and has been shown to be an essential catalytic residue involved in cleavage of the N-glycosyl bond.

The recognition of base lesions amongst thousands of non-damaged bases poses a considerable challenge to the glycosylases. Although a number of base lesions disturb the conformation of the DNA double helix, for example thymine glycol, many lesions such as 8-oxoG cause very little change in the structure or stability of the duplex. Verdine and Bruner, (1997), proposed that the DNA glycosylases locate their substrates on the tendancy of the lesion to become spontaneously extrahelical as opposed to being buried within the DNA. DNA de-stabilising lesions are more likely to adopt an extrahelical conformation and allow glycosylases to act on and remove the extruded bases. However, a different mechanism of recognition has to take place to remove lesions that do not destabilise the DNA structure significantly. For these lesions it was proposed that the glycosylase first extrudes a base at a distance from the lesion and thus promotes an extrahelical base conformation. The glycosylase then migrates along the DNA with each extruded base being inserted into the enzyme active site until a damaged base is encountered (Verdine and Bruner, 1997).

The three BER DNA glycosylases used at various stages of this project are discussed below. All three enzymes share homology to the *E. coli* endonuclease III (Nth) family of proteins, however they each possess different substrate specificities.

1.8.1 8-oxoguanine-DNA-glycosylase (OGG1)

As previously described in Section 1.4.5, 8-oxoG is a highly promutagenic lesion capable of forming base mispairs with adenine, which, during further rounds of replication lead to the formation of G:C to T:A transversion mutations. The 8-oxoG lesion is excised primarily by 8-oxoguanine-DNA-glycosylase (OGG1) in eukaryotes and by formamidopyrimidine-DNA-glycosylase Fpg/MutM in prokaryotes. The affinity of both Fpg and OGG1 for 8-oxoG in duplex DNA has been studied extensively and shows that 8-oxoG is preferentially removed from 8-oxodG:dC base pairs followed by dT and dG, while no activity is observed opposite dA (Castaing et al., 1993; Tchou et al., 1991; Bjoras et al., 1997; van der Kemp et al., 1996). Furthermore, the presence of clustered damage surrounding 8-oxoG has no effect on the ability of OGG1 to repair the lesion, except when paired opposite a single-strand break. This inhibition may prevent the appearance of double-strand breaks generated by the AP-lyase activity of the glycosylase (David-Cordonnier et al., 2001). Both Fpg and OGG1 also excise a number of other oxidised bases including, FaPy-G, 5-hydroxyuracil (5-OHU), 5-hydroxycytosine (5-OHC), and for Fpg, a number of other ring-opened pyrimidine products (Dr R Elder, personal communication; Cadet et al., 2000).

The role of both Fpg and OGG1 in maintaining genetic integrity has been studied extensively. Bacterial cells that have been mutated to inactivate Fpg display a 5-fold increase in G:C to T:A transversion mutations compared to wild-type cells (Cabrera et al., 1988). Similar findings have been shown in yeast, murine and human cells, whereby the deletion of OGG1 results in a 2-3-fold increase in the number of 8-oxoG lesions detected (Minowa et al., 2000; Mori et al., 2001; Singh et al., 2001), as well as an increase in G:C to T:A mutations (Klungland et al., 1999b). Analysis of the hOGG1 promoter region has shown that expression does not vary during the cell-cycle suggesting that OGG1 is a housekeeping gene (Dhenaut et al., 2000). Interestingly, Klungland et al., (1999b), showed that mOGG1 ko mice only accumulated 8-oxoG lesions in non-proliferating tissue and observed a slow repair rate in proliferating tissues, indicating that another glycosylase/pathway might also repair this lesion. Furthermore, while the ko mice diplayed a slight increase in G:C to T:A transversion mutations over time, no increase in tumour formation was observed in the ko mice over the wild-type. The overexpression of Fpg in mammalian cells has been shown to confer

protection against ionising radiation induced mutagensis (Laval, 1994) and a range of chemotherapeutic agents (Gill et al., 1996). Similar experiments using hOGG1 showed a 3-fold reduction in 8-oxoG levels, although no variation in mutations rates was observed (Hollenbach et al., 1999).

Despite the functional equivalence of these glycosylases, both Fpg and OGG1 share very little sequence homology, with OGG1 belonging to the *E. coli* Nth family of proteins and Fpg forming its own class. In addition to the glycosylase/AP-lyase function of these enzymes, both OGG1 and Fpg have been shown to possess a deoxyribophophodeisterase (dRpase) activity, which acts on abasic sites and cleaves the 5′-sugar-phosphate from the phosphate backbone, provided the damaged strand already contains a nick 5′ to the abasic site (Figure 1.10c) (Graves et al., 1992; Sandigursky et al., 1997).

A structural analysis of the Fpg protein has shown that it contains a single zinc finger region (consensus sequence: Cys-X_2-Cys-X_{16}-Cys-X_2-Cys), which is essential for efficient binding of the glycosylase to DNA; O'Connor et al., 1993). Once Fpg has bound a lesion, excision of the oxidised base is initiated by an N-terminal proline. This residue acts as the active site nucleophile forming a covalent link at the C1′ position of the sugar. Following this, a β/δ-elimination reaction cleaves the phosphate backbone both 3′ and 5′ to the abasic site, releasing the ring-opened sugar and generating both 3′ and 5′ phosphate termini (Figure 1.10c)(Bhagwat and Gerlt, 1996; Sidorkina and Laval, 2000; Zharkov et al., 1997). In addition, two lysine residues have been identified that effect the activity of Fpg. Substitution of lysine 55 was shown to decrease the efficiency of base cleavage (Sidorkina and Laval, 1998), while lysine 155 was found to provide substrate specificity for Fpg, possibly by direct interaction with the C-8 keto group of 8-oxoG and the carbonyl group of Fapy residues (Rabow and Kow, 1997; Tchou et al., 1994).

The eukaryotic functional homolog of Fpg (OGG1) has been isolated and cloned from yeast, mice, and humans (Aburatani et al., 1997; Arai et al., 1997; Bjoras et al., 1997; Lu et al., 1997; Nash et al., 1996; Radicella et al., 1997; Rosenquist et al., 1997; van der Kemp et al., 1996). The murine OGG1 protein shares 85% identity with hOGG1 and 36% identity with yOGG1, with all three homologs sharing five highly conserved domains. These include the HhH-GPD and Zinc finger motifs that contain the catalytic site, and three domains of unknown function. Mitochondrial and nuclear localization signals are also present at the N- and C-termini of the protein, respectively (Boiteux and Radicella, 2000; Tani et al., 1998). Unlike Fpg, the catalytic site is contained internally with Lys 249 acting as the nucleophile in mammalian OGG1, corresponding to Lys 241 in yOGG1 (Girard et al., 1997; Nash et al., 1997). So far, seven splice variants of the hOGG1 enzyme have been identified with each variation occurring in the C-terminal region of the protein. Of these, two isoforms (hOGG1-1a and 1b) are located in the nucleus, while the remaining 5 isoforms (hOGG1-2a to 2e) are located in the mitochondrion. The hOGG1-1a and hOGG1-2a proteins are the predominant isoforms in each compartment (Monden et al., 1999; Nishioka et al., 1999; Takao et al., 1998).

1.8.2 The GO-system

In addition to the activities of Fpg/MutM (and OGG1) a further two conserved mechanisms have been identified that protect the genome from the mutagenic effects of 8-oxoG. These defences are expressed through products of the MutY and MutT genes in prokaryotes and their respective homologs, MYH and MTH in eukayrotes. The importance of these complementary mechanisms in the repair of 8-oxoG has been demonstrated in *E. coli* using ko strains of Fpg, MutY and MutT. Both the single and double ko strains of Fpg and MutY showed a specific increase in the number of G:C to T:A transversion mutations (Cabrera et al., 1988; Michaels et al., 1992; Nghiem et al., 1988), while the MutT ko strain showed an increase in A:T to G:C transversions (Yanofsky et al., 1966).

The mechanism by which Fpg (OGG1), MutY (MYH) and MutT (MTH) co-operate to prevent the appearance of mutations caused by 8-oxoG is illustrated in Figure 1.11. As previously discussed, Fpg prevents the accumulation of 8-oxoG by the removal of the lesion when paired opposite cytosine in duplex DNA (a) (see Section 1.8.1) (Michaels et al., 1991; Tchou et al., 1991). However, if the lesion is not repaired a subsequent round of DNA replication may lead to the formation of an 8-oxoG:dA mis-pair. If this occurs, fixation of the mutation may be prevented by MutY (an adenine-DNA glycosylase), which excises adenine from G:A mis-pairs (Au et al., 1988) and, more efficiently from 8-oxoG:A mis-pairs (Michaels et al., 1992) (b). 8-oxoG lesions are generated in DNA not only by the *in situ* oxidation of guanine residues, but also by the incorporation of oxidised GTP precursors during DNA replication. The MutT gene product is an 8-oxodGTP-triphosphatase, which hydrolyses 8-oxodGTP to 8-oxodGMP, thereby depleting the dNTP pool of this oxidised precusor, thus preventing its incorporation during replication (c) (Mo et al., 1992). Recently a fourth activity has been characterised in mammalian cells conferred by the OGG2 glycosylase. This glycosylase excises 8-oxoG lesions when mis-paired with adenine (Hazra et al., 1998). However, in order to prevent the fixation of a mutation the activities of both OGG2 and MYH must act preferentially on the nascent strand of DNA and as such are probably directed in a replication associated manner (Boldogh et al., 2001; Hazra et al., 1998).

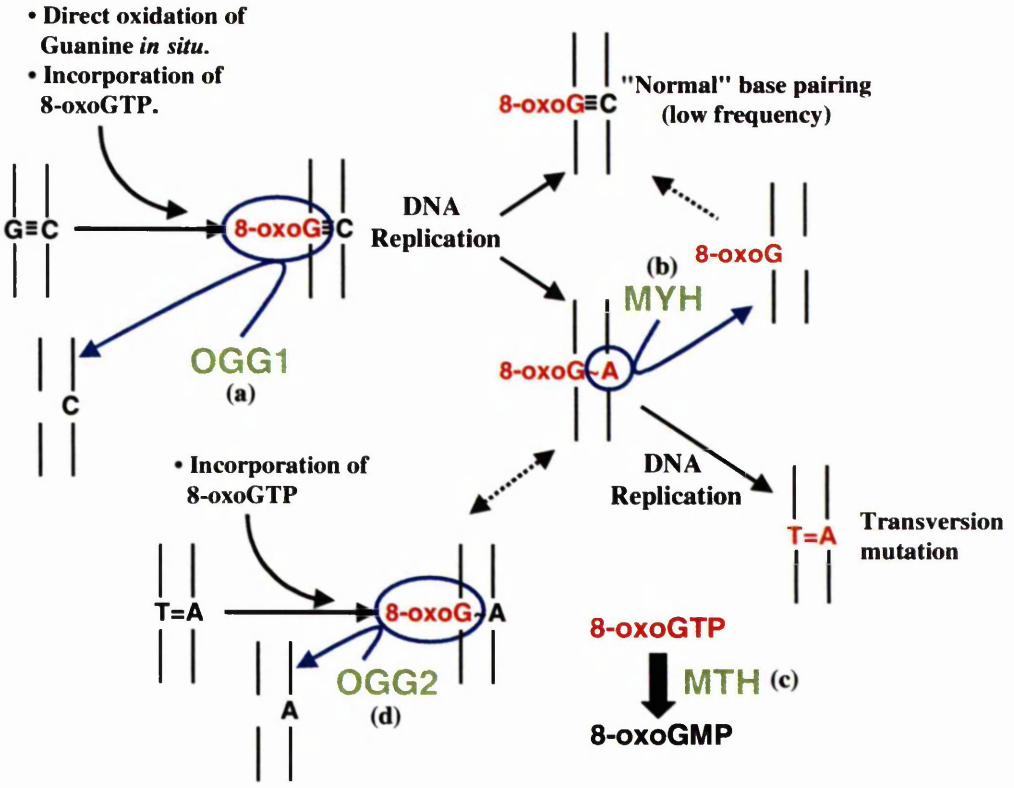

Figure 1.11. Mechanism for the removal of 8-oxoG lesions from DNA. (a) OGG1 (Fpg) preferentially removes the 8-oxoG lesion from 8-oxoG:dC base pairs, thereby preventing the incorporation of the lesion. (b) MYH (mutY) preferentially removes adenine when incorporated opposite 8-oxoG. (c) MTH (mutT) hydrolyses 8-oxoGTP to 8-oxoGMP thereby preventing the incorporation of the lesion into DNA. (d) OGG2 preferentially removes 8-oxoG lesions when paired opposite adenine.

1.8.3 Endonuclease III (NTH1)

While OGG1 provides the primary defence against oxidised purines, NTH1 confers protection from a variety of oxidised pyrimidines. These include among others, the ring saturated, fragmented or contracted thymine oxidation products, thymine glycol (Tg), 5,6-dihydrothymine (DHT), urea and cytosine oxidation products, 5-hydroxycytosine (5-OHC), 5-hydroxyuracil (5-OHU) and uracil glycol (Ug) (Figures 1.3 and 1.4). Thymine glycol, urea and DHT have all been charactised as cytotoxic lesions since they have the ability to inhibit both DNA and RNA polymerases (Evans et al., 1993). In contrast, the cytosine oxidation products, uracil glycol, 5-OHU and 5-OHC are potentially mutagenic (Feig et al., 1994; Purmal et al., 1994). While many of these lesions have been found to be substrates for other DNA glycosylases, importantly, NTH1 is the only glycosylase known to bind and remove thymine glycol.

Homologs of the endonuclease III gene have been isolated and cloned in *E. coli*, yeast, mice and humans (Aspinwall et al., 1997; Breimer and Lindahl, 1984; Eide et al., 1996; Sarker et al., 1998). These homologs share two highly conserved domains that include the HhH-GPD motif, which corresponds to the active site (including the nucleophile lysine 212 and conserved aspartic acid residues; Ikeda et al., 1998) and a $C\text{-}X_6\text{-}C\text{-}X_2\text{-}C\text{-}X_5\text{-}C$ segment containing an Fe-S centre involved in DNA binding (Sarker et al., 1998). Recently, NTH1 ko mice have been generated. However, to date, these animals have failed to show any deleterious effects from the deletion, including no increase in the levels of intracellular Tg (Dr R. Elder, personal communication).

1.8.4 Alkylpurine-DNA-N-glycosylase (APNG)

Alkylpurine-DNA-N-glycosylase (APNG) provides one defence against the cytotoxic effects of alkylating DNA damage. The substrate specificity of this enzyme includes 3-methyladenine (3-meA), 7-methylguanine (7-meG), $1,N^6$-ethenoadenine (εA) and deaminated adenine (hypoxathine, Hx) (Hang et al., 1997; Lindahl, 1976; Pandya and Moriya, 1996; Saparbaev and Laval, 1994). Though some repair activity has also been detected against 8-oxoG (Bessho et al., 1993) this activity is not thought to be biologically revelant *in vivo*. APNG deleted mice have been shown to contain an increased amount of 7-meG in the liver and a slight increase in A:T to T:A transversion mutations, generated by the 3-meA lesion. However, as with the NTH1 ko mice, these animals display a very mild phenotype, show no outward abnormalities and have a normal life span (Elder et al., 1998).

1.9 Aims of project

While the molecular function of most BER components has been studied extensively, the mechanism by which these proteins co-operate to repair DNA lesions is less well understood. Therefore, a number of studies have aimed to identify molecular interactions between BER core components using a variety of reconstitution and yeast two-hybrid experiments. These investigations have lead to the identification of numerous protein-protein interactions. For example, DNA polymerase β has been shown to interact directly with DNA ligase I (Prasad et al., 1996), XRCC1 (Dimitriadis et al., 1998; Kubota et al., 1996) and HAP1 (Bennett et al., 1997). Furthermore, the interaction of HAP1 with DNA polymerase β has been shown to stimulate the dRPase activity of DNA polymerase β (Bennett et al., 1997). In addition to DNA polymerase β, XRCC1 has been found to interact with DNA ligase III (Cappelli et al., 1997; Kubota et al., 1996) and polynucleotide kinase (PNK) (Whitehouse et al., 2001), potentially acting as a scaffold protein in BER to bring some of the post-incision components together at the site of resynthesis. XRCC1 has also been shown to interact with poly (ADP-ribose) polymerase (PARP)(Caldecott et al., 1996; Masson et al., 1998). As these studies intensify, more interactions are likely to be found and the function of these interactions clarified. However, enough information has been gathered so far, to propose a model for the mechanism of BER (described in Section 1.7.1).

The numerous protein-protein interactions observed between the BER core proteins indicates that they might act in a multiprotein complex. However, all of the proteins described above are involved in the latter stages of BER. Therefore, the main focus of this project was to assess if there was evidence for and then isolate novel protein partners for the DNA glycosylases (OGG1 and APNG), which act at the first step in the BER pathway. Unlike the core proteins, DNA glycosylases represent a diverse group of enzymes both structurally and in terms of substrate specificity. However, as they initiate the BER pathway it is likely that these enzymes recruit downstream components to complete the repair process. Furthermore, as DNA glycosylases generate abasic sites and in some cases SSBs, the potentially damaging nature of these enzymes would suggest that it is unlikely they dissociate from the site of damage until the repair process can be continued. In addition, several biochemical questions remain unanswered regarding the mechanism of BER, such as what determines the nature of the repair

synthesis pathway and the repair patch size in biological systems. These questions may potentially be answered by investigating the steps immediately downstream from the excision of the damaged base. A yeast two-hybrid analysis using the murine OGG1 and APNG DNA glycosylase cDNAs to probe a mouse testes cDNA library was undertaken to investigate these questions.

CHAPTER 2

2.0 Materials and Methods

2.1 Molecular biology

2.1.1 Enzymes

All enzymes were purchased from Promega (Southampton, UK) or New England Biolabs (NEB, Hertfordshire, UK). Enzymes were stored at –20°C and were used according to the conditions stated by the manufacturer.

2.1.2 Molecular biology kits

All molecular biology kits were obtained from Qiagen (West Sussex, UK). The kits used were; QIAfilter plasmid maxi kit, QIAprep spin miniprep kit, QIAquick gel extraction kit. All procedures were carried out as described in the appropriate protocol booklet.

2.1.3 Vectors

Listed below are the various vectors used in this project.

Vector	Description	Source
pTrcHisA pGEX4T-3	Bacterial overexpression vector	Invitrogen (Paisley, UK) Amersham Biosciences (Bucks, UK)
pGBTK7 pGADT7	Yeast two-hybrid vectors	Clontech (Hampshire, UK)
pcDNA3	Mammalian expression vector	Invitrogen
pM pVP16	Mammalian two-hybrid vectors	Clontech
pESC-leu	Yeast complementation vector	Stratagene (Amsterdam, NL)

2.1.4 Buffers and reagents

Listed below are the various reagents and buffers used in this project.

Reagent/buffer	Constituents
10x TAE buffer	0.4 M Tris-acetate, 10 mM EDTA, pH 8.5
10x TBE buffer	0.9 M Tris-borate, 20 mM EDTA, pH 8.3
Ethidium bromide	10 mg/ml stock solution in ddH_2O
Agarose gel DNA loading buffer (6x)	0.25% (w/v) Bromophenol blue, 0.25% (w/v) Xylene cyanol, 30% (v/v) glycerol, 10 mM EDTA
SDS-PAGE loading buffer	385 mg DTT, 2.5 ml of 20% SDS, 2ml of 1 M Tris-HCl pH 6.8, 3.75 ml Glycerol, 1 ml of 1.5% (w/v) Bromophenol blue
Non-denaturing loading buffer (3x)	30% (v/v) Glycerol, 0.25% (w/v) Xylene cyanol, 0.25% (w/v) Bromophenol blue
Denaturing loading buffer (3x)	90% (v/v) Formamide, 1.0 mM EDTA, 0.1% (w/v) Xylene cyanol, 0.1% (w/v) Bromophenol blue
2x Cleavage assay buffer	50 mM Tris-HCl, pH 7.6, 100 mM KCl, 10 mM EDTA, 1.0 mM DTT
Buffer I	50 mM Tris-HCl, pH 8.3, 3 mM DTT, 2 mM EDTA
Binding buffer	20 mM Tris-HCl pH 7.5, 10% (v/v) glycerol, 150 mM NaCl, 5 mM EDTA, 1 mM DTT, 0.1% (v/v) Tween 20, 0.75 µg/ml BSA, 0.5 mM PMSF, 0.8 µg/ml Leupeptin, 0.8 mg/ml Pepstatin.
His-binding buffer	20 mM $NaPO_4$, 500 mM NaCl, pH 7.8
His-wash buffer	20 mM $NaPO_4$, 500 mM NaCl, pH 6.0
Imidazole elution buffers	20 mM $NaPO_4$, 500 mM NaCl, pH 6.0 plus either 200, 350 or 500 mM Imidazole
Glutathione elution buffer	10 mM reduced Glutathione, 50 mM Tris-HCl pH 8.0.
SDS-PAGE resolving buf. (4x)	1.5 M Tris-HCl, 0.4% (w/v) SDS, pH 8.8
SDS-PAGE stacking buf. (4x)	0.5 M Tris-HCl, 0.4% (w/v) SDS, pH 6.8
SDS-PAGE running buf. (10x)	0.25 M Tris-HCl, 1.93 M Glycine, pH 8.3
Coomassie blue de-stain	50% ddH_2O, 40% (v/v) Methanol, 10% (v/v) Acetic acid.
Coomassie blue stain	50% ddH_2O, 40% (v/v) Methanol, 10% (v/v) Acetic acid, 0.25% (w/v) Coomassie brilliant blue R250

Transfer buffer	25 mM Tris-base, 190 mM Glycine, 20% (v/v) Methanol
50% PEG 3350	(Polyethylene glycol, avg .mol. wt = 3,350; (Sigma) 50% (w/v) ddH_2O
10x TE buffer	0.1 M Tris-HCl, 10mM EDTA, pH 7.5, Autoclave
10x LiAc	1.0 M Lithium acetate, pH 7.5, Autoclave
Herring testes carrier DNA (Clontech; 10 mg/ml)	Prior to use, denature the DNA by boiling in a water bath for 20 min and immediately cool on ice.
10x Phosphate buffer solution	1.0 M KH_2PO_4, 1.5 M $(NH_4)_2SO_4$, 0.75 N KOH, pH 7.0, Autoclave
1000x Mineral stock solution	2 mM $FeCl_3$, 0.8 M $MgSO_4.7H_2O$, Autoclave
100x Vitamin stock solution	0.04 mg/ml Thiamine, 2 µg/ml Biotin, 0.04 mg/ml Pyridoxine, 0.2 mg/ml Inositol, 0.04mg/ml Pantoethenoic acid. Filter sterilise (0.2 µm filter).
Zymolase solution	1.2 M Sorbitol, 100 mM Sodium phosphate pH 7.4, 2.5 mg /ml Zymolase 100-T (Bie-Berntsen, DK)

2.1.5 Oligonucleotides

Listed below are the various oligonucleotides used in this project.

Identification	Sequence 5′ to 3′	
pTrcHisA-mOGG1	5′	CGG GAT CCC GGT TAT TCC GTT CCT GGC TGC CTA GC
	3′	GGA ATT CCT CAA ATA GCT TCC TTT TTC CCT ATT G
pTrcHisA-hOGG1	5′	CGG GAT CCC GCA TCA CTG GCA TGG TGG
	3′	GGA ATT CAC TGC AGG CTG GGG AAG CCA TGG
pGBTK7-mOGG1	5′	CGG AAT TCC GGT TAT TCC GTT CCT GGC TGC CTA GC
	3′	CGG GAT CCC GCC CTC TGG CCT CTT AGA TCC
pGBTK7-mAPNG	5′	CGG AAT TCC CCC GCG GGT GGT AGT GCG CG
	3′	CGG GAT CCC GTT TTG AAC AAT TAA AAG CCC CTC
pGBTK7-mNTH1	5′	CGG AAT TCC CAG GCA TGA ACT CAG GGG TG
	3′	CGG GAT CCC GCC CTT AGA GAT CCT GGG CAG C
pGBTK7-mDnaja1	5′	CGG AAT TCC AAA TGG TGA AAG AAA CCA CTT ACT AC
	3′	CGG GAT CCC GAG GTC TGA CAC TGA ACG CCA C
pGBTK7-mDnaja3	5′	CGG AAT TCC AGA TGG CTG CGC GGT GC
	3′	CGG GAT CCC GAG GTA AAC ATT TTC TTA AGT TTG
pGBTK7-mDnaja1 N-term truncation	5′	GGA ATT CAC CAT GGA AGA ATT GAA AAA GGC ATA TAG
pESC-Leu-mDnaja1	5′	CGG GAT CCC ATC ATG GTG AAA GAA ACC ACT TAC TAC
	3′	CCG CTC GAG TTA AGA GGT CTG ACA CTG AAC GCC AC

2.2 DNA Protocols

2.2.1 PCR amplification of DNA

Polymerase chain reactions (PCRs) were performed to screen for the presence of an insert within a newly cloned construct, or for high fidelity PCR amplifications for gene cloning. Red Taq polymerase (Promega) was used to screen for newly cloned inserts whilst high fidelity PCRs were carried out using $Vent_R$ DNA polymerase (NEB). A Hybaid Onmi Gene thermal cycler was used for all PCR's. Amplification of 1-3 kb fragments was performed for: 1 cycle of 2 min at 94°C; 30 cycles of 60 s at 94°C, 60 s at 60°C, 90 s at 72°C, and 1 cycle of 5 min at 72°C. PCR products (5 µl) were assessed by agarose gel electrophoresis (Section 2.2.2).

2.2.2 Agarose gel electrophoresis

Agarose submarine gels were used to resolve DNA molecules by molecular weight. Different percentage gels were made by dissolving the appropriate amount of agarose (LE SeaKem, Flowgen, Staffordshire, UK) in 1x TAE containing 0.5 µg/ml ethidium bromide. 6x loading buffer was added to each sample prior to loading. DNA markers (ϕX174 DNA-*Hae*III, Lamba DNA-*Hin*dIII, and 1kb DNA ladder (Promega)) were routinely used to estimate the size of separated products. Electrophoresis was carried out in 1x TAE at 80-100 V for approximately 90 min. DNA bands within the gel were visualised under UV transillumination and digitally imaged using a UVP Imagestore system (Ultraviolet Products, Cambridge, UK).

2.2.3 Isolation of DNA fragments

Following agarose gel electrophoresis, DNA bands were cut from the gel with a sterile scalpel and the DNA was isolated from the agarose using a Qiagen gel extraction kit according to the manufacturer's instructions. The DNA concentration was determined using a GeneQuant II (Amersham Biosciences) capillary spectrophotometer.

2.2.4 Ligation reactions

Ligation reactions were performed using an insert : vector ratio of 3 : 1. T4-DNA ligase (Promega) was used in the reactions according to the manufacturer's instructions. Ligations were routinely performed in a 20 µl reaction volume and were incubated overnight at 15°C.

2.2.5 Plasmid purification (mini and maxi-preps)

Mini- and Maxi-prep procedures were carried out to isolate plasmid DNA from transformed bacteria. Both mini-prep and maxi-prep procedures were carried out as stated in the Qiagen kit protocols. For mini-preps; single colonies were picked, mixed in 10 ml of LB-broth containing the appropriate antibiotic (Section 2.3.2) and incubated overnight (37°C, 250 rpm). A QIAprep spin mini-prep kit was then used to yield between 5 and 10 µg of plasmid DNA.

For Maxi-preps, 1 ml of LB-broth was inoculated with a single bacterial colony and grown for 2-3 h (37°C, 250 rpm). The 1 ml starter culture was used to inoculate 200 ml of LB-broth, which was incubated overnight (37°C, 250 rpm). A QIAfilter plasmid maxi kit was then used to isolate plasmid DNA from this overnight culture. DNA concentrations were determined using the GeneQuant II (Pharmacia) capillary spectrophotometer and purity was determined by restriction enzyme digestion and agarose gel electrophoresis.

2.2.6 DNA sequencing

Plasmid DNA was sequenced using an *ABI* PRISM big-dye terminator kit (PE biosystems, Warrington, UK). For each reaction, 350 ng of plasmid DNA was added to 20 ng of sequencing primer and 4 µl big-dye terminator mix in a total volume of 20 µl. Samples were overlaid with mineral oil and amplified in a Hybaid Omni Gene thermal cycler for 1 cycle of 30 s at 94°C, 25 cycles of 30 s at 94°C, 15 s at 50°C, 4 min at 60°C. The DNA was precipitated by removing the 20 µl reaction to a fresh tube containing 50 µl of 96% ethanol and 0.1 M sodium acetate (NaOAc, pH 5.2). The tube was mixed and left to precipitate the DNA for >1 h at room temperature. Samples were centrifuged at 15,000 x *g* for 20 min, washed with 250 µl of 70% ethanol and re-spun for a further 10 min. The DNA pellet was dried and sequenced using an ABI 3100 capillary sequencer.

2.3 Bacterial work

2.3.1 Bacterial strains

Listed below are the various bacterial strains used in this project.

Bacterial Strain	Genotype	Source
HB101	F⁻, *mcr*B, *mrr*, *hsd*S20(r_B^-,m_B^-), *rec*A13, *sup*E44, *ara*14, *gal*K2, *lac*Y1 *pro*A2, *rps*L20(SM^r), *xyl*-5, *leuB6*, *mtl*1	Invitrogen
DH5α	F⁻, *phi*80 *dlac*ZΔ M15, Δ(*lac*ZYA-*arg*F), Δ*lacU169*, *deo*R, *rec*A1, *hsdR17*(r_k^-,m_k^+),*gal*⁻, *pho*A, *sup*E44, *thi*⁻1, *gyr*A96*m rel*A1	Invitrogen
TOP10	F⁻, *mcr*A Δ(*mrr-hsd*RMS-*mcrBC*) *phi80lac*ZΔM15 Δ*lac*X74 *deo*R *rec*A1 *ara*D139 Δ(*ara-leu*)*7697 gal/U gal/*K *rps*L *end*A1 *nup*G	Invitrogen
BLR	F⁻,*omp*T *hsdS*$_B$(r_B^-,m_B^-) *gal dcm*Δ(*srl-rec*A) *306::Tn10* (Tc^R) *(DE3) pLys*S (Cm^R)	Novagen

2.3.2 Bacterial culture media

Media components were obtained from Difco Laboratories (West Molesey, U.K.). Luria-Bertani broth (LB-broth) and LB-agar were used for all bacterial preparations. All broth and agar was autoclaved at 121°C / 1.05 kg/cm^2 for 30 min and stored at room temperature.

Media	Preparation
LB-broth :	10 g bacto-tryptone, 5 g bacto-yeast extract, 10 g NaCl in 1 L of ddH_2O.
LB-agar :	Same composition as L-broth with the addition of 20 g bacto-agar.
Antibiotics :	Ampicillin: 100 mg/ml stock soln in Methanol, used at 50 µg/ml. Kanamycin : 25 mg/ml stock solution in ddH_2O, used at 50 µg/ml Antibiotics (Sigma) were added to the media after autoclaving and cooling to below 55°C. Stock solutions were stored at –20°C.

2.3.3 Preparation of competent bacteria

LB-broth (10 ml) was inoculated with a single bacterial colony and grown overnight at 37°C / 250 rpm. The overnight culture was used to seed 100 ml of LB-broth to an optical density (OD_{600}) of 0.2. The culture was then incubated at 37°C with shaking until an OD_{600} of 0.6 was obtained. All subsequent centrifugations were carried out at 4°C and the resuspension steps on ice. The bacteria were collected by centrifugation at 2,700 x *g* for 20 min using a pre-cooled Sorvall centrifuge (DuPont, Hounslow, UK). The pellet was resuspended in 20 ml of ice-cold 0.1 M $CaCl_2$ and left on ice for 1 h. The suspension was then centrifuged once more and the bacterial pellet resuspended in 2 ml of 0.1 M $CaCl_2$. The cells were stored on ice and used up to 24 h after preparation.

2.3.4 Transformation of bacteria

For each transformation reaction, 100 µl aliquots of competent cells were transferred to cooled Eppendorf tubes. Plasmid DNA (~100 ng) was added to each of the reactions, mixed gently and incubated on ice for 30 min. The bacteria were heat shocked at 42°C for 90 s then transferred back to ice for 5 min. LB-broth (900 µl) was added to each reaction and the tubes were incubated at 37°C with shaking for 45 min. The cells were then centrifuged and the pellet resuspended in 100 µl of LB-broth. The bacteria were plated on LB-Agar plates containing the appropriate antibiotic selection.

2.3.5 Preparation of bacterial cell extracts

Bacterial cultures were centrifuged at 5,000 x*g* for 5 min and the pellet was resuspended in 50 µl of ice-cold buffer I (unless stated otherwise) per 1 ml of culture. The cells were sonicated in 10 s bursts until the sample was homogenous. Immediately after sonication PMSF was added to a concentration of 0.5 mM and the samples were centrifuged at 13,000 x *g* for 10 min at 4°C. The supernatant was removed to a fresh tube and the samples stored on ice.

2.3.6 Bradford assay for total protein estimation

Protein standards (40 µl; BSA in ddH_2O) ranging in concentration from 0-0.1 mg/ml (incremements of 0.01 mg) were pipetted in triplicate wells on a 96-well plate. ddH_2O (40 µl) was placed in each well along the top row as a control blank. Samples were pipetted (1:20, 1:40, and 1:80 dilutions in 40 µl) in triplicate on the same plate. BioRad/CBG reagent (200 µl) was added to each well and the resultant colour change was measured at 620 nm using a multiscan plate reader (Flow Ltd). A standard curve was produced using the protein standards and from this, the protein concentration of each sample was determined.

2.3.7 Overexpression of recombinant proteins

Single *E. coli* colonies containing a bacterial expression construct, were used to inoculate 5 ml of LB-broth containing 50 µg/ml ampicillin and the cultures were incubated overnight at 37°C with shaking (250 rpm). The overnight culture (0.5 ml) was then used to inoculate a further 200 ml of LB-amp medium and the culture was re-incubated until mid-log phase (OD_{600} = 0.6). Expression of the fusion protein was induced by the addition of 100 µl of 1 M IPTG (final concentration 1 mM) to the culture and incubating for a further 3 h, unless otherwise stated. The culture was transferred into a Sorvall tube, chilled on ice for 10 min, then centrifuged at 2,500 x *g* for 5 min. The supernatant was discarded and the pellets resuspended in 10 ml of ice cold buffer I. Bacterial extracts were prepared by sonication as described in Section 2.3.5.

2.4 Protein Protocols

2.4.1 Purification of His-mOGG1

BLR bacteria were transformed with pTrcHisA-mOGG1 and induced according to the method described in Section 2.3.7, unless otherwise stated. Sonicated bacterial cell extracts were prepared and the His-mOgg1 fusion protein was purified by Ni^{2+} chelating chromatography using ProBond resin columns (Invitrogen).

The Probond was prepared by centrifugation at 800 x *g* for 2 min to sediment the resin. The storage buffer was removed by careful aspiration and the resin was washed once with 7 ml of ddH_2O, followed by a further three washes with 7 ml of His-binding buffer, with aspiration after each step. The bacterial lysate (5 ml) was prepared following sonication (Section 2.3.5), by centrifugation at 5,000 x *g* for 10 min at 4°C, then filtration (0.8 µm filter) to remove any cellular debris which could block the column. The lysate was added to the column and mixed with the resin by gentle inversion for 10 min at 4°C. The column was clamped in a vertical position and the lower cap removed to allow unbound lysate to drain by gravity. The column was then washed three times with 5 ml of His-wash buffer. The bound fusion protein was eluted by the consecutive application of 5 ml of each of the 3 imidazole elution buffers containing increasing imidazole concentrations (200, 350, 500 mM imidazole). The samples were concentrated using a Millipore Ultra-free-15 centrifugation filter according to the manufacturer's instructions. Fractions from all the purification steps were analysed by SDS-PAGE.

2.4.2 Purification of GST-mOGG1

BLR bacteria were transformed with pGEX4T-3-mOGG1 and induced according to the method described in Section 2.3.7, unless otherwise stated. Sonicated bacterial cell extracts were prepared and the GST-mOGG1 fusion protein was purified using Glutathione Sepharose 4B beads (Amersham Biosciences).

To purify the protein, 1 ml of Glutathione Sepharose beads was placed in a 50 ml Falcon tube and washed 3 times in 10 ml of ice-cold PBS. The beads were sedimented by centrifugation at 500 x *g* for 5 min and the supernatant carefully removed. The beads were then washed in Binding buffer, centrifuged and resuspended in 5 ml of Binding buffer. Bacterial lysate (5ml), also prepared in Binding buffer was added to the beads and the lysate/GST beads were incubated at 4°C for 2 h on a rocking platform. The beads were centrifuged at 1000 x *g* at 4°C for 30 s and the supernatant carefully removed. Most of the non-specific lysate proteins were removed from the beads by washing 3 times in 5 ml of binding buffer. The bound GST-mOgg1 fusion protein was eluted using 5 ml of glutathione elution buffer. Millipore Ultra-free-15 centrifugation filters were used to concentrate the GST-mOgg1 eluate. Fractions from all the purification steps were analysed by SDS-PAGE (Section 2.4.3).

2.4.3 SDS-Polyacrylamide gel electrophoresis

SDS-PAGE was used to separate proteins by molecular weight. The BioRad mini-Protean gel apparatus was used in this protocol. Protein samples were mixed with SDS-PAGE loading buffer and heated to 95°C for 5 min, then centrifuged briefly to recollect the sample. Protein samples and prestained Kaleidoscope protein size markers (BioRad) were loaded onto a 0.75 mm thick SDS-PAGE gel with a 4.5% stacking gel (4.5% (w/v) acrylamide, 0.0125 M Tris-HCl, 0.1% (w/v) SDS, 0.2% (w/v) APS, 0.02% (v/v) TEMED, pH 6.8) lying above a 12.5% resolving gel (12.5% (w/v) acrylamide, 0.375 M Tris-HCl, 0.1% (w/v) SDS, 0.01% (w/v) APS, 0.01% (w/v) TEMED, pH 8.3). Electrophoresis was carried out at a constant 200 V for 45 min. The gel was either electroblotted onto Hybond-C super (Amersham Biosciences) for western blotting (Section 2.4.4), or stained with Coomassie brilliant blue at room temperature for 60 min. The gel was then de-stained at room temperature until the gel background had become clear and the protein bands were visible. Gel images were scanned onto a computer and stored.

2.4.4 Western blot analysis

Proteins separated by SDS-PAGE were transferred to a nitrocellulose membrane (Hybond-C super, Amersham Biosceinces) by electroblotting, using a BioRad Mini Trans-blot apparatus. Transfer was carried out at 100 V for 1 h in western transfer buffer. After blotting, the membrane was air dried and stored between two sheets of Whatman 3MM paper at 4°C until needed.

For processing, the membranes were washed with TBST (0.1% (v/v) Tween-20 in Tris 'buffered' saline pH 7.5) for 5 min, then blocked with 5% Marvel (non-fat milk powder made up in TBST) for 1 h. The primary antibody (~1:1000 dilution) was added to 0.5% Marvel and incubated with the membrane for a further hour. The membrane was then washed twice in TBST and incubated with the secondary Ab-HRP conjugate (horseradish peroxidase-conjugated secondary antibody ~1:2000 dilution; Dako) for a further 1 h. Membranes were then washed three times in TBST to remove any unbound antibodies. Bound secondary antibody was detected using BM-Chemiluminescence blotting substrate (Roche) according to the manufacturer's instructions. Blots were exposed to X-ray film (Fuji) for between 10 s and 5 min and the film was developed manually under a safe-light.

2.4.5 *In vitro* transcription/translation (IVTT) reaction

In vitro transcription/translation (IVTT) reactions were performed using the TnT coupled reticulocyte lysate system (Promega) according to the manufacturer's instructions. Positive yeast two-hybrid library clones were sub-cloned into either pcDNA3 or pGADT7 vectors which contain T7 promoter regions. IVTT reactions were set up in RNase-free 0.5 ml Eppendorf tubes.

Component	Volume
TnT rabbit reticulocyte lysate	25 µl
TnT Reaction buffer (x25)	2 µl
TnT T7 RNA polymerase	1 µl
Amino acid mixture minus Methionine	1 µl
[^{35}S]-labelled Methionine (>1,000 Ci/mmol)	2 µl
RNasin ribonuclease inhibitor (40 units/µl)	1 µl
DNA template (0.5 µg/µl)	2 µl
Nuclease free water to a final volume of	50 µl

The reaction mix was incubated at 30°C for 90 min and the products separated by SDS-PAGE (Section 2.4.3). The [^{35}S]-labelled protein was visualised within the gel using the STORM phosphorimager (Molecular Dynamics).

2.4.6 *In vitro* transcription/translation (IVTT) pull-down experiment

IVTT pull-down experiments were carried out to confirm positive yeast two-hybrid interactions. Purified GST-mOgg1 protein bound to GST beads (25 µl) was placed in a 1.5 ml Eppendorf tube for each pull-down experiment. The beads were first washed twice with binding buffer and then resuspended in 0.5 ml of the same. IVTT reactions were performed as described in Section 2.4.5 and 10 µl aliquots were added to each reaction tube. The tubes were incubated at 4°C for 2 h on a rocking platform. The beads were centrifuged at 1000 x*g* at 4°C and the supernatant carefully removed. After washing three times with 0.5 ml of binding buffer, the beads were resuspended in 50 µl of SDS-PAGE loading buffer. Samples were resolved on a 12% SDS-PAGE gel and the ^{35}S-labelled proteins imaged using a STORM phosphorimager (Molecular Dynamics).

2.4.7 OGG1 glycosylase activity assay

2.4.7.1 5' end-labelling of oligonucleotides using [γ-^{32}P]-ATP

Substrate oligonucleotides containing a single 8-oxodG base were synthesised by Invitrogen. Following quantitation using a GeneQuant II spectrophotometer oligos were 5′-[^{32}P]-end-labelled using T4-PNK (Roche) by incubating 2.5 pmoles of oligonucleotide (2.5 pmole/μl) with 40 μCi [γ-^{32}P]-ATP (6,000 Ci/mmol; Amersham Biosciences) and 0.2 μl PNK (10 units/μl) in 1x phosphorylation buffer at 37°C for 30 min. Following incubation the tube was stored on ice prior to purification of the [^{32}P]-labelled oligonucleotide. Sephadex G25 spin columns (Amersham Biosciences) were used to separate the oligonuclucleotide from un-incorporated [^{32}P]-ATP, according to the manufacturer's instructions.

Incision
↓

Oligonucleotides : 8-oxodG

5′ CCG CTA gCG GGT ACC GAG CTC GAA T 3′

3′ GGC GAT CGC CCA TGG CTC GAG CTT A 5′

g = 8-oxodG

normal

5′ CCG CTA GCG GGT ACC GAG CTC GAA T 3′

3′ GGC GAT CGC CCA TGG CTC GAG CTT A 5′

2.4.7.2 Annealing of [^{32}P]-labelled oligo to complementary oligo

The purified [^{32}P]-labelled oligonucleotide was annealed to its complement by heating the column eluate (approximately 2.5 pmol, determined using the GeneQuant II (Pharmacia) capillary spectrophotometer) with 5 pmol of complementary oligonucleotide to 95°C for 2 min in 50 mM NaCl and allowing the reaction to cool slowly to room temperature. An aliquot of the double-stranded [^{32}P]-labelled product (oligonucleotide substrate) was added to non-denaturing loading buffer and analysed on a 20% non-denaturing polyacrylamide gel (5 ml of 40% (v/v) BioRad acrylamide (19:1 acrylamide:bis-acrylamide solution), 1 ml 10x TBE, 4 ml ddH_2O), while a further aliquot was analysed by scintillation counting.

2.4.7.3 Oligonucleotide cleavage assay

The following reaction was set up in an Eppendorf tube on ice:

x µl [^{32}P]-labelled double-stranded 8-oxodG oligo (~150,000 cpm)

y µl cell free extract (10 µg/ml)

z µl 2x Cleavage assay buffer (up to 20 µl)

The reaction was mixed by vortexing, centrifuged briefly, then incubated at 37°C unless stated otherwise. Denaturing loading buffer (10 µl) was added at the required time point to stop the reaction. Samples were heated to 90°C for 5 min and then cooled on ice prior to analysis by PAGE.

A 20% polyacrylamide denaturing gel (5 ml of 40% (v/v) BioRad acrylamide (19:1 acrylamide:bis-acrylamide solution), 4.2 g urea; 0.5 ml 10x TBE made up to 10 ml with ddH_2O) was used to resolve the oligonucleotide cleavage fragments. Just prior to pouring, 75 µl of 10% APS was added to the tube and mixed followed by 7.5 µl of TEMED to initiate the polymerisation reaction. The gels were run in 0.5x TBE buffer at 200 V. The [^{32}P]-labelled oligonucleotide substrate and cleavage products were visualised within the gel using the STORM phosphorimager (Molecular Dynamics).

2.5 RNA protocols

2.5.1 RNA extraction and purification

The Qiagen RNeasy Midi Kit (Qiagen Ltd., West Sussex, UK) was used for RNA extraction from tissues. Frozen tissue (in liquid nitrogen) was ground to a fine powder using a stainless steel pestle and mortar, taking extreme care to avoid even partial thawing. Lysis buffer was added and the lysates homogenised by passing 5-10 times through a 21G needle and syringe. Ethanol was then added to the lysate, creating conditions that promote selective binding of RNA to the RNeasy membrane. Contaminants were efficiently washed away using the supplied buffers. RNA was eluted in RNase-free water. Qiagen RNeasy procedure selectively excludes most RNA molecules that are <200 nucleotides long (such as 5.8S rRNA, 5S rRNA, and tRNAs).

2.5.2 DNase treatment of total RNA

DNase treatment of the total RNA was performed as described in the Atlas™ Pure total RNA Labelling System user manual (PT3231-1, Clontech). Briefly, RNA was treated with DNase (0.1 unit/ug RNA) at 37°C for 30min, followed by the addition of 0.1 volumes of 10x termination mix (provided). This was followed by phenol and chloroform extraction. The RNA was then precipitated by the addition of 0.1 volumes of 2 M sodium acetate and 2.5 volumes of 95% (v/v) ethanol with glycogen (20µg) added as a carrier (Invitrogen). After air-drying the pellet was dissolved in RNase-free water.

2.5.3 Reverse-transcription PCR

The following reaction was set up in a 0.5 ml nuclease free Eppendorf tube:

Component	Amount (µl)
Oligo (dT) primers, (0.5 µg/µl)	1 µl
Random hexamer primers, (0.5 µg/µl)	1 µl
RNA sample, (1 µg/µl)	2 µl
Nuclease free water	9 µl

The mix was incubated at 65°C for 5 min to denature the secondary structure of the RNA and then cooled to room temperature for 2 min. After a short centrifugation, the following components were added in the order listed:

Component	Amount (µl)
$MgCl_2$, 25 mM	2 µl
Reverse transcription buffer (10x)	2 µl
dNTP mixture, 10 mM	2 µl
RNasin, ribonuclease inhibitor (40 u/µl)	1 µl
AMV reverse transcriptase (100 u/µl)	0.2 µl

The reaction was then mixed and incubated at 42°C for 1 h in a heating block. After incubation the AMV reverse transcriptase was heat inactivated at 95°C for 2 min, before the placing the tube on ice. The first strand synthesis could be stored at –20°C for longer periods of time. For PCR using specific primers, 2 µg of the first strand synthesis was used for each reaction (PCR conditions are described in Section 2.2.1).

2.6 Yeast work

2.6.1 Yeast strains

Listed below are the various yeast strains used in this project.

Yeast strain	Genotype	Source
Y190	*MATa, ura3-52, his3-200, ade2-101, lys2-801, trp1-901, leu2-3, 112, gal4Δ, gal80Δ, cyh^{r}2, LYS2 ::GAL1$_{UAS}$-HIS3$_{TATA}$-HIS3, URA3::GAL1$_{UAS}$-GAL1$_{TATA}$-LacZ,*	Clontech
W303	*MATa, leu2-3, 112 trp1-1, can 1-100, ura3-1, ade2-1, his3-11,15, phi+*	E. Schwarz
MDJ1 ko	*MATa, leu2-3, 112 trp1-1, can 1-100, ura3-1, ade2-1, his3-11,15, URA::mdj1, phi+*	E. Schwarz

2.6.2 Yeast culture media

YPD and SD minimal media components were obtained from Clontech. Media was autoclaved at 121°C / 1.05 kg/cm^2 for 30 min, then stored at room temperature. Synthetic dropout (SD) minimal media was supplemented with 10x dropout supplements to make the appropriate selective media.

Media/Reagent	Preparation	
YPD media	50 g YPD complete mix to 1 L of ddH_2O, pH 6.0.	
YPD agar	Same as YPD media with the addition of 20 g bacto-agar	
SD minimal media	26.7 g of SD minimal media mix + 1x SD Supplement in 1 L of ddH_2O, pH 5.8	
SD minimal agar	Same as SD minimal media with the addition of 20 g of bacto-agar	
10x SD supplements	SD -Trp	0.74 g in 1 L
	SD -Leu/-Trp	0.64 g in 1 L
	SD -Leu/-Trp/-His	0.62 g in 1 L

SD-Leu-Trp + X-Gal agar plates were made according to the method in "Methods in Yeast Genetics", 1994 Edition, Cold Spring Harbor Laboratory press, pp 211-213. (X-Gal = 5-bromo-4-chloro-3-indolyl-β-D-galactosidase).

Media/Reagent	Preparation	
Solution I : Mix in a 1 L flask	10x Phosphate buffer solution	100 ml
	1000x Mineral stock solution	1 ml
	SD-Leu-Trp 10x Dropout supplement	0.64 g
	Adjust the volume to 450 ml with ddH_2O.	
Solution II : Mix in a 2 L flask	Bacto-agar (Difco)	20 g
	ddH_2O	500 ml
Autoclave the solutions separately. After cooling to below 65°C, add the following to Solution I		
	Glucose 40% (v/v) (sterile)	40 ml
	X-Gal (20 mg/ml dissolved in dimethylformamide)	2 ml
	Mix Solution I and Solution II together and pour plates.	

2.6.3 Small-scale yeast transformation procedure

All the solutions were freshly prepared from 10x stock solutions. YPD or SD minimal media (50 ml) was inoculated with several colonies of yeast (2-3mm diameter) and incubated overnight at 30°C with shaking (250 rpm) to stationary phase (OD_{600} >1). Enough culture was transferred to 300 ml of media to obtain an OD_{600} of 0.2-0.3. The culture was then re-incubated at 30°C with shaking (250 rpm) until mid-log phase (OD_{600} 0.6). The yeast were then transferred to 50 ml Flacon tubes and centrifuged at 1,000 x *g* for 5 min at room temperature, the supernatant discarded and the cells washed with 30 ml of 1x TE. After centrifugation the cells were resuspended in 2 ml of freshly prepared sterile 1x TE/1x LiAc. Concurrently, 0.1 µg of plasmid DNA and 0.1 mg of herring testes carrier DNA were mixed in a fresh 1.5 ml Eppendorf tube. 0.1 ml of competent yeast cells were added to the mixture and mixed thoroughly before the addition of 0.6 ml of sterile 40% PEG/1x LiAc. The tubes were mixed vigorously and incubated at 30°C for 30 min with shaking (250 rpm) after which 70 µl of DMSO was added and the solution mixed thoroughly by inversion. The cells were heat shocked for 15 min at 42°C in a water bath and then chilled on ice for 5 min. Finally, the cells were centrifuged for 5 s at 5,000 x *g* at room temperature, the supernatant removed and the pellet resuspended in 0.5 ml of 1x TE buffer. Cells were plated on selective SD minimal media using the following dilutions; undiluted, 1:10, 1:100 and 1:1000.

2.6.4 Yeast two-hybrid experiment

A MATCHMAKER yeast two-hybrid system 3 kit (Clontech) was used to identify proteins that physically interact with the BER DNA glycosylase mOGG1. The pGBTK7 yeast expression vector contains the yeast GAL4 DNA binding domain motif and a Tryptophan (Trp) nutritional selection marker. The pGADT7 vector contains the GAL4 activating domain and a Leucine (Leu) nutritional selection marker.

2.6.4.1 Library screens

A pre-transformed MATCHMAKER mouse testes cDNA library inserted into pACT2 (pGADT7 sister vector) was purchased from Clontech. The library was amplified three times to ensure that 1 x 10^6 independent clones would be screened per yeast two-hybrid experiment (see Section 3.3). Y190 yeast carrying the pGBTK7-mOGG1 construct were transformed with 500 µg of amplified library plasmid DNA and plated onto SD -Leu-Trp-His + 25 mM 3-AT agar plates as described below.

All the solutions were freshly prepared from 10x stock solutions. SD-Trp media (150 ml) was inoculated with several colonies of Y190 yeast transfected with pGBTK7-mOGG1 and incubated overnight at 30°C with shaking (250 rpm) to stationary phase (OD_{600} >1). Enough culture was transferred to 1 L of media to obtain an OD_{600} of 0.2-0.3. The culture was then re-incubated at 30°C with shaking (250 rpm) until mid-log phase (OD_{600} 0.6). The yeast were then transferred to sterile Sorvall 300 ml bottles and centrifuged at 1,000 x *g* for 5 min at room temperature, the supernatant discarded and the cells washed with 200 ml of 1x TE. After centrifugation the cells were resuspended in 8 ml of freshly prepared sterile 1x TE/1x LiAc and split between two 50 ml Falcon tubes. Library plasmid DNA (250 µg) and 10 mg of herring testes carrier DNA was added to each tube and mixed. A further 30 ml of sterile 40% PEG/1x LiAc solution was added to each tube and mixed vigorously. The tubes were incubated at 30°C for 30 min with shaking (250 rpm). DMSO (7 ml) was then added and mixed thoroughly by inversion. The cells were heat shocked for 15 min at 42°C in a water bath and then chilled on ice for 5 min. Finally the cells were centrifuged for 5 s at 5,000 x*g* at room temperature, the supernatant removed and the pellet resuspended in 10 ml of 1x TE buffer. Cells were plated on selective SD-Leu-Trp-His + 25 mM 3-AT agar plates (20 cm diameter) at 200 µl per plate. The plates were incubated at 30°C for 14 days.

After incubation, colonies greater than 1 mm in diameter were picked carefully using a sterile toothpick and streaked on to SD-Leu-Trp + X-gal plates. These plates were incubated at 30°C for a further 10 days. Blue colonies were re-streaked onto SD-Leu-Trp-His + 25 mM 3-AT and SD-Leu-Trp + X-gal agar plates to confirm reporter expression.

2.6.4.2 Identification of library inserts

PCR amplification and DNA sequencing were used to identify the cDNA inserts producing positive two-hybrid colonies. SD-Trp-Leu media (5 ml) was inoculated with a single blue colony and incubated overnight at 30°C (250 rpm). The culture was centrifuged at 1,000 x *g* for 5 min and the supernatant completely removed. Using a 200 µl pipette tip, a dab of the yeast was taken from the pellet and resuspended in 5 µl of Zymolase solution in a 0.5 ml Eppendorf tube. The tube was incubated at 37°C for 5 min and then cooled at room temperature. PCR reactions were prepared (50 µl) using Perkin-Elmer Taq polymerase and 1 µl of the yeast/zymolase solution. Amplification of fragments fragments was performed using the following conditions: 1 cycle of 2 min at 94°C, 50 cycles of 30 s at 94°C, 3 min at 68°C and 1 cycle of 5 min at 68°C. PCR products (5 µl) were assessed by agarose gel electrophoresis (Section 2.2.2) and were sequenced as described in Section 2.2.6.

2.6.5 Yeast mutation analysis

Mutation analysis was performed by assessing the number of Tryptophan (Trp) revertants in the *S. cerevisiae* yeast strains; W303 wild-type (wt) and W303 MDJ1::URA3 knockout (mdj1). Two mutational analysis experiments were performed as described below.

2.6.5.1 Mutation analysis using SD-Trp liquid medium

This procedure was carried out for each *S. cerevisiae* strain in parallel. Fresh 1-2 mm colonies were grown on YPD agar plates at 20°C. YPD media (10 ml) was inoculated with a single colony and incubated overnight at 20°C (250 rpm). The culture was diluted in 50 ml of YPD to produce an OD_{600} of 0.3 and re-incubated at 20°C until an OD_{600} of 0.6 was obtained. The cells were transferred to a 50 ml Falcon tube and centrifuged at 1,000 x *g* for 5 min, washed in 20 ml of SD-Trp media to remove any residual YPD and resuspended in 5 ml of SD-Trp media. Yeast cells were counted on a haemocytometer and diluted to 4 x 10^5 cells/ml in 240 ml SD-Trp media. Aliquots of the culture (1 ml) were pipetted into each well of 10 x 24 well plates. The plates were sealed with tape and left undisturbed on the bench for 14 days for Trp revertant colonies to grow. After incubation the number of cells in 3 representative wells were re-counted on a haemocytometer and wells containing Trp revertant colonies were scored. These values were used to calculate the number of mutations/cell/generation for each strain.

2.6.5.2 Mutation analysis using SD-Trp agar medium

The propagation and incubation of each *S. cerevisiae* strain was carried out as in the first mutational analysis experiment. However, once cells had reached an OD_{600} of 0.6, they were pelleted and resuspended in 5 ml of SD-Trp media. The yeast cells were counted on a haemocytometer and diluted to a concentration of 1 x 10^8 cells/ml. Serial x10 dilutions of this culture were made to 1 x 10^3 cells/ml and 1 ml of each of the dilutions was placed in a 1.5 ml Eppendorf tube. Following centrifugation at 1,000 x *g* for 5 min, the pellet resuspended in 100 µl of SD-Trp media and the cells plated on SD-Trp agar plates. Further dilutions were made to allow the plating of 500 and 50 cells onto YPD agar plates to assess cell survival.

2.6.5.3 Mutation analysis after treatment with chemical agents

Hydrogen peroxide (H_2O_2) treatment (0-20 mM): Once an OD_{600} of 0.6 had been reached, the cells were split equally between five 50 ml Falcon tubes. The yeast were treated with H_2O_2 concentrations from 0 to 20 mM (0, 0.125, 2.5, 5, 10, 20 mM in 30 ml of SD-Trp media) for 1 h at 20°C on a rocking platform. After incubation each tube was centrifuged at 1,000 x *g* for 5 min and the pellet resuspended in 2 ml of SD-Trp. The cells were counted on a haemocytometer and appropriate dilutions were made depending on the mutational analysis experiment to be used. Treatment of cells with TEMPO (0-20 mM; Sigma) was carried out using the same procedure.

2.7 Cell culture work

2.7.1 Tissue culture cell lines

Listed below are the various mammalian cells lines used in this project.

Cell line	Description	Source
NIH 3T3	*Mus musculus* (mouse) primary embryonic fibroblasts	ATCC (Virginia, USA)
HeLa	*Homo sapiens* (human) adenocarcinoma; cervix; epithelial	ATCC (Virginia ,USA)

2.7.2 Maintenance and subculture of cell lines

Cells were maintained as adherent monolayer cultures in RPMI-1640 (Invitrogen). Culture medium was supplemented with 10 % foetal calf serum (FCS; Biological industries), and 1 mM L-glutamine (Invitrogen; complete medium). Cells were grown to confluence at 37°C in humidified air containing 5% CO_2.

Cells were routinely passaged (subcultured) weekly by removing the culture medium and washing the monolayer with 10 ml of PBS. To harvest the cells, 2 ml of 0.05% trypsin/EDTA (Sigma) was added to the culture flask and incubated at 37°C until the cells detached. Complete medium (10 ml) was carefully added to neutralise the trypsin and to wash the cells from the base of the flask. Cells were then pelleted by centrifugation (1000 x *g* for 5 min). The supernatant was removed and the pellet was resuspended in complete medium. Cells were counted using a haemocytometer before 2 x 10^5 cells were used to re-seed 10 ml of medium in a new T-75 flask. The cells were incubated as described above. All cell manipulations were carried out in a class II microbiological safety cabinet.

2.7.3 Mammalian two-hybrid experiment

The mammalian two-hybrid system (Clontech) was used to confirm positive yeast two-hybrid interactions *in vivo*. A T-75 flask of either NIH 3T3 or HeLa cells was grown to confluence. The cells were harvested and counted using a haemocytometer. Duplicate 6-well plates were seeded with 1.5 x 10^5 cells per well and were incubated overnight at 37°C. The following reactions were set up under sterile conditions in 1.5 ml Eppendorf tubes.

Reagent	Description	Amount
SFM	RPMI Serum free media	100 µl
pM-x	Binding domain construct	0.6 µg
pVP16-x	Activating domain construct	0.6 µg
pFR- luc	Luciferase reporter construct	0.6 µg
pRL-TK	Renilla reporter internal control	0.2 µg
Superfect	Qiagen transfection reagent	10 µl

After incubation for 10 min at room temperature, a further 0.6 ml of complete medium was added to each tube. The cells were washed twice with PBS (5 ml) and the transfection reagent mix was added. The plates were then incubated at 37°C for 3 h. After incubation the cells were washed twice in PBS (5 ml), fresh media was added and the cells were re-incubated for 24 h. Luciferase reporter activity was measured using the Dual luciferase reporter assay system (Promega) to assess positive two-hybrid interactions. The data was corrected for transfection efficiencies using the Renilla internal control reporter gene.

CHAPTER 3

3.0 Results: Yeast two-hybrid screens

3.1 Introduction

In order to study protein-protein interactions that may affect DNA glycosylase function, yeast two-hybrid analyses were carried out using mOGG1 and mAPNG DNA glycosylase cDNAs to probe a mouse testes cDNA library. A yeast two-hybrid MATCHMAKER system III kit (Clontech) was used to carry out these screens.

3.2 The principle of the yeast two-hybrid system

The principle of the yeast two-hybrid system relies on the separation of the two functionally independent domains of the *S. cerevisiae* GAL4 transcription factor. These domains consist of the DNA-binding domain (BD) that binds to a GAL4-specific upstream activation sequence (UAS) and the activating domain (AD), which interacts with the promoter region and directs RNA polymerase II to transcribe the gene downstream of the UAS. When the BD and AD (amino acids 1-147 and 768-881, respectively) are separated by recombinant technology they cannot activate transcription independently. However, transcription can be initiated if both domains are brought into close physical proximity in the promoter region.

Two constructs are used to generate a fusion between each of the GAL4 domains and two proteins that potentially interact with each other. The fusion proteins are then co-expressed in a yeast reporter strain. Any interactions between the 'bait' protein (fused to the BD) and a test protein (fused to the AD) create a novel transcription factor, with binding affinity for a GAL4-UAS. This factor can then direct transcription of the downstream reporter genes, allowing the detection of yeast colonies that express interacting proteins. For this project, two reporter genes (HIS3 and LacZ) were used to increase the ability to detect false-positive interactions. The HIS3 reporter provided a nutritional marker to allow selective growth, while the LacZ reporter allowed the analysis of β-galactosidase activity. An overview of the yeast two-hybrid principle is illustrated in Figure 3.1.

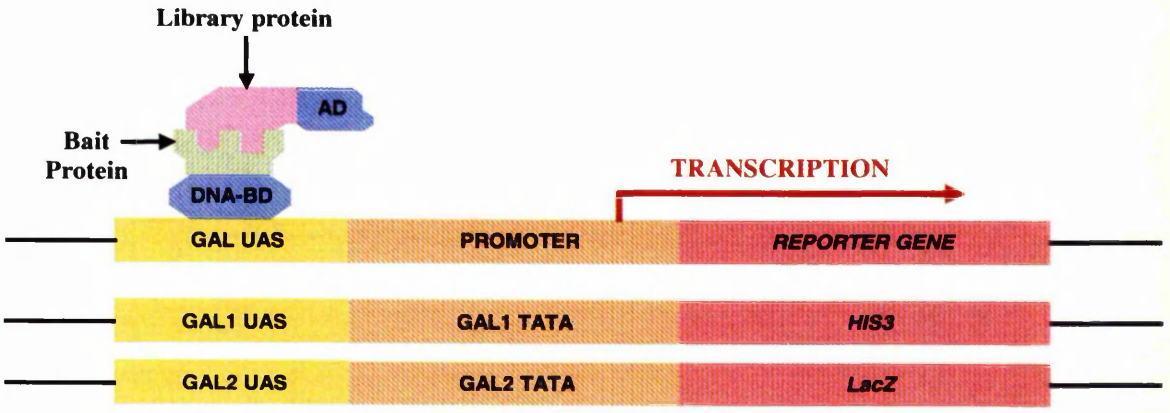

Figure 3.1. Yeast two-hybrid principle. Two constructs are generated that express either the 'bait' protein fused to the BD and a library-encoded protein fused to the AD of the yeast GAL4 protein. When expressed, the BD-fusion protein binds to the GAL UAS of the reporter genes. If the 'bait' protein and library protein physically interact, the AD domain is brought into close proximity of the promoter and transcription of the reporter gene is initiated. In the system used, there are two reporter gene constructs, encoding *HIS3* and *LacZ* that are integrated into the yeast genome.

In this project the yeast two-hybrid system was used both to screen a cDNA library for the expression of any proteins that interact with the glycosylases (mOGG1 or mAPNG), and more specifically, to test several proteins involved in DNA repair for any interaction with the glycosylases. In each case, both the BD and AD constructs were co-transformed into the yeast reporter strain (Y190) and plated onto SD media without Leu, Trp or His amino acid supplements (SD-Leu-Trp-His). Once transformed, selection of the plasmids was maintained by tryptophan (TRP1) and leucine (LEU2) nutritional markers contained within the BD and AD constructs, respectively (Figures 3.4 and 3.3, respectively). In addition, the nutritional requirement for His production allowed the selective growth of colonies containing two-hybrid interactions by the expression of the HIS3 reporter gene.

After incubation at 30°C for 14 days colonies >1 mm in diameter were picked and restreaked onto SD-Leu-Trp + X-gal agar plates, a medium that maintained the plasmid selection and also allowed the visual identification of two-hybrid interactions. Following hydrolysis of X-gal by β-galactosidase, the product of the LacZ reporter gene, a blue coloured product is formed, turning colonies blue. For the library screenings, colonies that turned blue after 10 days incubation at 30°C were isolated and the cDNA library inserts were amplified by PCR, sequenced and identified using BLAST (http://www.ncbi.nlm.nih.gov/BLAST/). An overview of the two-hybrid experimental procedure is illustrated in Figure 3.2, while a detailed account is given in Section 2.6.4.

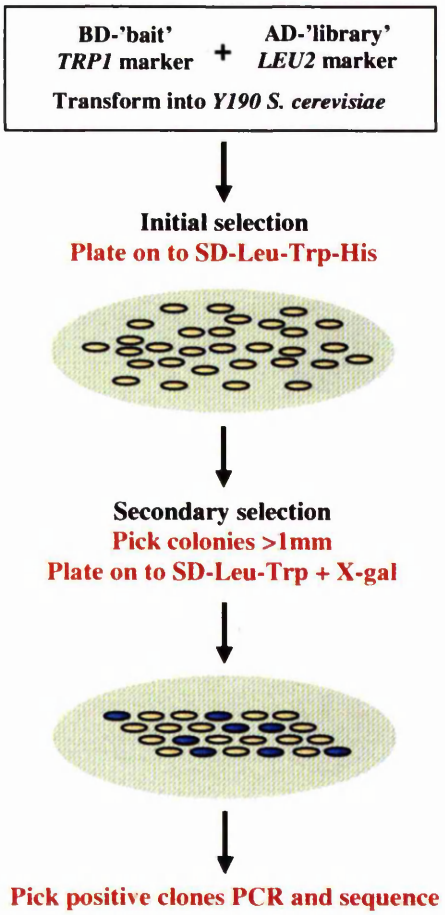

Figure 3.2. Yeast two-hybrid experimental method.

3.3 Amplification of the mouse testes cDNA library

As most base excision repair enzymes are highly expressed in the testes, it was decided to use a mouse testes cDNA library (Clontech) for the two-hybrid screens. The library contained 1 x 10^6 independent clones, which were both pre-cloned into pACT2 (yeast two-hybrid AD-fusion construct; Figure 3.3) and pre-transformed into *E. coli*. In order to ensure that every clone would be screened in the two-hybrid experiment, the library was amplified three times. Ideally this would have been carried out in liquid medium, however the library constructs that contain larger inserts are unstable and are quickly lost under these conditions leading to the generation of a biased library. Therefore, the amplification procedure was carried out on solid media.

Assuming that a single plasmid is contained within each bacterial cell, when plated, every individual colony formed on the agar plate (colony forming unit: cfu) will represent one library clone. Therefore, in order to amplify the library 3 times, it was first necessary to calculate the titer of the pre-transformed library. This was done by plating out known dilutions of the library onto LB-amp agar plates and counting the number of colony forming units (cfu) formed after incubation at 37°C for 24 h. Using this method the library titer was estimated to be 6 x 10^8 cfu/ml. The amount of library culture needed to amplify the library three times was calculated by dividing the number of clones to be screened by the library titer:

$$\frac{\text{no. clones to be screened}}{\text{library titer}} = \frac{3 \times 10^6 \text{ cfu}}{6 \times 10^8 \text{ cfu/ml}} = 5 \text{ µl of library culture needed.}$$

Finally, the number of LB-amp agar plates (25 cm x 25 cm square plates) needed to plate the library was calculated by dividing the number of colonies to be plated by the plating capacity of each plate:

$$\frac{3 \times 10^6 \text{ colonies}}{60{,}000 \text{ cfu/plate}} = 50 \text{ plates needed.}$$

After incubation at 37°C for 24 h the bacterial colonies were scraped off the plates, made into 10 % glycerol stocks and frozen at –80°C. The plasmid DNA was extracted using a Qiagen maxi-prep kit, ethanol precipitated and stored at 4°C until use.

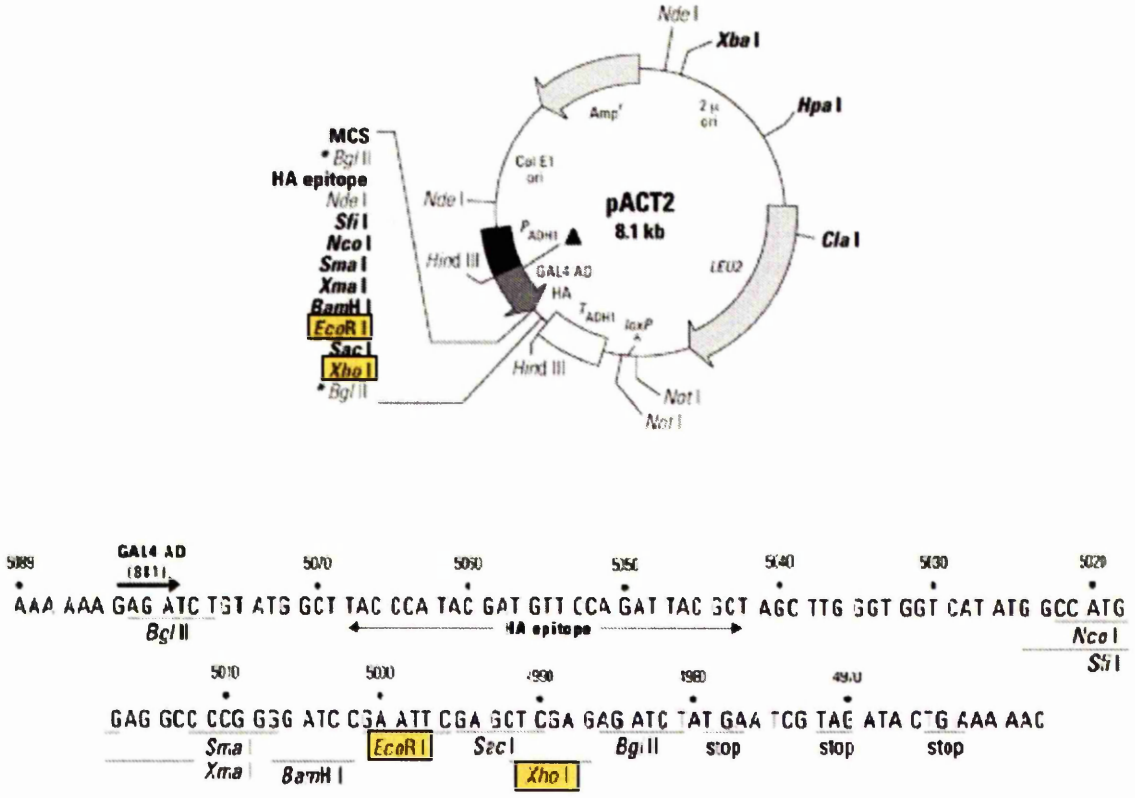

Figure 3.3. pACT2 vector map and multiple cloning site (MCS). pACT2 was used to generate the mouse testes cDNA library in fusion with the GAL4 AD (amino acids 768-881). The library cDNA was cloned into the MCS site of pACT2 using *Eco*RI/*Xho*I restriction sites (yellow). The fusion proteins are expressed from the ADH1 promoter. This vector also contains an Amp^R marker for selection in *E. coli* and a LEU2 marker for selection in yeast.

3.4 Production of the yeast two-hybrid constructs

The mOGG1 cDNA (IMAGE clone: 0416941) was amplified by high fidelity PCR and cloned into the multiple cloning site (MCS) of pGBTK7 using *Eco*RI/*Bam*HI restriction sites. Both the *Eco*RI and *Bam*HI restriction sites were engineered into the design of the 5′ and 3′ PCR primers respectively (see Section 2.1.5). Correct fusion between the GAL4 binding domain and mOGG1 ORFs was confirmed by DNA sequencing as was the fidelity of the sequence. The remaining yeast two-hybrid constructs used in this project (pGADT7-mOGG1, pGBTK7-mAPNG and pGADT7-mAPNG) were produced using the same procedues. The BD and AD yeast expression vectors are shown in Figures 3.4 and 3.5 respectively.

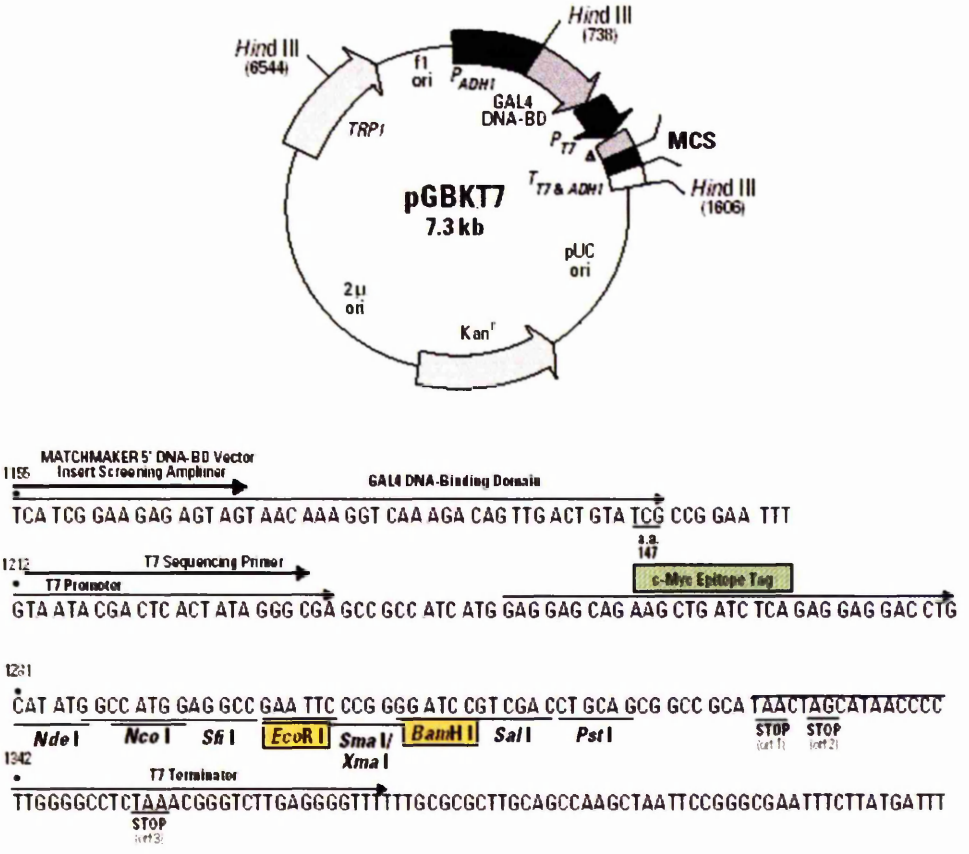

Figure 3.4. pGBTK7 vector map and MCS. pGBTK7 was used to generate the amino-terminal fusion proteins of the two DNA glycosylases (mOGG1 and mAPNG) and the GAL4 BD (amino acids 1-147). The cDNA inserts were cloned into the MCS site of pGBTK7 using *Eco*RI/*Bam*HI restriction sites (yellow). The fusion proteins are expressed from the ADH1 promoter. This vector also contains an Amp^R marker for selection in *E. coli* and a TRP1 marker for selection in yeast. The green box indicates the position of the c-myc epitope tag used for the detection of expressed proteins by c-myc specific antibodies.

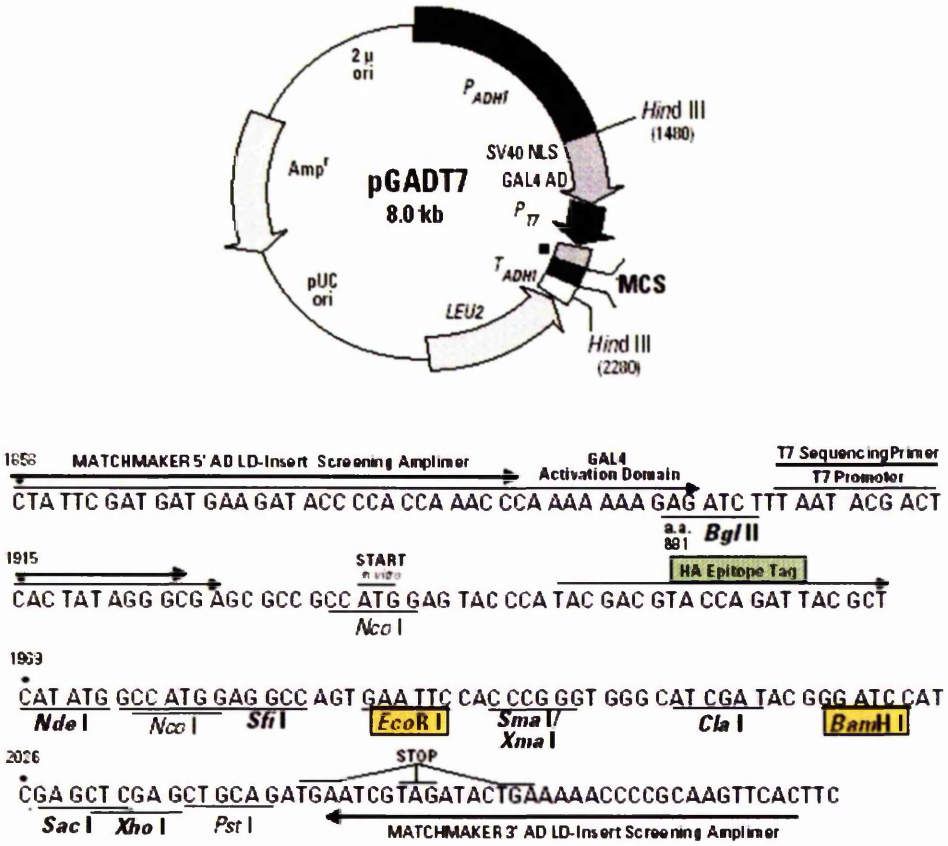

Figure 3.5. pGADT7 vector map and MCS. pGADT7 was used to generate the fusion proteins of the two DNA glycosylases (mOGG1 and mAPNG) and the GAL4 AD (amino acids 786-881). The cDNA inserts were cloned into the MCS site of pGADT7 using *Eco*RI/*Bam*HI restriction sites (yellow). The fusion proteins are expressed from the ADH1 promoter. This vector also contains an Amp^R marker for selection in *E. coli* and a LEU2 marker for selection in yeast. The green box indicates the position of the Hemagglutinin (HA) epitope tag used for the detection of expressed proteins by c-HA specific antibodies.

To test that the BD-'bait' fusion proteins were being expressed, each of the BD-constructs (including pGBTK7-p53, provided as positive controls in the MATCHMAKER kit) was transformed into Y190 *S. cerevisiae* and plated onto SD-Trp media. Expression of the BD-fusion proteins was confirmed by western blot analysis of yeast cell extracts, using an anti-myc antibody (Invitrogen; Figure 3.6). The estimated molecular weights of recombinant BD-p53, BD-mOGG1 and BD-mAPNG are 69.2 kDa, 55 kDa and 51.6 kDa, respectively (p53, 53 kDa; mOGG1, 38.8 kDa; mAPNG, 35.4 kDa; BD, 16.2 kDa). Each of the bands shown in Figure 3.6 corresponded to the predicted molecular weight confirming that each protein was being expressed as a BD-fusion protein. The multiple banding seen in lane 1 represents degradation of the BD-p53 protein and indeed, similar bands had been observed for all of the expressed proteins in previous experiments. Subsequently however, the addition of higher concentrations of protease inhibitors, when preparing the yeast extracts, reduced the observed protein degradation. Expression of the AD-fusion proteins was not tested at this time because of the lack of availability of anti-HA (hemagglutinin) antibodies.

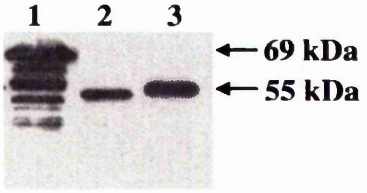

Figure 3.6. Western blot analysis of extracts from Y190 *S. cerevisiae* transformed with the two-hybrid expression constructs. Lane 1, pGBTK7-p53; lane 2, pGBTK7-mAPNG; lane 3, pGBTK7-mOGG1. The molecular weight of each protein was estimated by comparison to the nitrocellulose membrane labelled with broad-range Kaleidoscope rainbow markers (BioRad).

3.5 Viability of the yeast containing the two-hybrid constructs

Before proceeding with the two-hybrid experiments, several control experiments were performed to determine whether the glycosylases were suitable bait proteins for use in the two-hybrid system. These experiments were designed to ensure that expression of the fusion proteins did not produce false-positive two-hybrid results and was not detrimental to the growth of the yeast.

Initially, each construct was tested to verify that the GAL4 BD and AD did not activate the *LacZ* reporter gene in the presence of mOGG1 or mAPNG alone. This was carried out by performing the various control transformations shown in Table 3.1. Each transformation was plated onto SD-Leu-Trp + X-gal media and incubated at 30°C for 5 days. The results of the various mOGG1/mAPNG co-transformations are shown in Figure 3.7. The initial observation from these plates was the clear nutritional requirement of the yeast for both of the construct nutritional markers (Leu and Trp). They also showed that none of the co-transformations initiated expression of the *LacZ* reporter gene, except for the positive control transformation between pGBTK7-p53 and pGADT7-T. Furthermore, these experiments also showed that neither DNA glycosylase formed homozygous interactions in this environment.

Construct 1 Binding domain	Construct 2 Activating domain	SD selection medium	LacZ phenotype
pGBTK7	-	SD-Leu-Trp + X-gal	no growth
-	pGADT7	SD-Leu-Trp + X-gal	no growth
pGBTK7	pGADT7	SD-Leu-Trp + X-gal	white
pGBTK7-mOGG1[a]	pGADT7	SD-Leu-Trp + X-gal	white
pGBTK7	pGADT7-mOGG1[a]	SD-Leu-Trp + X-gal	white
pGBTK7-mOGG1[a]	pGADT7-mOGG1[a]	SD-Leu-Trp + X-gal	white
pGBTK7-p53	pGADT7-T	SD-Leu-Trp + X-gal	(+ve con) blue

Table 3.1. Table showing the control transformations used to confirm that the GAL4 BD and AD did not auto-activate the LacZ reporter gene in the presence of mOGG1 or mAPNG. This experiment was carried out with both the DNA glycosylases; Key: [a], indicates substitution of the mOGG1 construct with the respective mAPNG construct as appropriate.

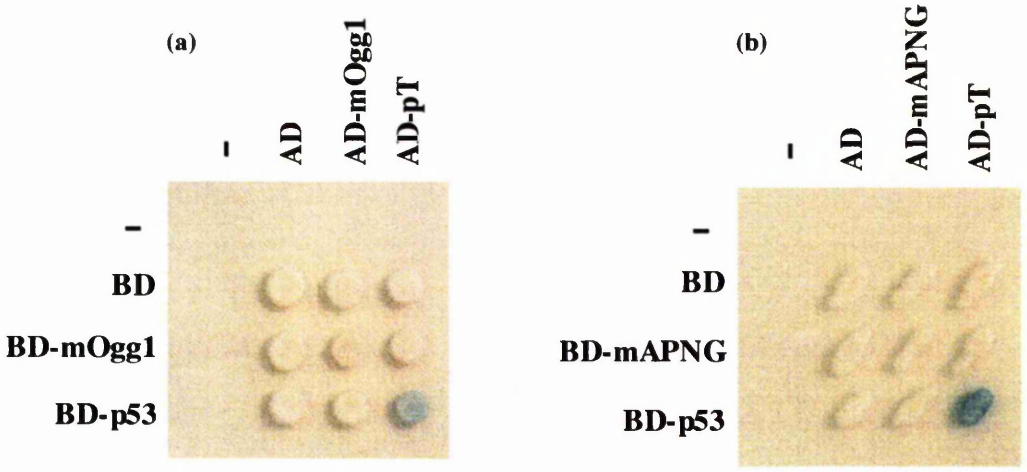

Figure 3.7. Photograph of *Y190 S. cerevisiae* co-transformation testing for the auto-activation of the LacZ reporter gene. (a) Represents the mOGG1 constructs, and (b), the mAPNG constructs. The yeast were plated onto SD-Leu-Trp + X-gal agar plates. BD-p53 and AD-pT were used as a positive control for interacting proteins.

In order to check that the constructs did not activate the HIS reporter, selected co-transformants (pGBTK7-mOGG1/pGADT7; pGBTK7-mAPNG/pGADT7 and control pGBTK7-p53/pGADT7-T) were plated onto SD-Leu-Trp-His media and incubated at 30°C for 5 days. Examination of these plates showed a low amount of background growth on the test plates (mOGG1 and mAPNG), while as expected, the positive control grew healthy colonies (results not shown). However, an indication was given by the Clontech two-hybrid user manual that low level background growth might be encountered with the Y190 strain on media lacking His, generated by leaky expression from the *HIS* reporter and that this could be corrected by the addition of 3-AT (3-Amino-1,2,4-Triazole) to the media. 3-AT is a competitive inhibitor of the yeast *HIS3* protein (His3p) and can be used to inhibit low levels His3p and thus to suppress background growth on selective medium lacking His. A concentration of 25 mM 3-AT added to the media (determined by titration) was found to be sufficient to suppress the background growth of the two test strains and was used in all subsequent experiments.

3.6 Clone specific two-hybrid experiments

In addition to the library screens, several individual co-transformations were carried out involving the two DNA glycosylases (mOGG1 and mAPNG) and various other DNA repair proteins. These were made available through a collaboration with Dr L.J. Rasmussen, Roskilde University, Denmark. Each of the proteins (shown in Table 3.2) used in these experiments was chosen because of its involvement in different aspects of DNA repair and any positive interactions detected would have indicated a novel interaction.

To perform the experiments each of the test constructs was co-transformed into Y190 yeast with the respective two-hybrid mOGG1/mAPNG construct and the transformants were plated onto both SD-Leu-Trp-His and SD-Leu-Trp + X-gal media. After incubation at 30°C for 5 days the plates were removed and examined for colony growth on the His selection media and the formation of blue colonies on the X-gal media. However, none of these experiments yielded any evidence of a two-hybrid interaction between the respective proteins.

Construct	Description	Human/mouse aa seq homology (%)
AD-hUDG	BER DNA glycosylase; Uracil recognition	83%
AD-RPA1	NER protein; binds DNA in preincision complex	-
AD-hRPA2	NER protein; binds DNA in preincision complex	87%
BD/AD-hMSH2	MMR; Mismatch and loop recognition	93%
AD-hMSH6	MMR; Mismatch recognition	86%
BD-hMLH1	MMR; MutL homolog, function unknown	88%
AD-hMGMT	DNA repair protein; Alkyl group acceptor	69%
AD-hTREX	DNA editing and processing nuclease; 3′ nuclease	-
BD/AD-hFEN1	DNA editing and processing nuclease; 5′ nuclease	96%
BD-hHEX1	DNA editing and processing nuclease; 5′ nuclease	-
BD-hExo1b	Partial clone of hHEX1	72%
BD-hC-Ter Exo1	Partial clone of hHEX1	72%

Table 3.2. Table showing the identification of all the human DNA repair proteins used in the yeast two-hybrid experiments with mOGG1 and mAPNG, including the percentage amino acid sequence homology between the human and murine homologs (a dash indicates no homology data was found for this clone). All of the sequence homology data was obtained from the human proteome database (www.proteome.com).

While no protein-protein interactions were observed in these experiments, several factors have to be taken into account before discounting any possible interactions between these proteins. One potential drawback of these experiments was that all of the clones encoded the human homolog of each protein, while the bait protein was, of course, of murine origin. Nevertheless, the high degree of amino acid sequence homology (Table 3.2) and functional homology between mouse and human DNA repair genes suggested that this series of experiments was worth pursuing. Furthermore, the two-hybrid system may not suit the detection of protein-protein interactions for all proteins. Interactions may be lost via steric interference of the interacting domains generated by the N-terminal fusions, or more subtly, certain proteins may only interact when adopting certain conformations brought about by the presence of a substrate (*e.g.* binding to a DNA lesion) or environmental conditions.

3.7 Yeast two-hybrid library analysis

The main focus of the yeast two-hybrid work was to assess if there was evidence for and then isolate novel protein partners for either mOGG1 or mAPNG. Thus, a mouse testes cDNA library cloned into an AD expression construct was co-transformed with the BD-mOGG1 or BD-mAPNG construct. Initially, Y190 yeast were transformed sequentially, first with the BD-mOGG1/mAPNG construct, then the library constructs. The yeast were then plated onto SD-Leu-Trp-His media to select for *HIS* reporter activity. After incubation at 30°C for 14 days, the plates were examined for colonies >1 mm in diameter. For the mOGG1 screen, this produced 768 colonies, which were re-streaked onto SD-Leu-Trp + X-gal media. However, only limited growth was observed on the mAPNG plates. This indicated that the co-transformation of mAPNG/library constructs was exerting a toxic effect on the cells, although at this stage it was unclear why this should be so since the control plates showed no obvious growth defects.

In an attempt to obtain viable colonies for mAPNG, a second round of experiments was performed using a simultaneous transformation procedure. Using this method the yeast would be exposed to BD-mAPNG expression for a shorter period of time prior to the screen and, therefore, might be less prone to the toxic effects. However, using this method similar results were obtained, with the mOGG1 screening producing 844 colonies while the mAPNG screening produced none. Because of this, no further attempts were made using the BD-mAPNG construct. Therefore, I decided to concentrate on screening for partners of mOGG1. A further 3 sequential experiments were carried out generating a total of 24 two-hybrid clones for mOGG1.

3.7.1 Summary of the mAPNG two-hybrid analysis

The mechanism by which mAPNG removes damaged purines may provide a possible explanation for the toxic effects seen in this work. mAPNG can excise a wide variety of base adducts and has also been shown to remove normal purine bases from DNA. Therefore, overexpression of mAPNG could increase the rate at which normal purine bases are lost from the genome. However, yeast transformed only with mAPNG showed no growth defects and it was the transformation of a second construct that caused a pronounced growth defect. In contrast, the co-expression of the BD-mOGG1 and library constructs did not result in such overt toxicity. The explanation for this remains obscure. While it is possible that the second plasmid facilitated the overexpression of mAPNG leading to increased DNA damage, it might alternatively be that mAPNG expression interferes with auxotrophy.

While the expression of mAPNG was not tolerated in the two-hybrid screens performed in this study, this system has since been used successfully to identify an interaction between hAPNG and hHR23 (human RAD23 protein; Maio *et al.*, 2000). The most significant differences between these studies were the use of the human APNG, which might be less toxic to the yeast than the murine homolog, and the pAS2-1 host vector used to create the BD-construct. While the pGBTK7 vector used in this project contains an *ADH1* (700bp) promoter producing a high level of constitutive expression, the pAS2-1 vector used by Maio *et al*, utilises the *ADH1* (400bp) promoter and expresses proteins at a far lower level, and this therefore might significantly reduce the toxicity of APNG. If the protein levels of APNG were indeed the problem in this project, an alternative *LexA* yeast two-hybrid system could be adopted that allows IPTG controlled expression of constructs. Indeed it would be interesting to measure DNA damage (*e.g.* by comet assay) in single and double transformants using such a system. However, at this stage it was decided to focus on the analysis of the mOGG1 two-hybrid clones rather that repeat the experiments using either of these systems.

3.7.2 Summary of the mOGG1 two-hybrid analysis

In the mOGG1 screens a total of 4,788 colonies were obtained from the His selection plates and these were re-streaked onto SD-Leu-Trp + X-gal media to screen for β-galactosidase activity. After incubation at 30°C for 10 days, 24 colonies that had turned blue were re-streaked onto both sets of selective media to confirm the two-hybrid phenotype. In order to identify the library inserts, specific primers were designed on either side of the pGADT7 MCS and were used to amplify the cDNA by PCR (method described in Section 2.2.1). Each clone was then sequenced using the 5′ primer and the DNA sequences were submitted to a standard nucleotide-nucleotide BLAST search. A summary of all the clone identifications gained from the BLAST search is given in Table 3.3. Each clone that remained un-identified after BLAST analysis was labelled as an unknown clone (UNK 'X').

Clone number	BLAST identification
2, 5, 13, 16, 19, 24	mDnaja1
3, 11, 12, 17	mRanBP9
23	mDnaja3
1	UNK A
4	UNK B
6	UNK C
7	UNK D
8	UNK E
9, 10	UNK F
14, 15	UNK G
18	UNK H

Table 3.3. Table showing the number and identification of two-hybrid clones generated from the mOGG1 analysis.

3.7.2.1 Dnaja1

The most frequently occurring clone obtained in the two-hybrid screens encoded a partial cDNA for mDnaja1 (Acc no. NM_008298) in fusion with the AD. mDnaja1 is a murine homolog of the bacterial DnaJ molecular chaperone protein (Dnaj-like or HSP40 family in eukaryotes), and is located specifically within the mitochondrion (Hata and Ohtsuka, 2000; Royaux et al., 1998). While very little is known about mDnaja1 specifically, DnaJ is known to complex with at least two other molecular chaperones, DnaK and GrpE (Langer et al., 1992). Together, these proteins are primarily involved in the transport of proteins across the mitochondrial membrane, but have also been associated with protein stability, disagregation and the targeting of proteins for degradation (Ben-Zvi and Goloubinoff, 2001; Hartl, 1996). Analysis of the DNA sequence showed that each of the 6 clones was missing the N-terminal 57 bp of the coding sequence. Figure 3.8 shows the 5´ sequence homology between mDnaja1 and clones 2, 5 and 13, and a schematic overview showing the cDNA fragments obtained from the library screens compared to the published sequence of mDnaja1.

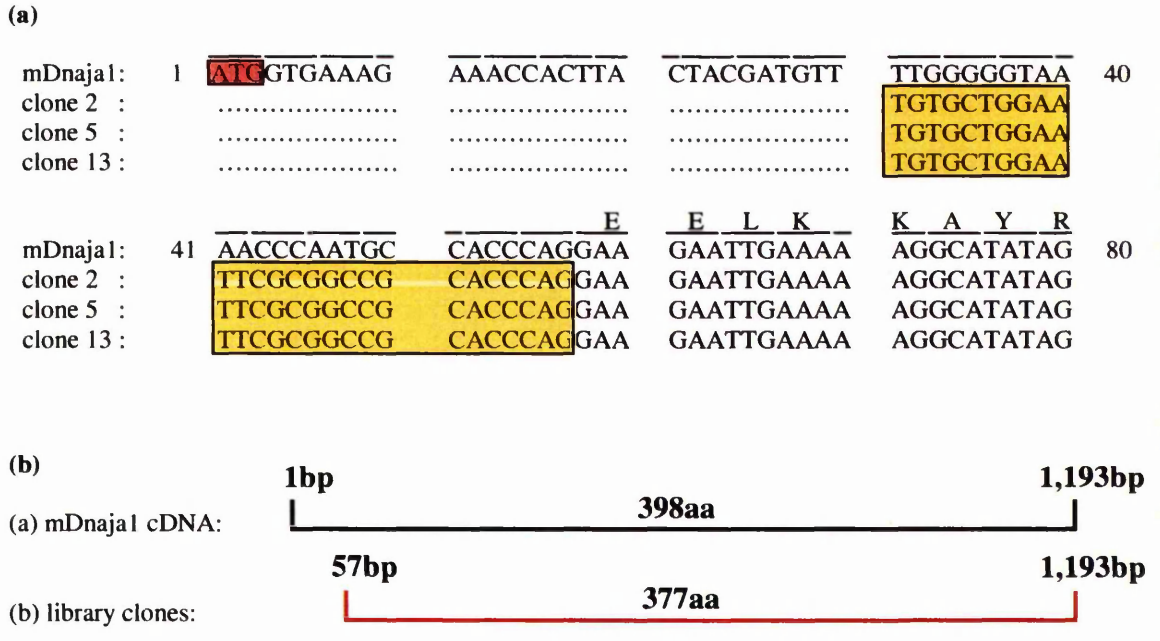

Figure 3.8. **(a)** Sequence data showing the N-terminal sequence homology between the two-hybrid clones 2, 5 and 13, and mDnaja1 (Acc no. NM_008298). The red box indicates the position of the ATG codon in the full-length cDNA, while the yellow box indicates the pACT2 vector sequence and adapter region. **(b)** Representation of, (a) the full-length cDNA encoding mDnaja1 and, (b) the 6 cDNA library clones that encode mDnaja1.

3.7.2.2 mRanBP9

The cDNA sequence encoding mRanBP9 (Acc no. NM_019930) was identified four times in the library screens. This protein has been recently identified as a novel Ran binding protein and has been localised to both the nucleus and cytoplasm surrounding the centrosome (Nakamura et al., 1998; Nishitani et al., 2001). The Ran protein is a Ras-like small nuclear GTPase whose primary function is to act as a carrier, shuttling macromolecules between the nucleus and the cytoplasm. Several Ran-binding proteins (RanBPs) have been identified that aid Ran as either nuclear import or export factors. In addition to nucleocytoplasmic transport, Ran is also thought to be involved in ribosomal RNA processing and cell cycle regulation and several other RanBP's have been identified that provide a role in these functions (Kunzler and Hurt, 2001). Sequence analysis of the Ran BP9 cDNA showed that each of the 4 library clones was missing between 128 and 210 bp of the N-terminal coding sequence (Figure 3.9).

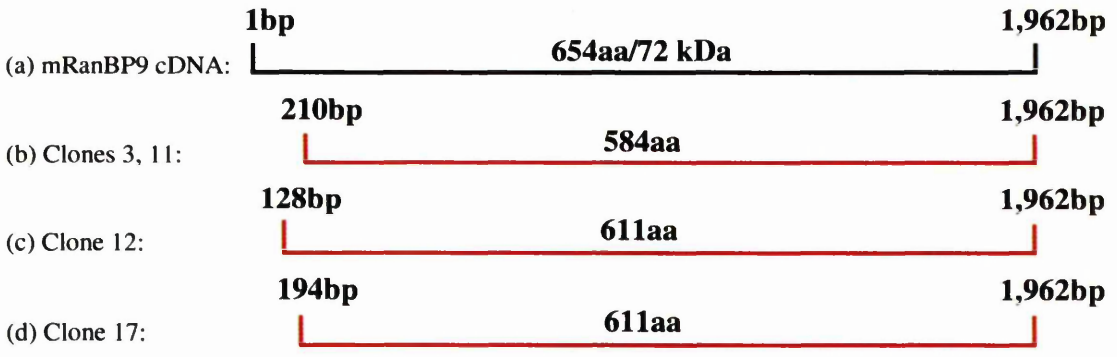

Figure 3.9. Representation of (a) the full-length cDNA encoding mRanBP9 (Acc no. NM_019930) and the 4 cDNA library clones that encode mRanBP9: (b) Clones 3, 11; (c) Clone 12; and (d) Clone 17.

3.7.2.3 mDnaja3

The cDNA encoding mDnaja3 (Acc no. NM_023646) was identified once in the library screens. Interestingly, this clone is also a member of the bacterial DnaJ molecular chaperone family providing further support for the involvement of molecular chaperones with DNA glycosylases. As with mDnaja1, this protein has only been recently identified and very little is known about its specific cellular function. Sequence analysis showed that this clone was missing the 330 bp of the N-terminal coding sequence (Figure 3.10).

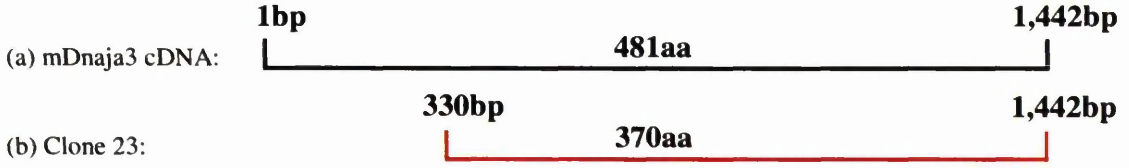

Figure 3.10. Representation of (a) the full-length cDNA encoding mDnaja3 (Acc no. NM_023646) and (b) clone 23 from the cDNA library that encodes mDnaja3.

3.7.2.4 Library clone 7

Library clone 7 contained homology to a cDNA clone that was part of an enriched cDNA library database (Acc no. AK016033). The database identified the clone as having a predicted ORF that was incomplete at the 5´ end of the gene. Analysis of the DNA sequence from clone 7 showed that this clone coded for the C-terminal 159 aa of the predicted ORF (Figure 3.11).

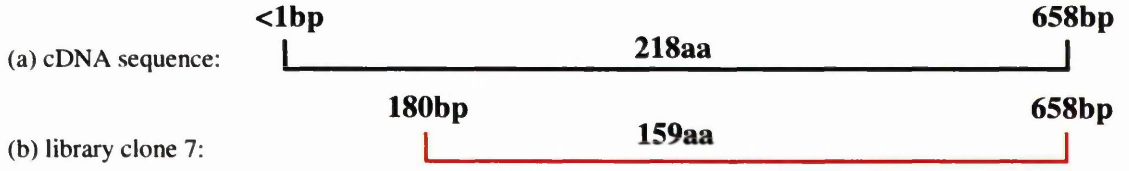

Figure 3.11. Representation of (a) the enriched library cDNA (Acc no. AK016033) and (b) library clone 7.

3.7.2.5 Unidentified or novel sequences

Several of the library clones contained "unknown" sequences according to the BLAST search (Table 3.3). Furthermore, of these sequences all but clones 7 and 8 contained sequences encoding short peptides. The 5 aa peptide fused to the AD in clone 1 was characteristic of several of the library clones identified (Figure 3.12). A list of the two-hybrid clones with similar short peptide sequences is shown in Table 3.4.

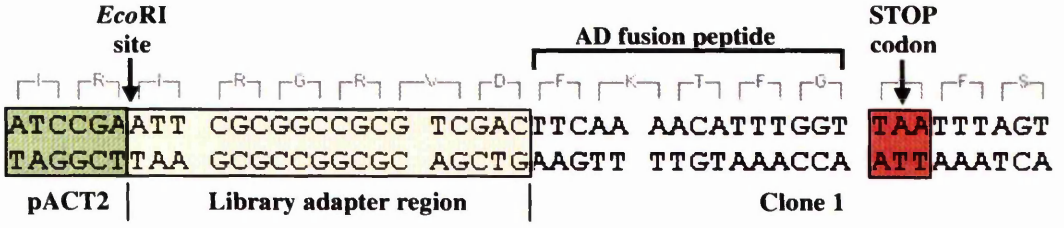

Figure 3.12. N-terminal sequence of Clone 1. The green box indicates the C-terminal region of the GAL4-AD fusion (pACT2). This is fused to the library adapter region (yellow box), used by Clontech to generate the fusion between the AD and the library cDNA. Next follows the library cDNA of clone 1, which expresses a 5 aa peptide fused to the AD before translation is terminated by a STOP codon (red box). The sequence is translated in the same ORF as the AD (ORF1).

Clone no.	Peptide sequence
1	FKTFG-
4	FHIRNCL-
6	AQRALHVA-
9, 10	PRAA-
14, 15	VFTVHVARPWH-
18	LTFT-

Table 3.4. Table showing the short fusion peptides expressed by two-hybrid clones. Termination codons are denoted by (-).

While it is not uncommon for short peptide sequences to facilitate protein-protein interactions, as shown by both nuclear and mitochrondrial localisation signals, as well as numerous protein binding motifs, none of the peptides listed in Table 3.4 shared any sequence homology, or strong property similarities (*e.g.* basic sidechains) that might help to indicate how or why these interactions occur. Therefore, although it is likely that these peptides are responsible for the interactions with mOGG1 or indeed the *GAL4* binding domain, it was decided to analyse the data further for alternative explanations for the yeast two-hybrid interactions.

Other possible explanations for the interaction could include frame shift mutations or mRNA splicing events, introduced by the yeast transcription processing and resulting in the expression of an alternative ORF in fusion with the AD. In order to investigate whether frame-shift mutations could be involved, the DNA sequence of each clone was examined for alternative ORF's and compared to the BLAST analysis of the complete DNA sequence from each clone (Table 3.5). For example, both clone 4 and 18 were found to encode large proteins in an alternative ORF that would be expressed if a frame-shift mutation occurred at the AD junction (Figure 3.13). Clone 4 encoded the C-terminal 225 aa of a 617 aa novel protein (Acc no. AK014463) in ORF2, while clone 18 encoded a 531 aa novel protein (Acc no. NM_025851) in ORF3. Similarly, clones 1 and 6 also encoded large polypeptides in an alternative ORF, however the BLAST analysis did not produce any matches to known cDNA sequences for these clones. Since a frame shift mutation at the AD junction would allow the expression of each of these large ORF's, it is tempting to assume that these clones are likely candidates for frame-shift expression. However, contrasting data is provided by clone 8, which encodes a significant proportion of subunit I of Cytochrome c oxidase in ORF3, while also encoding a 77 aa novel peptide in fusion with the AD in ORF1, which is more likely to be generating the two-hybrid interaction.

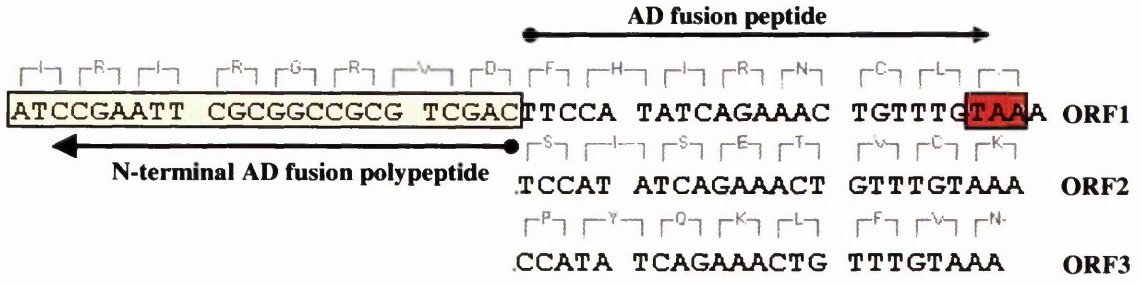

Figure 3.13. Example of a frame shift mutation using the 5′ mRNA sequence of clone 4. The diagram shows the possible results of a splicing event at the AD junction whereby one or more bases have been removed from the 5′ end of the library insert by the yeast transcription machinery. This process alters the translated coding sequence of the library insert from this junction onwards, thereby allowing the expression of peptides encoded by ORF2 or ORF3 in fusion with the AD polypeptide sequence.

In addition to frame-shift mutations, yeast also has the ability to carry out mRNA splicing events that could generate alternative AD-fusion proteins. Clones 14 and 15 both contained identical DNA sequences, encoding the C-terminal region (238 aa) of a 258 aa novel protein in ORF1 (Acc no. AK006951). However, homology to this protein occurs 102bp into the library clone sequence and after 3 termination codons (at bases 33, 48 and 60). Therefore, expression of this protein could only occur via a splicing event that would eliminate the termination codons (Figure 3.14). Similarly, clones 9 and 10 also contain identical sequences with BLAST homology that occurs far downstream of the AD junction. However, as with clones 1 and 6, no cDNA sequence match was found.

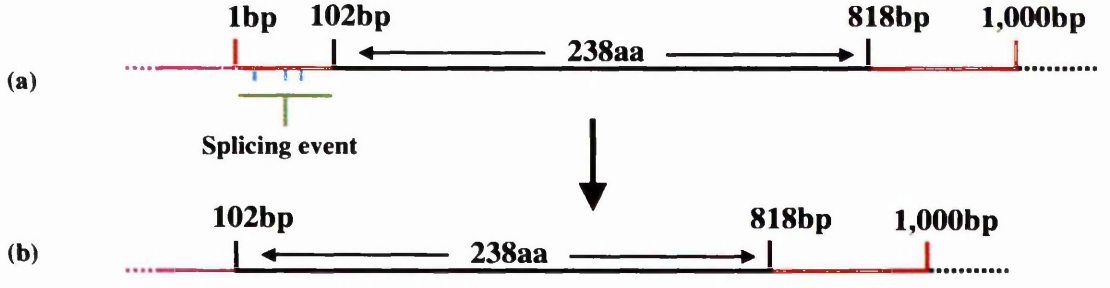

Figure 3.14. Representation of an mRNA splicing event using library clones 14 and 15. (a) Shows the complete library insert (shown in red) fused the AD region of the pACT2 vector (shown in pink) in the form of an mRNA sequence. The black lines represent an ORF identified by BLAST. Three termination codons are present in the N-terminal region of the library insert (shown in blue). (b) Shows a splicing event of the N-terminal 102bp of the library insert allowing an alternative fusion protein to be generated with the coding sequence.

Clone No.	ORF (in aa)			BLAST Identification	Predicted peptide
	1	2	3		
Candidates for frame shift mutations					
4	7	**150+**	8	Novel cDNA	225 aa of a 617 aa protein
18	4	1	**150+**	Novel cDNA	515 aa of a 531 aa protein
1	5	53	6	-	-
6	8	28	87	BAC Library	-
8	77	30	**150+**	Novel cDNA	266 aa of a 298aa protein
Candidates for mRNA splice events					
14/15	**11**	3	36	Novel cDNA	232 aa of a 258 aa protein
9/10	4	80	10	Library insert	-

Table 3.5. Table showing the peptides formed in each of the 3 ORF's and BLAST search identification for each of the two-hybrid clones. The ORF that contains the BLAST identification is in red.

In an attempt to gain more information about the novel polypeptides encoded within clones 4, 8 and 18, both the nucleotide and amino acid sequences were submitted for bioinformatic analysis (Bioinformatics department, PICR). Using these sequences a variety of databases were searched for both nucleotide and amino acid homology as well as conserved domains, motifs, and signalling molecules. However, no significant similarities were found for any of the clones with the search parameters used.

3.8 Summary

The yeast two-hybrid analyses were carried out in an attempt to isolate novel protein partners that might affect the regulation or function of the DNA glycosylases, mOGG1 and mAPNG. In total, 2 library screens were carried out using mAPNG. However, while the yeast tolerated the expression of mAPNG alone, the co-expression of mAPNG and a library protein was found to be toxic and therefore no yeast two-hybrid clones were generated from these screens. In contrast, the expression of mOGG1 did not result in the same toxicity and 5 screens were carried out resulting in the generation of 24 yeast two-hybrid clones. The most frequently occurring clone encoded the molecular chaperone mDnaja1. In addition, a second molecular chaperone, mDnaja3, was found to be encoded by a single library clone providing further evidence for the involvement of molecular chaperones in DNA glycosylase function. A third identifiable clone occurred 4 times in the screens and encoded the cDNA for a novel Ran binding protein, Ran BP9. The majority of the two hybrid clones were found to encode for novel or unknown cDNA sequences.

In addition to the two-hybrid library screens several individual co-transformations were carried out involving the two DNA glycosylases and various other BER enzymes. None of these experiments yielded positive protein-protein interactions, however, although these experiments were carried out across species, these results gave a strong indication that none of these proteins interacted with the DNA glycosylases in the two-hybrid system and allowed these proteins to be eliminated from the investigations.

In order to confirm the two-hybrid interactions an attempt was made to clone each of the library cDNA sequences obtained from the screens. These were then used to further investigate the protein-protein interactions using *in vitro* transcription/translation pull-down experiments as described in Chapter 5.

CHAPTER 4

4.0 Results: Purification of mOGG1

4.1 Introduction

The purification of recombinant mOGG1 protein was carried out to provide protein for use in *in vitro* transcription/translation pull-down experiments, activity assays, and for the production of anti-mOGG1 antibodies.

4.2 The His-tag purification system

Initially a His-tag fusion system, using the pTrcHisA bacterial expression vector, was adopted for the expression and purification of mOGG1 protein from *E. coli*. The system works by cloning the mOGG1 cDNA downstream and in frame with a sequence that encodes an N-terminal fusion peptide. This sequence codes for (5′ to 3′ from the promoter) an ATG translation initiation codon, 6 histidine residues (6xHis-tag) in series that function as a metal binding domain in the translated protein, the bacteriophage T7 gene translation enhancer, and an enterokinase (EK) cleavage recognition sequence that allows cleavage of the 6xHis-tag from the protein (Figure 4.1). Transcription occurs from a trc promoter (trp-lac hybrid promoter) that contains the –35 region of the trp promoter together with the –10 region of the lac promoter. Expression of recombinant His-mOGG1 protein is induced by the addition of IPTG to a pTrcHisA-mOGG1 transformed *E. coli* culture that has been grown to mid-log phase. The protein is purified from the soluble fraction of sonicated bacterial extracts.

The 6xHis-tag metal binding domain of the fusion peptide allows one-step purification of recombinant proteins by immobilized metal affinity chromatography. Recombinant His-mOGG1 is captured from the bacterial extract using a Ni^{2+} chelating column (ProBond purification column; Invitrogen). Bound proteins are eluted from the column by washing with an imidazole buffer gradient that competitively displaces the 6xHis containing fusion proteins from the matrix.

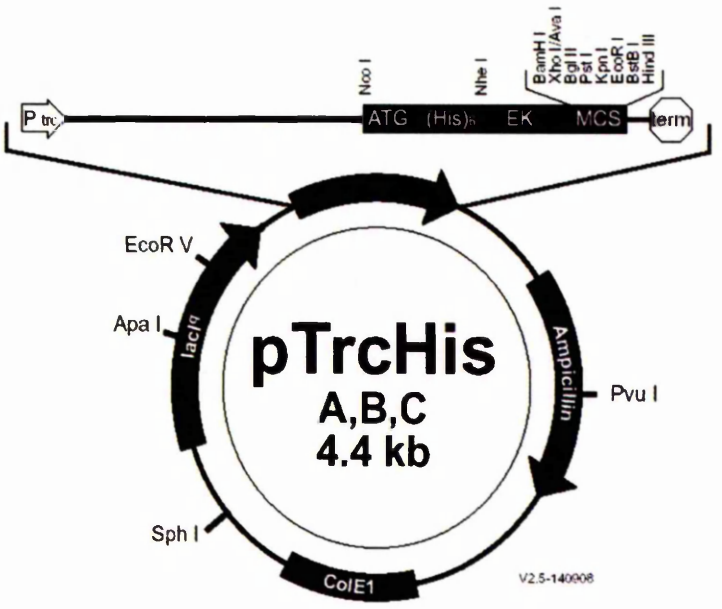

Figure 4.1. pTrcHisA vector map. The 3 forms of the pTrcHis vector (A, B and C), denote the 3 ORFs available for the cloning of cDNA inserts in frame with the fusion peptide. The pTrcHisA form of this expression was used in the experiments. Key: P_{trc} – trc promoter region; $(His)_6$ -6x His-tag; EK – enterokinase recognition site. The anti- Xpress™ epitope tag lies between the latter two regions (not shown).

4.2.1 Production of the pTrcHisA-mOGG1 construct

The complete mOGG1 cDNA was purchased from the IMAGE consortium (IMAGE clone: 0416941). Specific PCR primers complementary to the 5′ and 3′ ends of the gene were then used to amplify the cDNA and introduce both 5′ *Bam*HI and 3′ *Eco*RI restriction sites at the ends of the gene. Furthermore, the 5′ primer was designed to eliminate the 5′ start codon to prevent any expression of mOGG1 protein that did not contain the N-terminal fusion peptide. Correct fusion between the N-terminal 6xHis-tag and mOGG1 ORF was confirmed by DNA sequencing (Figure 4.2), as was the fidelity of the mOGG1 sequence. The construct was then transformed into TOP10 *E. coli* and expressed under varying conditions (see below). Recombinant His-mOGG1 protein has an estimated molecular weight of 44.8 kDa (mOGG1, 38.8 kDa; His-tag 6 kDa). Expression of the fusion protein was confirmed by western blot analysis of bacterial cell extracts, using an anti-Xpress™ antibody against an anti-Xpress™ epitope tag contained within the N-terminal fusion peptide (Figure 4.2a).

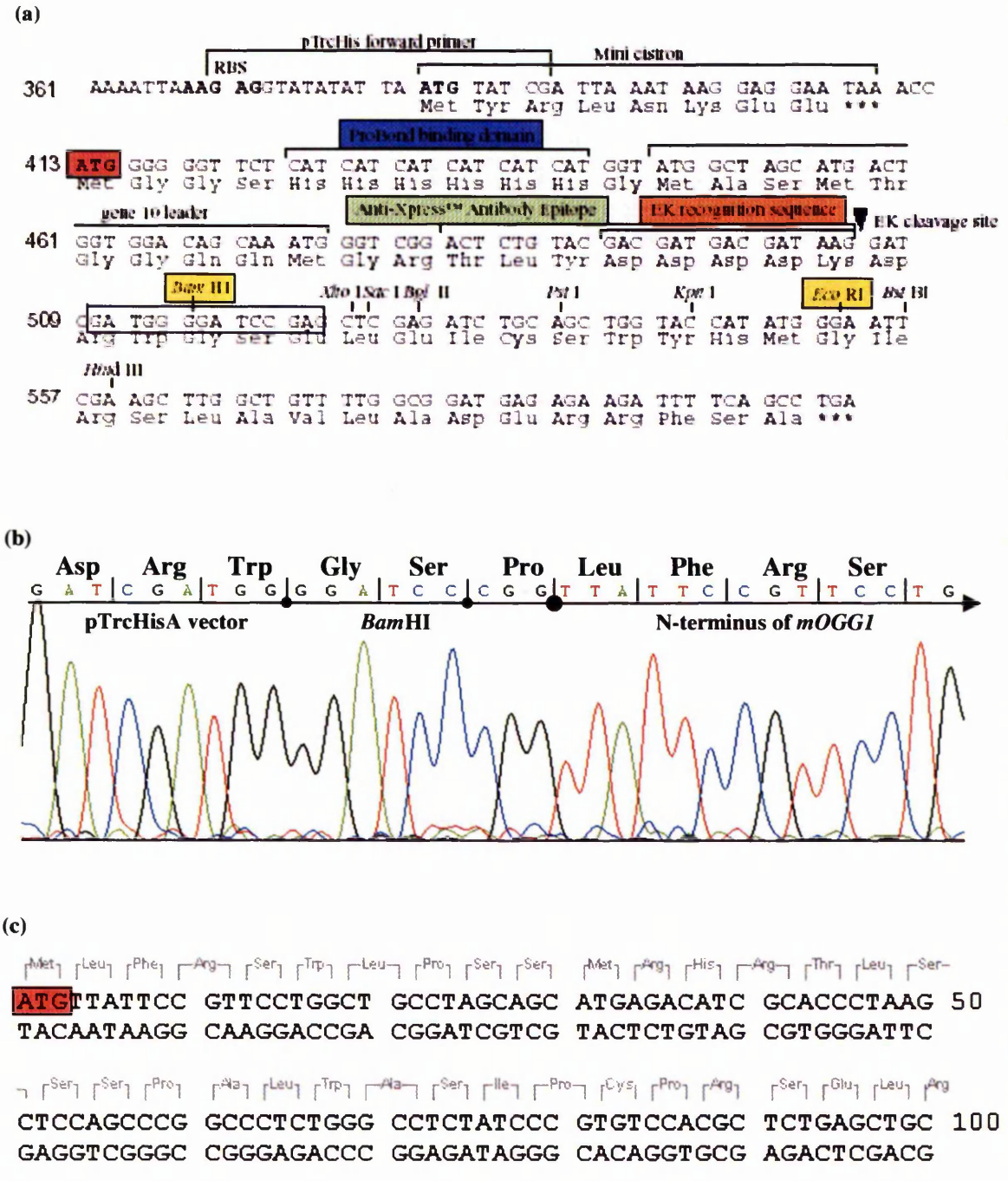

Figure 4.2. (a) Sequence map of the pTrcHisA MCS. The red box indicates the ATG translation initiation codon. The blue box indicates the metal binding 6xHis-tag. The green box indicates the position of the anti-Xpress™ antibody epitope tag used for the detection of expressed proteins by western blot analysis. The orange box indicates the enterokinase recognition sequence for the cleavage of the peptide. The yellow boxes indicate the positions of the *Bam*HI/*Eco*RI restriction digest sites used to insert the mOGG1 cDNA. (b) Chromatogram showing the in frame N-terminal fusion between the pTrcHisA vector and mOGG1 cDNA (c) Sequence data showing the N-terminal region of mOGG1 cDNA (Acc no. U96711). The red box indicates the start of the coding sequence.

4.2.2 Expression of recombinant His-mOGG1 protein

To assess the level of protein expressed using the pTrcHisA system, the pTrcHisA-mOGG1 construct was transformed into TOP10 *E. coli* and induced using 1 mM IPTG, for 4 h at 37°C. The pTrcHisA vector was also transformed and induced in the same way to provide a negative control. Aliquots (1 ml) were removed from both sets of cells every hour and both soluble and insoluble bacterial extracts were prepared. The extracts were analysed by SDS-PAGE and the results are described below.

Western blot analysis of the soluble bacterial extracts showed expression of a 45 kDa protein, with an optimal induction time of 3 h in the pTrcHisA-mOGG1 transformed cells (Figure 4.3). Visualisation of this protein on the Coomassie blue stained gel was hindered by the expression of an endogenous 45 kDa protein, seen in the soluble extracts for both pTrcHisA-mOGG1 and pTrcHisA transformed cells. However, since the intensity of the endogenous band was similar in both gels, the expression level of soluble His-mOGG1 protein was estimated to be low. The protein expression level within several other transformed colonies was also assessed, though no increased expression was seen in any of these colonies.

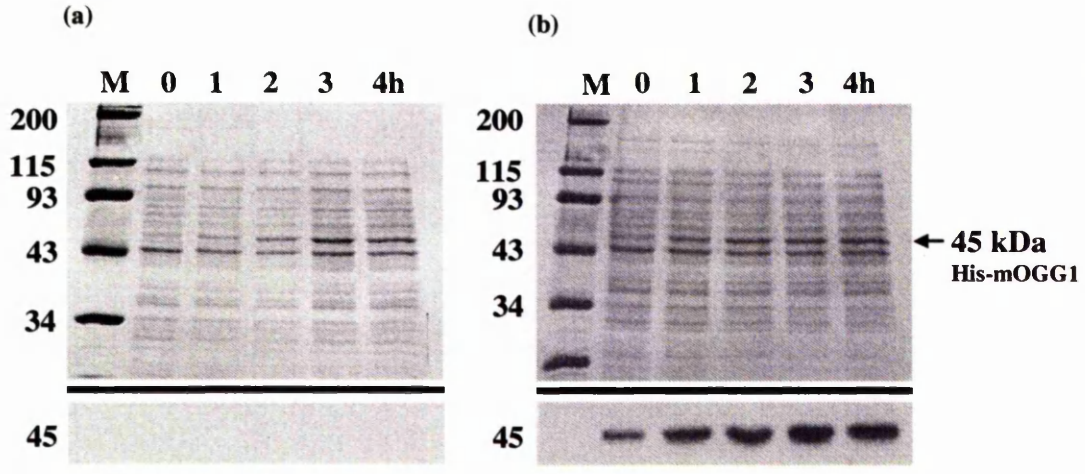

Figure 4.3. Coomassie blue stained SDS-PAGE gel (top) and western blot (bottom) of bacterial cell extracts (9 µg per lane) from (a) 'control' pTrcHisA transformed and (b) pTrcHisA-mOGG1 transformed TOP10 *E. coli* induced over 4 h time period. Transformed bacteria were induced using 1 mM IPTG, for 4 h at 37°C and 1 ml aliquots were removed every hour.

As a low yield of His-mOGG1 protein was seen in the soluble extract, the insoluble extract was also analysed to see if the protein was being expressed in an insoluble form. Figure 4.4 shows the insoluble extract from the 0 and 3 h time points, from the pTrcHisA-mOGG1 and pTrcHisA transformed cells.

As seen previously with the soluble extract, there was no apparent difference between the Coomassie blue stained gels from the pTrcHisA-mOGG1 and pTrcHisA transformed cells after induction. Furthermore, although western blot analysis clearly showed expression of His-mOGG1 after 3h induction, as the protein was not visible on the Coomassie gel the expression levels were once again estimated to be low.

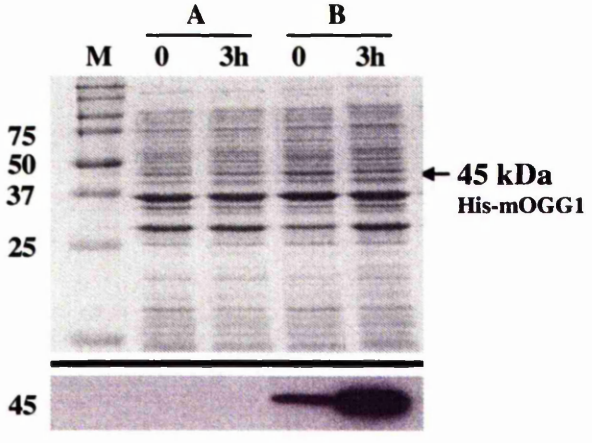

Figure 4.4. Coomassie blue stained SDS-PAGE gel (top) and western blot (bottom) of insoluble bacterial cell extracts (9 µg per lane) from (A) 'control' pTrcHisA transformed and (B) pTrcHisA-mOGG1 transformed TOP10 *E. coli* induced over a 3 h time period. Bacteria were induced using 1 mM IPTG, for 3 h at 37°C and 1 ml aliquots were removed at 0 h and 3 h.

4.2.3 Increasing the expression levels of His-mOGG1

In an attempt to increase mOGG1 protein expression, both the levels of IPTG and incubation temperatures were altered. Transformed bacteria were induced using increasing concentrations of IPTG (0, 0.5, 1 and 3 mM), for 3 h at 37°C and 1 mM IPTG, for 3 h at decreasing incubation temperatures (37, 30 and 22°C). However, as far as can be assessed using western blot analysis, neither alteration affected the expression levels of His-mOGG1 in either a soluble or insoluble form (Figure 4.5; data for insoluble fraction not shown).

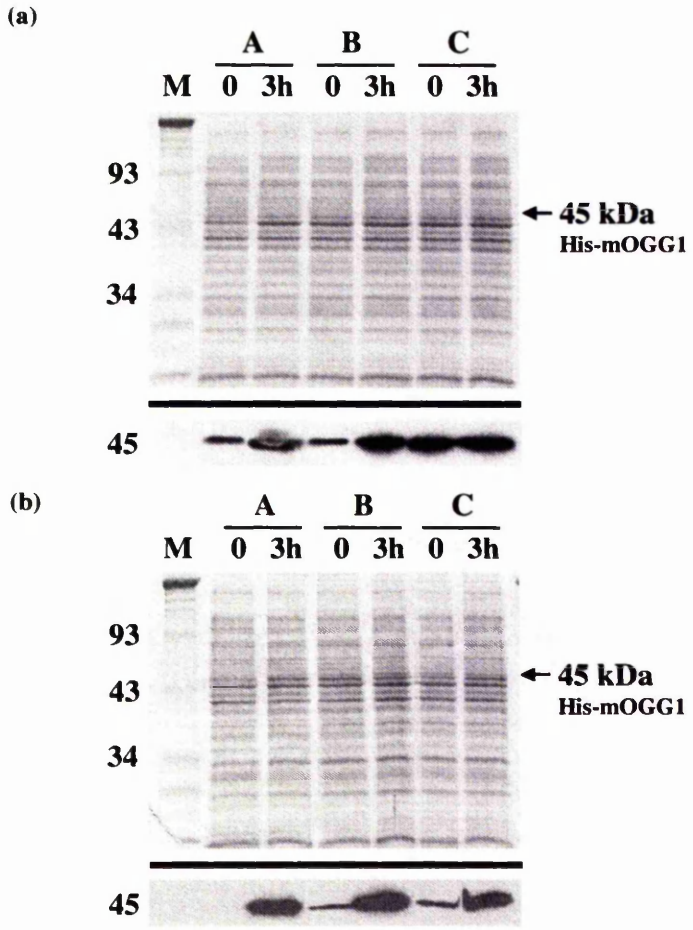

Figure 4.5. Coomassie blue stained SDS-PAGE gel (top) and western blot (bottom) of bacterial cell extracts (9 µg per lane) from induced *TOP10 E. coli* transformed with pTrcHisA-mOGG1. Bacteria were induced using (a) IPTG concentrations of (A) 0.5, (B) 1 and (C) 3 mM for 3 h at 37°C, (The western blot for the Section C, 0 h time point represent shows there was a error with extract from the 3 h time point being loaded accidentally.) and (b) 1 mM IPTG for 3 h at (A) 22, (B) 30 and (C) 37°C.

4.2.4 Purification of His-mOGG1

Despite relatively low expression levels, an attempt was made to purify His-mOGG1 protein using a ProBond purification column. A culture (200 ml) of pTrcHisA-mOGG1 transformed bacteria was induced using 1 mM IPTG, for 3 h at 37°C. Bacterial cell extracts were prepared and the soluble fraction was applied to the ProBond column. The column was washed 3 times and the protein eluted using an imidazole buffer gradient (5 ml of: 200 mM, 350 mM and 500 mM imidazole buffer applied consecutively). The eluate samples were pooled and concentrated to total volume of 0.75 ml using a Millipore Ultra-free-15 centrifugation filter. The complete purification method is described in Section 2.4.1.

Western blot analysis of the bacterial extracts showed similar protein expression levels to those seen previously, with His-mOGG1 protein being present in both the soluble and insoluble fractions (Figure 4.6; Lanes 2,3). The blot also shows that a relatively small amount of recombinant protein was lost during the washing of the column (lanes 4,5). The final concentration of protein in the concentrated eluate was 120 ng/µl (calculated by Bradford total protein assay), though both the western blot and Coomassie blue stained gel showed that the protein yield was low (lane 6). Furthermore, the Coomassie blue stained gel showed that the overall purity of the protein was poor, with approximately 10 bands of endogenous protein of various molecular weights also present, none of which correspond clearly to the molecular weight of His-mOGG1.

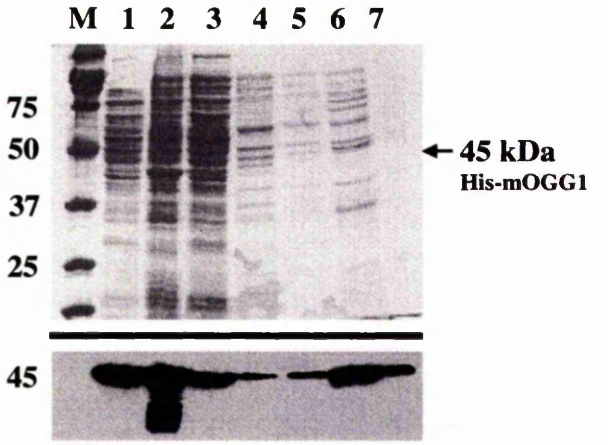

Figure 4.6. Coomassie blue stained SDS-PAGE gel (top) and western blot (bottom) of His-mOgg1 purification scheme. Lane 1, Crude extract; lane 2, Insoluble extract; lane 3 Soluble extract; lane 4, Wash 1; lane 5, Wash 3; lane 6, recombinant His-mOGG1 eluate; lane 7, Residual binding to resin.

4.3 The GST-tag purification system

Since little success was gained by manipulating the pTrcHisA system to generate significant quantities of protein, it was decided to try an alternative method. The glutathione-S-transferase (GST) expression system was chosen which involves the generation of a fusion protein between the 26 kDa GST protein and the N-terminal region of mOGG1 via a linker peptide. The linker peptide contains a thrombin cleavage recognition sequence to allow cleavage of the GST-tag from the fusion protein. Transcription is driven from a tac promoter and translation is initiated from an ATG site immediately upstream from the GST-tag. Figure 4.7 illustrates the vector map and MCS region of the pGEX4T-3 vector used for this experiment.

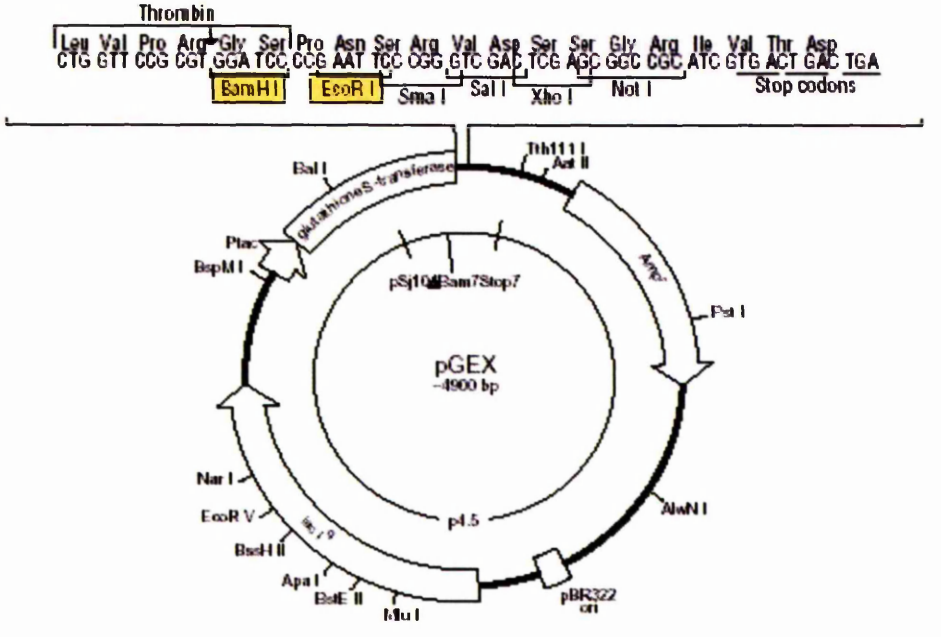

Figure 4.7. Vector and MCS sequence map of pGEX4T-3. The yellow boxes indicate the positions of the *Eco*RI/*Bam*HI restriction digest sites used to insert the mOGG1 cDNA.

4.3.1 Production of the GST-mOGG1 construct

Since the pTrcHisA and pGEX4T-3 vector ORFs were identical, the mOGG1 cDNA was cleaved out of the pTrcHisA-mOGG1 construct and introduced into the MCS of pGEX4T-3 using *Bam*HI/*Eco*RI restriction sites (Figure 4.7). Correct fusion between the N-terminal GST-tag and mOGG1 ORFs was confirmed by DNA sequencing (Figure 4.8). The construct was transformed into BLR *E. coli* and induced using 1 mM IPTG, for 3 h at 37°C. The estimated molecular weight of recombinant GST-mOGG1 is 66 kDa (mOGG1, 38.8 kDa; GST-tag 27 kDa). Expression of the fusion protein was confirmed by western blot analysis, using an anti-GST antibody (Invitrogen).

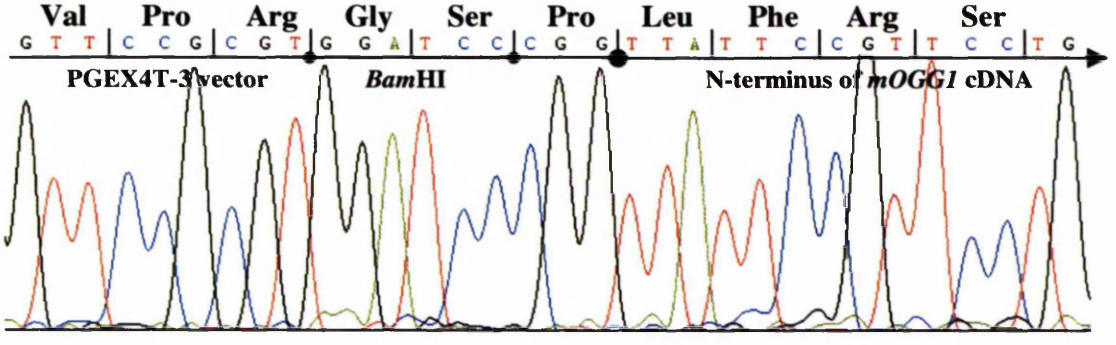

Figure 4.8. Chromatogram showing the in frame N-terminal fusion between the pGEX4T-3 and mOGG1.

4.3.2 Expression and purification of GST-mOGG1

For this purification, Glutathione Sepharose-4B beads were used to purify GST-mOGG1 protein according to a protocol received from a collaborating laboratory (Dr L Rasmussen, Roskilde University, Denmark). A culture (200ml) of pGEX4T-3-mOGG1 transformed BLR *E. coli* was induced with 1 mM IPTG, for 3 h at 37°C. Bacterial cell extracts were prepared and the soluble fraction was applied to the GST-beads and incubated for 2 h at 4 °C. The beads were then washed 3 times and the protein eluted using reduced glutathione elution buffer (5 ml). The eluate was concentrated to a total volume of 1 ml using a Millipore Ultra-free-15 centrifugation filter. The complete purification method is described in Section 2.4.2.

The Coomassie blue stained gel showed that this method purified GST-mOGG1 protein to a high yield and with few contaminants (Figure 4.9; lane 8). Interestingly, a clear GST-mOGG1 band can be seen in the soluble extract from this induction that was previously unseen in any of the inductions using pTrcHisA (Figure 4.9; lane 3). The identity of the purified protein was confirmed by western blot analysis (Figure 4.9b) and subsequent enzyme assays (see Section 4.3.4). The protein concentration was determined to be 4 µg/µl using the Bradford total protein assay. Later purifications of GST-mOGG1 protein resulted in a similar high yield of GST-mOGG1 protein.

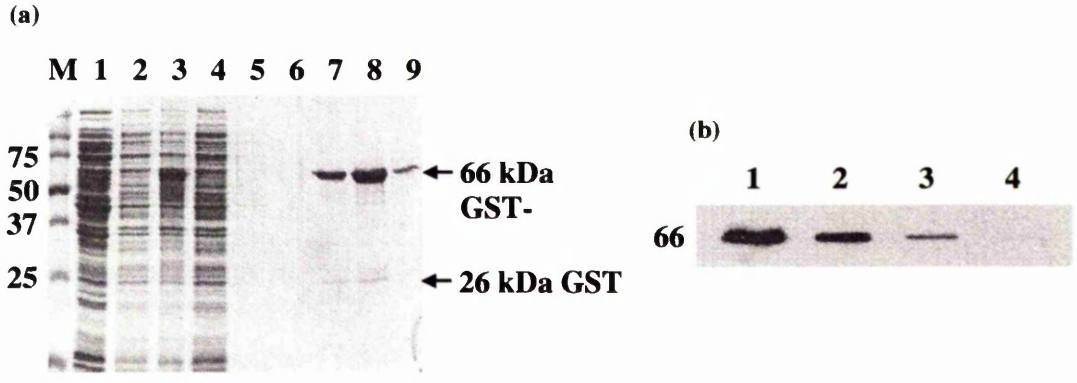

Figure 4.9. (a) Coomassie stained SDS-PAGE gel of GST-mOGG1 purification scheme. Lane 1, Crude extract; lane 2, Insoluble extract; lane 3 Soluble extract; lanes 4-6, Wash 1-3; lane 7 recombinant GST-mOGG1 bound to GST-beads; lane 8, Purified GST-mOGG1 eluate; lane 9, Residual binding to GST-beads. (b) Western blot analysis of purified GST-mOGG1 protein. Lane 1, 1:500 dilution; lane 2, 1:1000 dilution; lane 3 1:2000 dilution; lane 4, 1:4000 dilution.

4.3.3 Expression and purification of GST-hOGG1a

As the GST-purification scheme had proved successful with mOGG1 it was decided to use this method to also purify the major human isoform of OGG1 (hOGG1a). The hOGG1a cDNA (IMAGE clone: 0826352) was purchased from the IMAGE consortium. Specific PCR primers complementary to the 5′ and 3′ ends of the cDNA were then used to amplify the cDNA and introduce both 5′ *Bam*HI and 3′ *Eco*RI restriction sites at the ends of the cDNA. The PCR products were then digested and ligated into pGEX4T-3 and the construct was checked by DNA sequencing. After transformation of BLR *E. coli* with the construct, the culture was induced with 1 mM IPTG, for 3 h at 37°C. The preparation of bacterial cell extracts and the purification procedure was carried out as previously described. Recombinant GST-hOGG1a protein has the same estimated molecular weight as GST-mOGG1 (GST-hOGG1a, 66 kDa; hOGG1a, 38.8 kDa; GST-tag 26 kDa).

The Coomassie blue stained gel showed that this system successfully purified GST-hOGG1a protein with a moderate yield and few contaminants (Figure 4.10; lane 6). Western blot analysis and subsequent enzyme assays of the bacterial cell extracts confirmed its identity (Figure 4.10b and Section 4.3.4, respectively). The protein concentration was determined to be 0.3µg/µl using the Bradford total protein assay. Later purifications resulted in a higher yield of GST-hOGG1a protein.

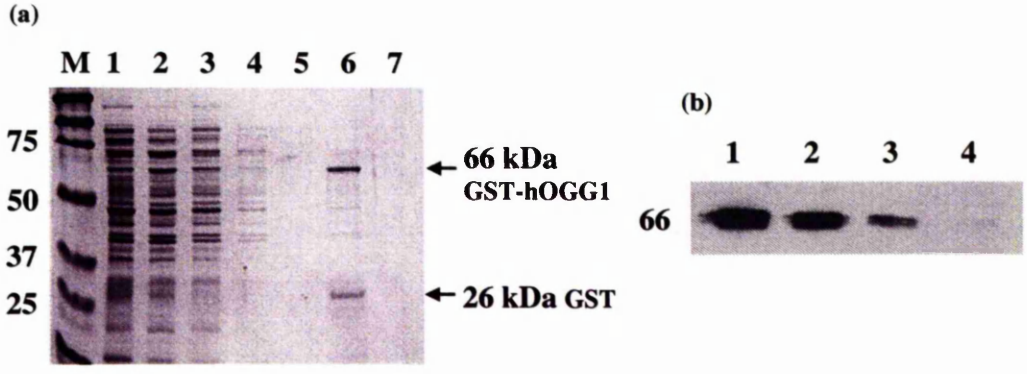

Figure 4.10. (a) Coomassie stained SDS-PAGE gel of GST-hOGG1a purification scheme. Lane 1, Insoluble extract; lane 2, Soluble extract; lanes 3-5, Wash 1-3; lane 6, Purified recombinant GST-hOGG1a eluate; lane 7, Residual binding to GST-beads. (b) Western blot analysis of purified GST-hOGG1a protein. Lane 1, 1:50 dilution; Lane 2, 1:100 dilution; lane 3 1: 200 dilution; lane 4, 1:400 dilution.

4.3.4 Functional activity of purified GST-mOGG1

The activity of the purified GST-mOGG1 and GST-hOGG1a proteins was assessed using the OGG1 glycosylase assay. A double stranded oligo containing a single 8-oxodG lesion was labelled with [^{32}P] and used as a substrate to measure the cleavage activity of the proteins over time. Both the GST-mOGG1 and GST-hOGG1a proteins (32 ng of each) were incubated at 37°C for up to 4 h with the substrate (approximately 70,000 cpm per time point). The bacterial FPG protein was included in this assay as a positive control. Figure 4.11 shows that both GST-mOGG1 and GST-hOGG1a proteins had functional activity against the 8-oxoG containing oligo. While neither protein showed as high affinity for the substrate as Fpg, GST-mOGG1 did cleave an equal amount of the oligo (~80%) over the 4 h incubation. GST-hOGG1a had a reduced activity showing only cleaving 40% of the oligo, however, subsequent purifications showed an increased activity of this protein.

As previously discussed in Section 1.8.1, to my knowledge none of the Nth-like glycosylases have been characterised with δ-elimination activity. However, these initial experiments clearly showed the occurrence of partial β,δ-elimination activity from GST-mOGG1 and to a lesser extent with GST-hOGG1a (Figure 4.11a). To check that the new activity was not derived from any contaminants, the purified GST-mOGG1 protein was subjected to a further gel filtration purification step and the experiment was repeated (Gel filtration and activity work was carried out by Dr J. Parsons, Carcinogenesis Group, PICR). As shown in Figure 4.12, the GST-mOGG1 protein retained significant δ-elimination activity.

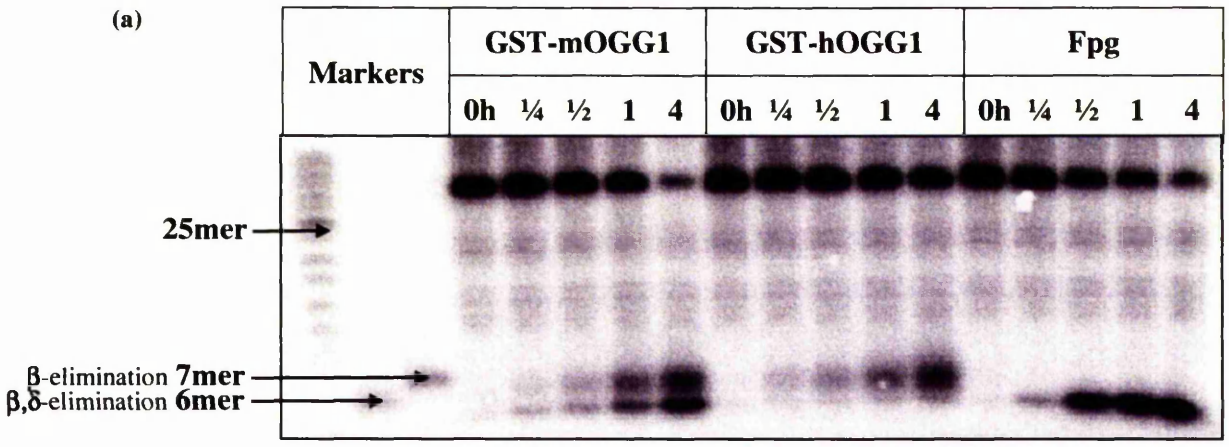

(b) OGG1 glycosylase assay of purified GST-m/hOGG1 protein

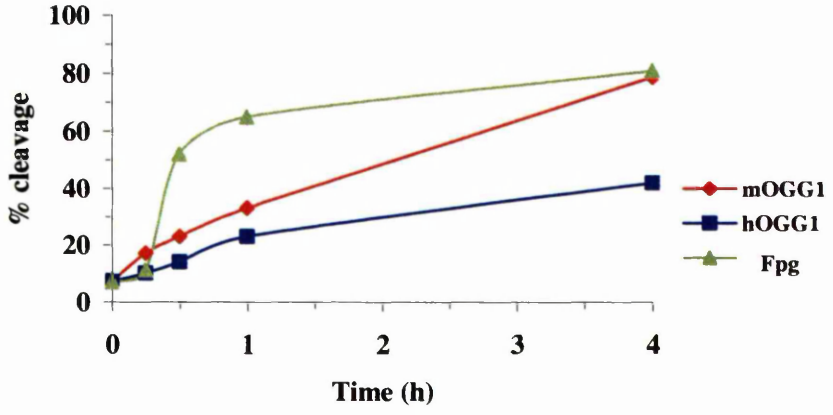

Figure 4.11. (a) Phosphorimage of OGG1 glycosylase assay using purified GST-mOGG1, GST-hOGG1a and Fpg proteins. Each protein (32 ng) was incubated with the radiolabelled substrate for 4 h (80 µl total volume). Aliquots (20 µl) were removed after 0, 30 min, 1 hr and 4 h incubation. (b) Graph showing the percentage cleavage of the 8-oxodG oligo substrate over time.

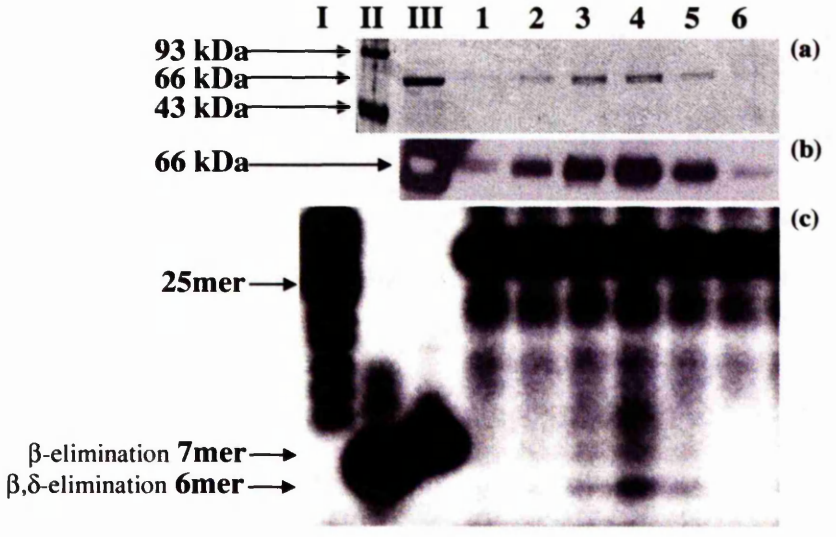

Figure 4.12. Functional activity of GST-mOGG1 protein after gel filtration. (a) Coomassie blue stained SDS-PAGE gel of purified GST-mOGG1 fractions after gel filtration (Key; II, Broad range protein markers (BioRad); III, GST-mOGG1 un-filtered; Lanes 1-6, represent gel filtration fractions 4-9). (b) Western blot of SDS-PAGE gel using anti-GST antibodies (Key; III, GST-mOGG1 un-filtered; Lanes 1-6 as previously stated). (c) OGG1 activity assay of gel filtration extracts (Key; I, II, III, nucleotide markers; Lanes 1-6, as previously stated).

4.3.5 Thrombin cleavage of GST-tag

In an attempt to cleave the bulky GST-tag from the fusion protein, GST-mOGG1 was treated with thrombin. Initially, the protein was treated with the recommended dose of 0.01 units of thrombin per mg of protein, though after 18 h incubation at 22°C no visible cleavage of the GST-tag was seen on the Coomassie blue stained gel (Figure 4.13a). Next, the protein was treated with increasing doses of thrombin (1x to 100x recommended dose) for 18 h (Figure 4.13b). Though some cleavage of the GST-tag was seen in this experiment for each thrombin concentration, the cleavage efficiency was still poor. Furthermore, any cleavage of the GST tag also resulted in the digestion of the mOGG1 protein, as shown by the faint degradation bands seen above the GST-tag in Figure 4.13b. In order to assess the cleavage efficiency of thrombin, both native and heat-denatured (heated to 90°C for 5 min) GST-mOGG1 was incubated with thrombin (1x) for 18 h. Once again the native protein was left un-cleaved, while the activity of the thrombin was confirmed by the degradation of the denatured protein after 4 h (Figure 4.13c). Similar results were obtained for the thrombin digestion of GST-hOGG1a protein (data not shown).

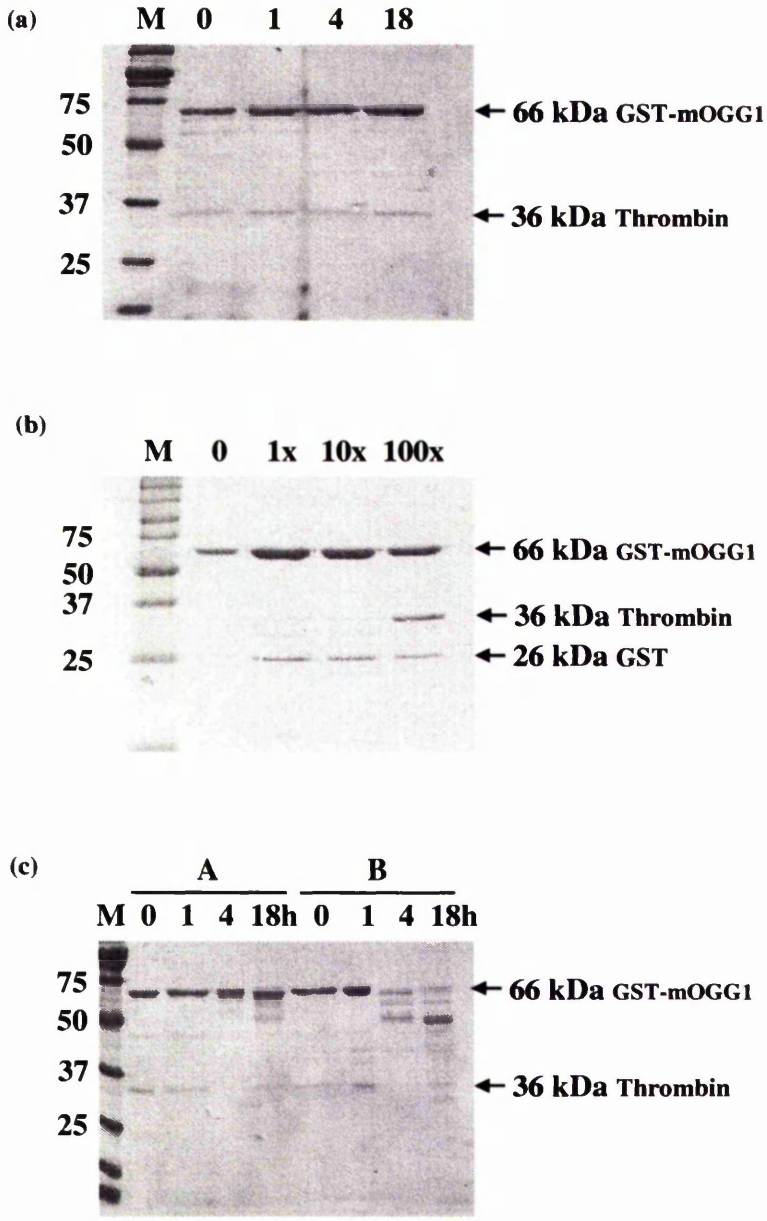

Figure 4.13. Coomassie blue stained gel showing thrombin cleavage of the GST-tag from GST-mOGG1. (a) Purified GST-mOGG1 (8 µg) was incubated for up to 18 h with thrombin (0.08 units) in a total volume of 80 µl. Aliquots (20 µl) were removed after 0, 1, 4 and 18 h incubation. (b) Purified GST-mOGG1 (2 µg per lane) was incubated for 18 h with increasing doses of thrombin (0 units, 1x, 10x, 100x). (c) Purified GST-mOGG1 (A) (8 µg) and heat-denatured GST-mOGG1 (B) were incubated for 18 h with thrombin (0.08 units) in a total volume of 80 µl per reaction. Aliquots (20 µl) were removed for after 0, 1, 4 and 18 h incubation.

4.4 Summary

The overexpression and subsequent purification of mOGG1 proved to be fraught with difficulty and no ideal solution was obtained. Thus while the His-tag system produced low expression levels of His-mOGG1 protein, better levels of expression were obtained with the GST fusion protein. Indeed, this method was subsequently used to purify GST-hOGG1a protein. However, the GST system did have the drawback that both the mOGG1 and hOGG1a proteins were themselves sensitive to thrombin digestion while the engineered thrombin site was probably buried within the fusion proteins rendering it resistant to cleavage. Therefore, although this GST fusion protein was active and conveniently tagged for pull-down experiments, it was not ideal as an immunogen for obtaining specific anti-m/hOGG1 antibodies as the immunisation of rabbits with a fusion-protein containing a GST-tag would produce a mixed set of polyclonal antibodies that was rich with anti-GST antibodies. However, the majority of these contaminating antibodies could probably be separated from the anti-m/hOGG1 antibodies by the incubation of the serum with Glutathione sepharose 4B beads coated with purified GST protein.

The reasons for the low level of expression seen from the pTrcHisA system have not been established. However, it may have resulted from poor levels of transcription from the trc promoter, since similar induction conditions provided good expression levels from the tac promoter used in the GST system. Even if the expression had been high, the smaller His-tag protein has the potential to be buried within the protein when folding, unlike the larger GST-tag (26 kDa for the GST-tag compared to 6 kDa for the His-tag). This may have provided difficulties for the capture of the fusion protein.

Interestingly, the purification and subsequent functional assay of GST-mOGG1 allowed the discovery of a novel δ-elimination activity for this protein. The characterisation of this new activity will be pursued within the Carcinogenesis Group by assessing the cleavage characteristics with various lesion substrates.

CHAPTER 5

5.0 Results: *In vitro* transcription/translation pull-down experiments

5.1 Introduction

In vitro transcription/translation (IVTT) pull-down experiments were used to verify the positive protein-protein interactions obtained from the yeast two-hybrid system. The IVTT reactions were performed using a rabbit reticulocyte IVTT kit according to the manufacturer's instructions (Promega).

5.2 The principle of the IVTT pull-down system

The IVTT reaction allows both the transcription and translation of a target gene in an *in vitro* environment. To perform the reaction, the target gene is first ligated into an expression vector that contains a T7 promoter region. This construct is then added to a mixture containing, T7 RNA polymerase, polymerase buffer, [^{35}S]-labelled methionine, amino acids (minus methionine), an RNase inhibitor, and rabbit reticulocyte lysate. All of the enzymes required for protein synthesis are provided in the reticulocyte lysate. The reaction is initiated by incubation at 30°C for 90 min. During this time T7 RNA polymerase binds to the T7 promoter and transcribes the target gene. Translation of the newly synthesised mRNA may occur from any ATG codon that is surrounded by a reasonable Kozak sequence (Kozak consensus sequence: GCC ACC ATG G). Therefore, if multiple ORF's exist within the mRNA several different polypeptides may be expressed in the same reaction. Expression of the polypeptide is confirmed by SDS-PAGE followed by phosphorimaging. The strength of the signal gained from the phosphorimage is determined by the amount of [^{35}S]-labelled methionine incorporated into the polypeptide. Therefore, the intensity of the signal will vary depending on the number of methionine residues present in the polypeptide. Furthermore, the efficiency of expression may vary between target genes. A complete description of the IVTT reaction protocol is given in Section 2.4.5.

To perform the GST pull-down experiment, purified GST-mOGG1 protein (described in Chapter 4) was re-bound to Glutathione sepharose 4B beads. The IVTT reaction product was then added to the beads, bound with GST-mOGG1, and incubated at 4°C for 2 h to allow protein-protein interactions to occur. The beads were then sedimented by centrifugation, washed extensively to remove unbound proteins and resuspended in SDS-PAGE loading buffer. Bound polypeptides were dissociated and denatured by heating at 95°C for 5 min and then analysed by SDS-PAGE. Any [^{35}S]-labelled polypeptides pulled-down with the beads were visualised by phosphoimaging using a STORM phosphoimager. A complete description of the pull-down experiment is given in Section 2.4.6.

5.3 Production of the IVTT constructs

The PCR products obtained from the mOGG1 library screens all contained 5′ *Eco*RI and 3′ *Xho*I restriction sites, introduced by Clontech during the construction of the cDNA library. Thus, each clone was digested with *Eco*RI/*Xho*I and ligated into pcDNA3 unless stated otherwise (Figure 5.1). Correct ligation was confirmed by DNA sequencing.

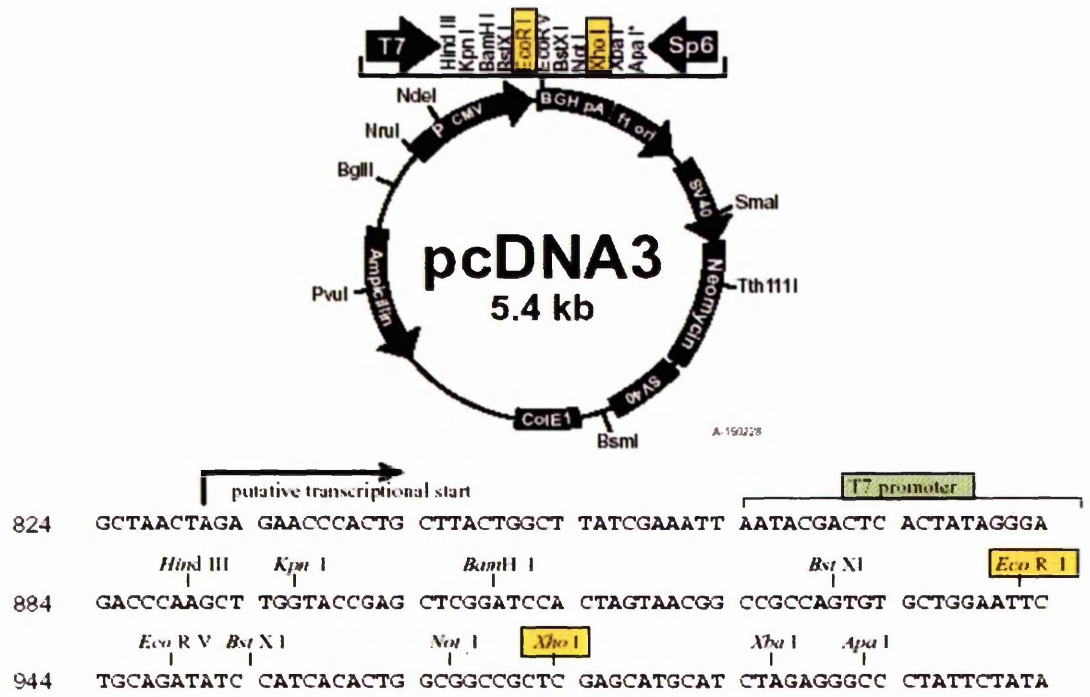

Figure 5.1. pcDNA3 vector map and MCS. pcDNA3 was used as the host cloning vector for the library cDNA PCR products. Each PCR product was ligated on *Eco*RI/*Xho*I sites, shown in yellow. The T7 promoter region used to initiate transcription by T7 RNA polymerase is shown in green.

5.4 IVTT pull-down experiments

The following section describes the results for each of the library clones tested using the IVTT pull-down method.

5.4.1 mDnaja1

The interaction between mOGG1 and mDnaja1 was tested using 3 of the 6 library clones obtained from the yeast two-hybrid screens (Figure 5.2a; clones 2, 5 and 13). In order to predict the molecular weight of proteins that would be expressed in the IVTT reaction the DNA sequence of both the library clones and full-length mDnaja1 cDNA was examined. This analysis showed that the first ATG codon present in the library clones (at position 253bp in the full-length mDnaja1 sequence) was the most favourable to initiate expression due to its proximity to the T7 promoter, and because the surrounding bases contained significant homology to the Kozak consensus sequence (Figure 5.2b). Expression from this codon would generate a 35 kDa protein, incorporating 11 out of the 12 methionine residues present in the full-length cDNA (Figure 5.2a).

The downstream ATG codons present within the mDnaja1 ORF could also initiate protein expression, producing further truncations of mDnaja1. However, a reduced expression level would be expected from these sites as they only contained moderate homology to the Kozak consensus sequence and translation efficiency would decrease as the distance from the T7 promoter region increased. Finally, the sequences were examined for large polypeptides contained within ORF2 and ORF3, which if expressed, would generate visible IVTT products that might confuse any pull-down results obtained. However, no significant alternative ORFs were found within the mDnaja1 sequence.

(a)

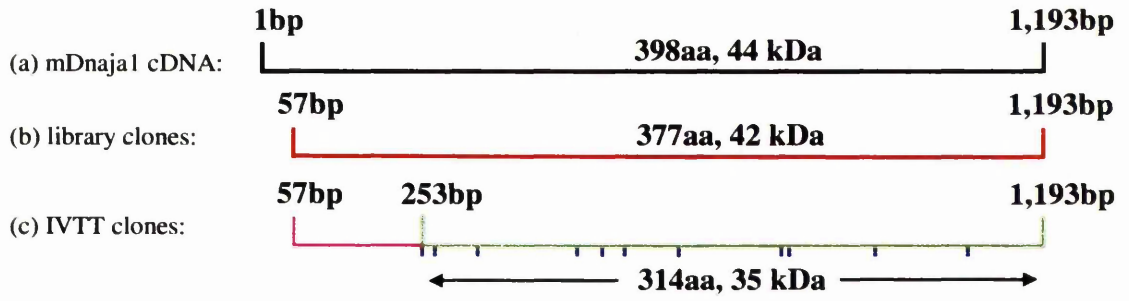

(b)

Position (in bp)	start codon sequence	Position (in bp)	start codon sequence
1 :	AAA ATG G	532 :	TGC ATG G
253 :	CCC ATG G	646 :	GGC ATG A
268 :	GAT ATG T	778 :	TTA ATG T
292 :	AGG ATG C	784 :	TGT ATG G
472 :	GGT ATG C	922 :	GGT ATG C
505 :	GGA ATG G	1072 :	GAA ATG G

Kozak consensus sequence: **ACC ATG G**

Figure 5.2. **(a)** Representation of (a) the full-length mDnaja1 cDNA (Acc no.NM_008298); (b) the two hybrid library clones 2, 5 and 13; and (c) the IVTT clones 2, 5 and 13, indicating the position of methionine residues within the cDNA sequence (shown in blue), regions of un-translated sequence (shown in pink) and regions open to translation (shown in green). **(b)** Comparison of the start codon sequences within the mDnaja1 cDNA sequence. DNA bases that match the Kozak consensus sequence directly are shown in red, while bases that do not match exactly, but are from the same family (*i.e.* purine or pyrimidine) are shown in green. The start codon at position 1 (bp) is labelled in grey as this codon is missing from all the IVTT clones.

The phosphorimage (Figure 5.4a) shows the products generated in the IVTT reactions of clones 2, 5 and 13. As predicted a protein of approximately 35 kDa was efficiently expressed from all three clones. Interestingly, a small difference in size was seen between the clones on the phosphorimage. DNA sequence analysis of the clones did not show any premature termination codons or sequence truncations, however two of the clones did contain point mutations that altered the coding sequence of the gene (Figure 5.3). This in turn may have caused a conformational change in the protein effecting its migration through the SDS-PAGE gel even after denaturation. Several shadow bands were also present on the phosphorimage for each clone that represented either degradation products of mDnaja1, or translation from downstream ATG codons.

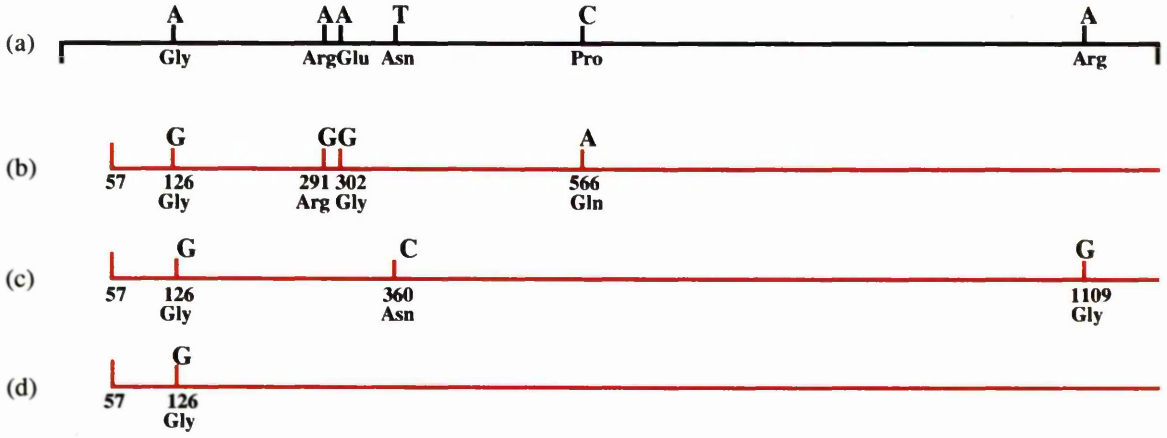

Figure 5.3. Illustration showing the point mutations occurring in each of the library cDNA clones compared to the published full-length mDnaja1 sequence (Acc number: NM_008298). (a) published sequence, (b) clone 2 (c) clone 5, and (d) clone 13.

The IVTT pull-down experiment result is shown in Figure 5.4b. Each of the test clones (clones 2, 5, and 13 shown in lanes 4, 5 and 6, respectively) produced a signal of moderate strength on the phosphorimage, which confirmed that mOGG1 and mDnaja1 interacted *in vitro*. Interestingly, none of the point mutations described above affected the protein interactions with mOGG1. Furthermore, this result also indicated that the N-terminal region of mDnaja1 (253bp; 84 aa) was not directly involved in the interaction. Once again shadow bands could be seen clearly in the pull-down experiment (lanes 4, 5 and 6). A weak signal was also seen in two of the negative controls (lanes 2 and 3) indicating that mDnaja1 interacted, though weakly, with both the Sepharose beads and GST protein bound to the beads.

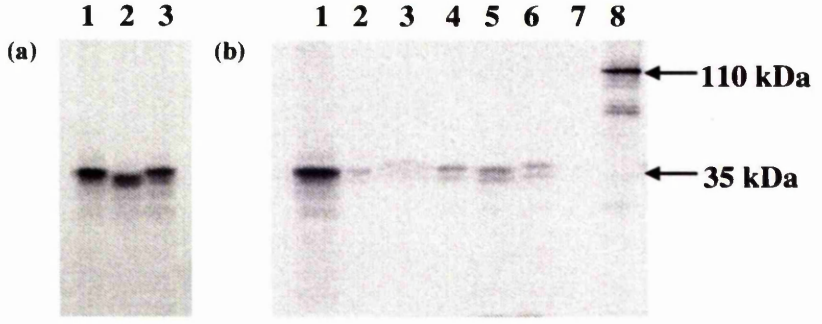

Figure 5.4. Phosphorimage of IVTT products for clones 2, 5 and 13. [^{35}S]-Met labelled proteins were expressed by *in vitro* transcription/translation. (key: The IVTT reaction from each clone is labelled as 'IVTT' followed by the clone number e.g. IVTT-2 for the IVTT reaction involving pcDNA3-clone 2. (a) Lane 1, IVTT-2; Lane 2, IVTT-5; Lane 3, IVTT-13. (b) IVTT pull-down experiment for clones 2, 5 and 13. Lane 1, IVTT-5; Lane 2, IVTT-5 incubated with beads (-ve con); Lane 3, IVTT-5 incubated with pGST-beads (-ve con); Lane 4, IVTT-2 incubated with pGST-mOGG1-beads; Lane 5, IVTT-5 incubated with pGST-mOGG1-beads; Lane 6, IVTT-13 incubated with pGST-mOGG1-beads; Lane 7, IVTT-pcDNA3 incubated with pGST-mOGG1-beads (-ve con); Lane 8, IVTT-hPMS2 incubated with pGST-hMLH1-beads (+ve con). Kaleidoscope broad-range protein markers (BioRad) were used to estimate the molecular weight of IVTT products.

5.4.2 mRanBP9

The ligation of the library clones encoding mRanBP9 proved to be more difficult since these clones contained an internal *Eco*RI restriction digest site 1009bp into the coding sequence of the full-length cDNA (Figure 5.5). Several attempts were made to ligate the 3′ terminal region of the cDNA into pcDNA3 using the internal *Eco*RI and 3′ *Xho*I sites, however, this scheme was unsuccessful for reasons unknown. A further effort was made to clone full-length cDNA by RT-PCR, using mRNA derived from mouse testes. The mRNA was reverse transcribed using a mixture of oligodT and random primers to generate the first strand cDNA, then specific primers complementary to sequences at the 5′ end (incorporating a *Bam*HI site not present in the RanBP9 sequence) and 3′ end of the gene were used for PCR. Unfortunately however, no bands were obtained despite attempts to modify both the RT-PCR and PCR conditions. Subsequently, an attempt was made to obtain the complete cDNA from the authors of the published sequence, however, unfortunately they were unable to provide a copy of the RanBP9 cDNA. With these difficulties in mind, it was decided to concentrate on the investigation of other two-hybrid clones. However, if time had allowed, several cloning schemes could be envisaged to attempt the successful cloning of RanBP9. These include PCR-based schemes, or alternatively *Eco*RI digestion of the cDNA fragment to ligate the N-terminal region of mRanBP9 into pcDNA3.

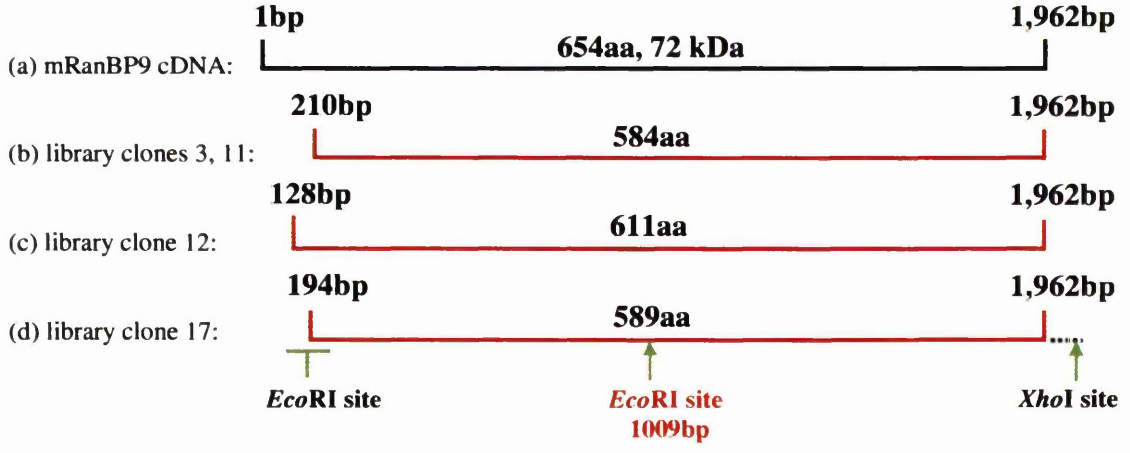

Figure 5.5. Representation of (a) the full-length cDNA encoding mRanBP9 (Acc no. NM_019930) and the four cDNA library clones that encode mRanBP9 - (b) Clones 3, 11; (c) Clone 12; and (d) Clone 17. Also marked are the 5′ *Eco*RI and 3′ *Xho*I restriction sites together with the internal *Eco*RI site (1009bp).

5.4.3 mDnaja3

The library clone encoding mDnaja3 contained an N-terminal truncation of 330bp (110aa). Therefore, prior to testing the mOGG1/mDnaja3 interaction an attempt was made to obtain the full-length cDNA. Following a literature search the full-length clone was kindly donated by Dr K. Munger, Harvard Medical School, Boston, USA. This clone was amplified by PCR and ligated into pGADT7 using *Eco*RI/*Bam*HI sites. Both the 5′ *Eco*RI and 3′ *Bam*HI restriction sites were incorporated into the design of the PCR primers. A Kozak consensus sequence (ACC ATG A) was also incorporated into the sequence flanking the ATG initiation codon of the PCR product to ensure efficient translation of the full-length clone. Expression from this codon would generate a 53 kDa protein, incorporating 8 methionine residues (Figure 5.6).

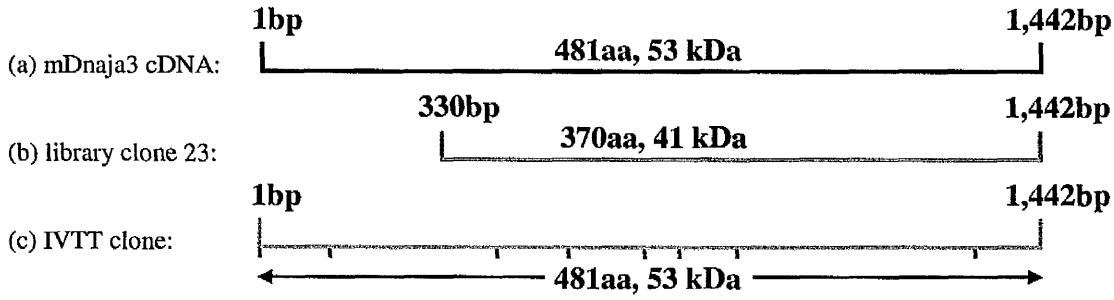

Figure 5.6. Representation of (a) the full-length cDNA encoding mDnaja3 (Acc no. NM_023646); (b) the Library clone 23; and (c) the IVTT cDNA clone, indicating the position of methionine residues within the cDNA sequence (shown in blue) and regions open to translation (shown in green).

Figure 5.7 shows the phosphorimage for the mOGG1/mDnaja3 IVTT pull-down experiment. Expression of the full-length mDnaja3 protein can be seen as a single band in lane 1. The lack of any shadow bands on the phosphorimage might be due to the incorporation of the Kozak consensus sequence providing efficient translation at the N-terminus. In the pull-down experiment, a weak signal was observed in lane 4 indicating that mOGG1 and mDnaja3 did interact *in vitro*. However, an equal interaction was seen with the Sepharose beads and a stronger interaction with the GST protein alone. Thus, these results were inconclusive and demonstrated that an alternative method was needed to test the validity of any interaction between mOGG1 and mDnaja3 (described in Chapter 6).

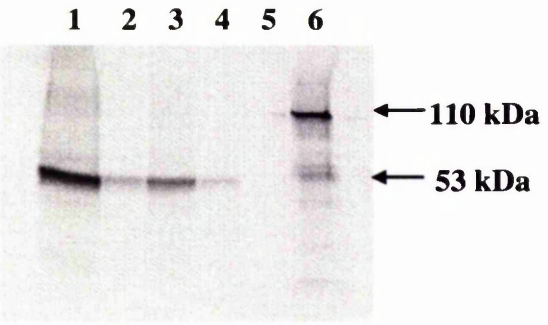

Figure 5.7. Phosphoimage of IVTT pull-down experiment for mDnaja3. Lane 1, IVTT-mDnaja3; Lane 2, IVTT-mDnaja3 incubated with beads (-ve control); Lane 3, IVTT-mDnaja3 incubated with pGST-beads (-ve control); Lane 4, IVTT-mDnaja3 incubated with pGST-mOGG1-beads; Lane 5, IVTT-pcDNA3 incubated with pGST-mOGG1-beads (-ve control); Lane 6, IVTT-hPMS2 incubated with pGST-hMLH1-beads (+ve control). Kaleidoscope broad-range protein markers (BioRad) were used to estimate the molecular weight of IVTT products.

5.4.4 Library clone 7

Library clone 7 was found to encode the C-terminal 159 aa of a RIKEN clone predicted ORF (Acc no. AK016033). However, restriction digest analysis of the DNA sequence from clone 7 revealed the presence of an internal *Eco*RI site 427bp into the coding sequence of the RIKEN cDNA (Figure 5.8). This C-terminal fragment was ligated into pcDNA3 using the internal *Eco*RI and 3′ *Xho*I sites. Further sequence analysis showed that the clone contained 4 methionine residues and would express a 70 aa (7.7 kDa) polypeptide, provided that translation was initiated at the first ATG codon (position 448 bp).

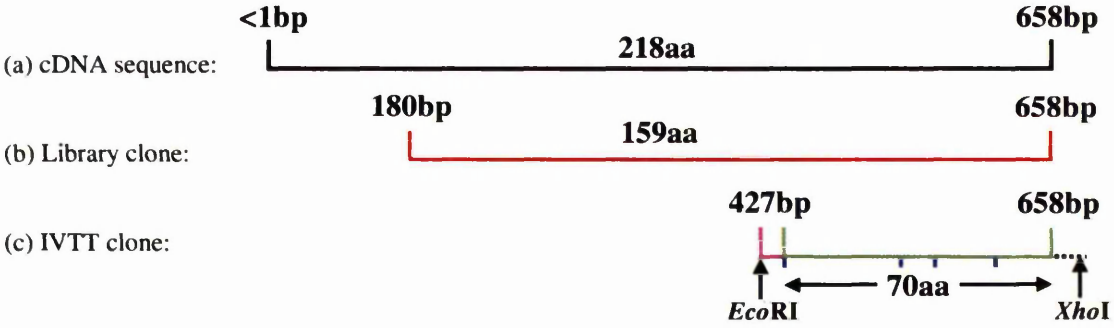

Figure 5.8. Representation of (a) the RIKEN enriched full-length cDNA (Acc no. AK016033) and (b) library clone 7 and (c) the IVTT cDNA clone, indicating the position of methionine residues within the cDNA sequence (shown in blue), regions of untranslated sequence (shown in pink) and regions open to translation (shown in green).

The results of the IVTT pull-down experiment for clone 7 are shown in Figure 5.9. As predicted a 7.7 kDa polypeptide was expressed in the IVTT reaction (lane 1). While no signal was observed in the negative controls, unfortunately the addition of GST-mOGG1 also showed no positive interactions in the pull-down experiment (lane 4). This result may have been generated for several reasons. (i) The two-hybrid interaction involving clone 7 was a false-positive and therefore was not confirmed in the IVTT experiment, (ii) the N-terminal un-translated region of this clone was necessary for the protein interaction to occur, or (iii) the incorporation of 4 methionine residues may not have generated a sufficiently strong signal to be seen in the pull-down experiment (indicated by the weak signal seen in lane 1). Therefore, an alternative method would be needed to confirm the initial yeast two-hybrid interaction for this clone.

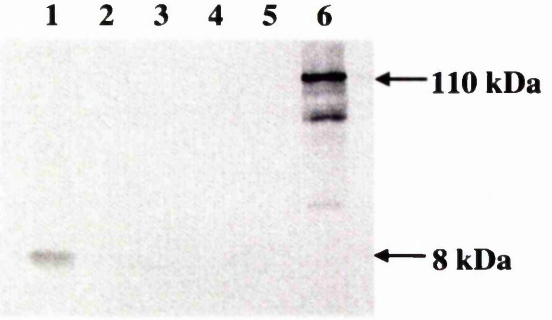

Figure 5.9. Phosphorimage of IVTT pull-down experiment for clone 7. Lane 1, IVTT-7; Lane 2, IVTT-7 incubated with beads (-ve con); Lane 3, IVTT-7 incubated with pGST-beads (-ve control); Lane 4, IVTT-7 incubated with pGST-mOGG1-beads; Lane 5, IVTT-pcDNA3 incubated with pGST-mOGG1-beads (-ve control); Lane 6, IVTT-hPMS2 incubated with pGST-hMLH1-beads (+ve control). Kaleidoscope broad-range protein markers (Biorad) were used to estimate the molecular weight of IVTT products.

5.4.5 Library clone 18

As previously discussed in Section 3.7.4 the AD fusion peptide of clone 18 was only 4 aa in length (ORF1; peptide sequence: L T F T -). However, an alternative 515 aa polypeptide was encoded in ORF3 (C-terminal 515 aa out of 533 aa protein; Acc no. NM_025851). While the pull-down experimental method was not designed to detect interactions with short peptide sequences and so could not confirm the interaction with the ORF1 product, the IVTT reaction would be expected to express the polypeptide in ORF3. Interestingly, the expression of this protein would allow the investigation of frame shift mutations in the yeast two-hybrid system, since an interaction between the polypeptide and mOGG1 in the IVTT pull-down would indicate this might have occurred in the yeast two-hybrid system via a frame shift mutation or splicing event.

In order to predict the molecular weight of proteins that would be expressed in the IVTT reaction the DNA sequence of the library clone was examined. This analysis showed that the polypeptide would be the only large polypeptide expressed in the IVTT reaction. Furthermore, the first ATG codon present in the library clone occurred 282 bp into the coding sequence and would express a 439 aa (48 kDa) protein incorporating 8 methionine residues. The downstream ATG codons present in this ORF could also initiate the expression of truncated proteins (Figure 5.10).

(a)

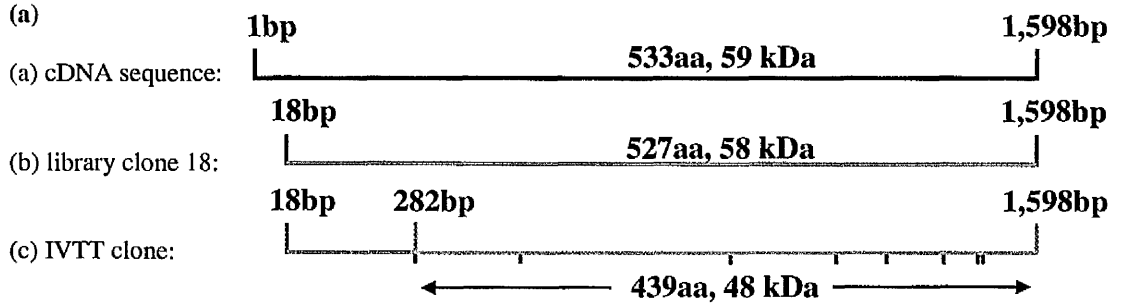

(b)

Position (in bp)	start codon sequence	Position (in bp)	start codon sequence
1 :	GCA ATG G	1221 :	AAC ATG G
282 :	GAG ATG A	1344 :	CAG ATG A
484 :	GAC ATG G	1410 :	GCG ATG G
913 :	TAC ATG G	1416 :	GAG ATG C
1110 :	AAA ATG A		

Kozak consensus sequence: **ACC ATG G**

Figure 5.10. **(a)** Representation of (a) the full-length novel cDNA sequence (Acc no. NM_02585) (b) the library clone 18; and (c) the IVTT clone indicating the position of methionine residues within the cDNA sequence (shown in blue), regions of untranslated sequence (shown in pink) and regions open to translation (shown in green). **(b)** Comparison of the start codons sequences within the novel cDNA sequence. Bases that match the Kozak consensus sequence directly are shown in red, while bases that do not match exactly but are from the same family (i.e. purine or pyrimidine) are shown in green. The start codon at position 1 is labelled in grey as this codon is missing in the IVTT clone.

Figure 5.11 shows the phosphorimage for the mOGG1/clone 18 IVTT pull-down experiment. Three bands can be seen on the phosphoimage in lane 1 generated in the IVTT reaction. The sequence data indicates that the predominant 40 kDa band was most likely expressed from the second ATG codon (484bp into the coding sequence and surrounded by a strong Kozak consensus sequence), however this data alone is not conclusive. The IVTT pull-down result raises two interesting points. First, the novel protein produced a positive interaction with mOGG1 (lane 4), although weak interactions were also observed with the negative controls (lanes 2 and 3). Second, this experiment was designed to give an indication of whether frame shift events may occur in the yeast two-hybrid system and while this result was encouraging it does not prove that the protein expressed here generated the initial yeast two-hybrid interaction. Therefore, further investigations are needed to both confirm the interaction with mOGG1 *in vivo* and to identify whether a frame shift mutation occurred in yeast with this clone.

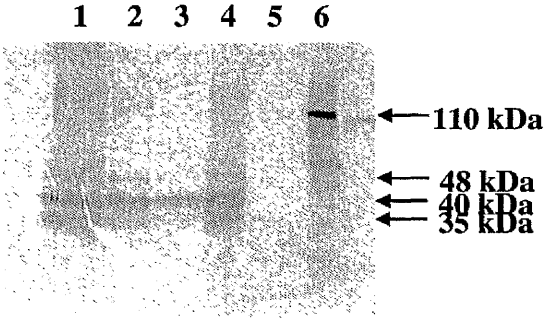

Figure 5.11. Phosphorimage of IVTT pull-down experiment for clone18. Lane 1, IVTT-clone 18; Lane 2, IVTT-clone 18 incubated with beads (-ve control); Lane 3, IVTT-clone 18 incubated with pGST-beads (-ve control); Lane 4, IVTT-clone 18 incubated with pGST-mOGG1-beads; Lane 5, IVTT-pcDNA3 incubated with pGST-mOGG1-beads (-ve control); Lane 6, IVTT-hPMS2 incubated with pGST-hMLH1-beads (+ve control). Kaleidoscope broad-range protein markers (BioRad) were used to estimate the molecular weight of IVTT products.

5.4.6 Library clone 4

The sequence analysis of clone 4 showed similar results to those seen for clone 18 with a short peptide fused to the AD (ORF1; 7 aa peptide sequence: F H I R N C L -), and suspected of generating the two-hybrid interaction, while the BLAST analysis identified a novel protein sequence in ORF2 (617 aa; Acc no. AK014463). The C-terminal 225 aa of the novel protein, containing 4 methionine residues, was encoded in the library clone. However an internal *Eco*RI site present 1,632bp into the coding sequence of the novel protein significantly reduced the size of the of the clone that was ligated into pcDNA3 and removed all of the methionine residues (Figure 5.12A). Thus, while the IVTT pull-down experiment was completed as normal, as expected no [^{35}S]-labelled products were generated from the IVTT reaction (Figure 5.12b). As with clone 18, this clone is also worth further investigation by the generation of specific constructs to test interactions with mOGG1 and the possibility of frame shift mutations in yeast.

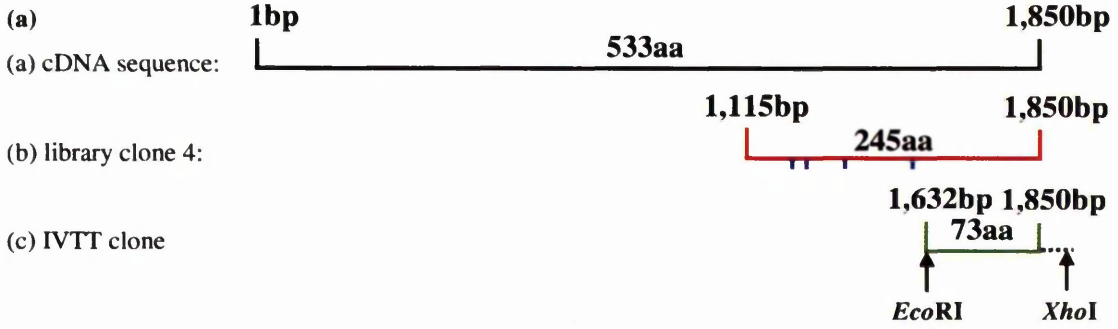

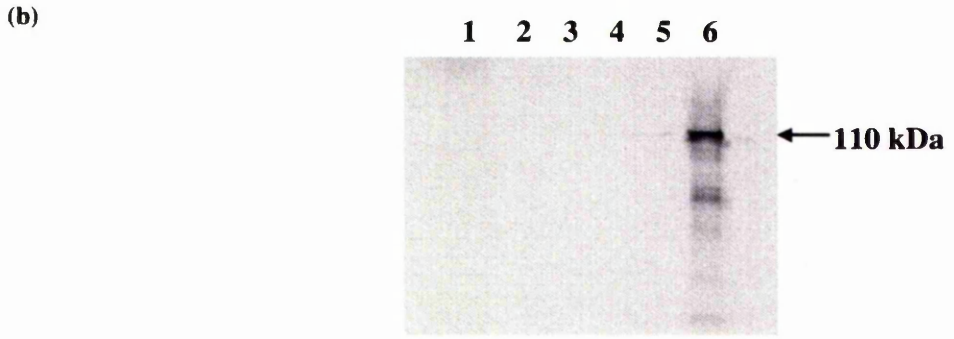

Figure 5.12. **(a)** Representation of (a) the full-length novel cDNA sequence (Acc no. AK014463) (b) the library clone 4; and (c) the IVTT clone. **(b)** Phosphorimage of IVTT pull-down experiment for clone14. Lane 1, IVTT-clone 4; Lane 2, IVTT-clone 4 incubated with beads (-ve control); Lane 3, IVTT-clone 4 incubated with pGST-beads (-ve control); Lane 4, IVTT-clone 4 incubated with pGST-mOGG1-beads; Lane 5, IVTT-pcDNA3 incubated with pGST-mOGG1-beads (-ve control); Lane 6, IVTT-hPMS2 incubated with pGST-hMLH1-beads (+ve control). Kaleidoscope broad-range protein markers (BioRad) were used to estimate the molecular weight of IVTT products. As expected no radiolabelled products were generated from the IVTT reaction (shown in lane 1), therefore all the pull-down results were also negative.

5.4.7 Remaining library clones

While all of the library clones obtained in the yeast two-hybrid screens warranted further investigation to either confirm or disprove the protein interactions with mOGG1, both time constraints and in some cases technical difficulties, made it impossible to test all of the clones using the IVTT pull-down system. Therefore, no further experiments were carried out using library clones 1, 6, 9/10, 14/15 and 8. However, each of these clones and the sequence data derived from them has been stored and are available for use in future experiments.

5.5 Summary

The IVTT pull-down experiments were used to verify positive protein-protein interactions obtained from the yeast two-hybrid screens. These experiments confirmed the interaction observed with the most frequently obtained yeast two-hybrid clone, mDnaja1. Interestingly however, doubt was cast over the interaction with the second molecular chaperone, mDnaja3, since this protein produced a weak signal for the interaction with GST-mOGG1, while reacting strongly with both the sepharose beads and the GST protein bound to the beads, suggesting a non-specific interaction.

An internal restriction site prevented the RanBP9 library cDNA being cloned and despite repeated attempts to clone the full-length cDNA by RT-PCR no success was gained. Therefore, this clone was shelved and may be investigated further at a future date. The cloning of library cDNAs 7 and 4 both resulted in a N-terminal truncation of the clones. While the polypeptide encoded in clone 7 still produced a product in the IVTT reaction, no signal was seen in the pull-down experiment possibly indicating that the interacting domain may have been lost in the truncation. Similarly, the truncation of clone 4 removed all of the methionine residues from this polypeptide and therefore no experimental results were gained.

Clone 18 provided an opportunity to study frame shift mutations and/or mRNA splicing events that might have occurred in the yeast-two hybrid experiments. Interestingly, the IVTT pull-down experiment produced a positive interaction with a polypeptide expressed from ORF3, providing circumstantial evidence for such events. However, specific 'controlled' experiments need to be designed to properly investigate whether frame-shift mutations occur in the yeast two-hybrid system. Either way, the interaction with mOGG1 indicated that this novel protein warranted further investigation.

Several of the library clones were not investigated further using the IVTT pull-down experiments for various reasons. These included insufficient amounts of DNA to clone the library inserts into pcDNA3, the presence of an internal restriction site that prevented the cloning of these cDNAs, and time constraints, which made it necessary to continue investigating clones that had produced promising results.

The IVTT pull-down experiments were designed to provide a simple and effective screen to augment the yeast two-hybrid experimental data. While this was successfully achieved, several modifications to the pull-down method would enhance any future experiments. These include, the use of a host vector that incorporates an N-terminal start codon (with Kozak consensus sequence) in frame with ORF1 of the library clones, therefore ensuring the efficient translation of the cDNA. Furthermore, some of the library inserts would have been better served by expressing the IVTT reactions with radiolabelled [^{35}S]-Leu instead of [^{35}S]-Met. However, the choice of [^{35}S]-Met in these experiments was based on the sequence analysis of the major clones that were to be tested. Finally, several of the library clones produced a significant background signal with both the Sepharose beads and GST protein bound to the sepharose beads, indicating that any results gained from these experiments should be taken only as a further indication of a protein-protein interaction, rather than a confirmation of the yeast two-hybrid results.

CHAPTER 6

6.0 Results: Investigation of protein interactions between DNA glycosylases and molecular chaperones

6.1 Introduction

While the IVTT pull-down experiments produced several interesting results that warranted further study, it was decided to concentrate the investigations on a specific set of protein interactions. Therefore, as the molecular chaperone mDnaja1 was the most frequently obtained clone in the yeast two-hybrid screens and produced a positive result in the IVTT pull-down experiment it was chosen as the primary focus for this work. Subsequently, these studies were expanded to include the second molecular chaperone, mDnaja3, and another DNA glycosylase, mNTH1. The mDnaja3 protein was obtained once in the yeast two-hybrid screens and while the IVTT pull-down experiment produced inconclusive results, this protein was included as it was a member of the DnaJ family of proteins. The DNA glycosylase, mNTH1, was cloned by RT-PCR in parallel with the attempted cloning of mRanBP9 (for RT-PCR and PCR, see Section 2.5.3). This glycosylase was included as it carries out a similar function to mOGG1 and utilises the same downstream components of the BER pathway. It was therefore argued that if the molecular chaperones interacted in complex with mOGG1 they might also interact with mNTH1. Finally, before proceeding with these experiments the entire mDnaja1 cDNA was cloned by RT-PCR, thereby producing a clone with the previously missing N-terminal region of the protein.

Ideally, the putative protein interactions obtained from the two-hybrid analysis needed to be confirmed in an *in vivo* environment, preferably by co-immunoprecipitation (co-ip) of the endogenous proteins from murine cell extracts. However, this avenue was blocked due to the lack of specific antibodies against either of the murine glycosylases, mOGG1 and mNTH1 or the chaperones mDnaja1 and mDnaja3. Therefore, as each protein would have to be artificially expressed with a peptide tag to perform the co-ip experiments, it was decided instead to use the mammalian two-hybrid system for these analyses.

6.2 The principle of the mammalian two-hybrid experiment

The mammalian two-hybrid assay is used primarily to determine the relevance of protein interactions obtained from the yeast two-hybrid system in an *in vivo* environment. While the principle behind the mammalian and yeast two-hybrid system is the same (the yeast two-hybrid system is described in Section 3.2), there are slight differences in the experimental procedures with both the constructs used and the detection of positive interactors. Both the BD- and AD-fusion constructs are generated using the pM and pVP16 vectors, respectively (Figure 6.1). The pM construct utilises the GAL4 DNA-BD (amino acids 1-147) used in the yeast two-hybrid system, while the VP16 AD (amino acids 411-455) is used in the pVP16 construct. Protein expression from both constructs is driven from the constitutive SV40 early promoter.

A dual luciferase reporter assay was used to detect protein interactions in the mammalian two-hybrid experiments. The term 'dual reporter' refers to the simultaneous expression and measurement of two individual reporter enzymes within a single system. In this experiment, firefly luciferase activity was used as the reporter to detect the protein interactions (pFR-luc vector), while renilla luciferase activity provided an internal control (pRL-TK vector), which served as the baseline response. Normalising the activity of the experimental reporter to the activity of the internal control allowed for any experimental variability caused by differences in cell viability and transfection efficiency. Furthermore, as the reporter system was plasmid based there was no specific requirement for the host cell line, therefore the murine cell line NIH 3T3 was used in these experiments.

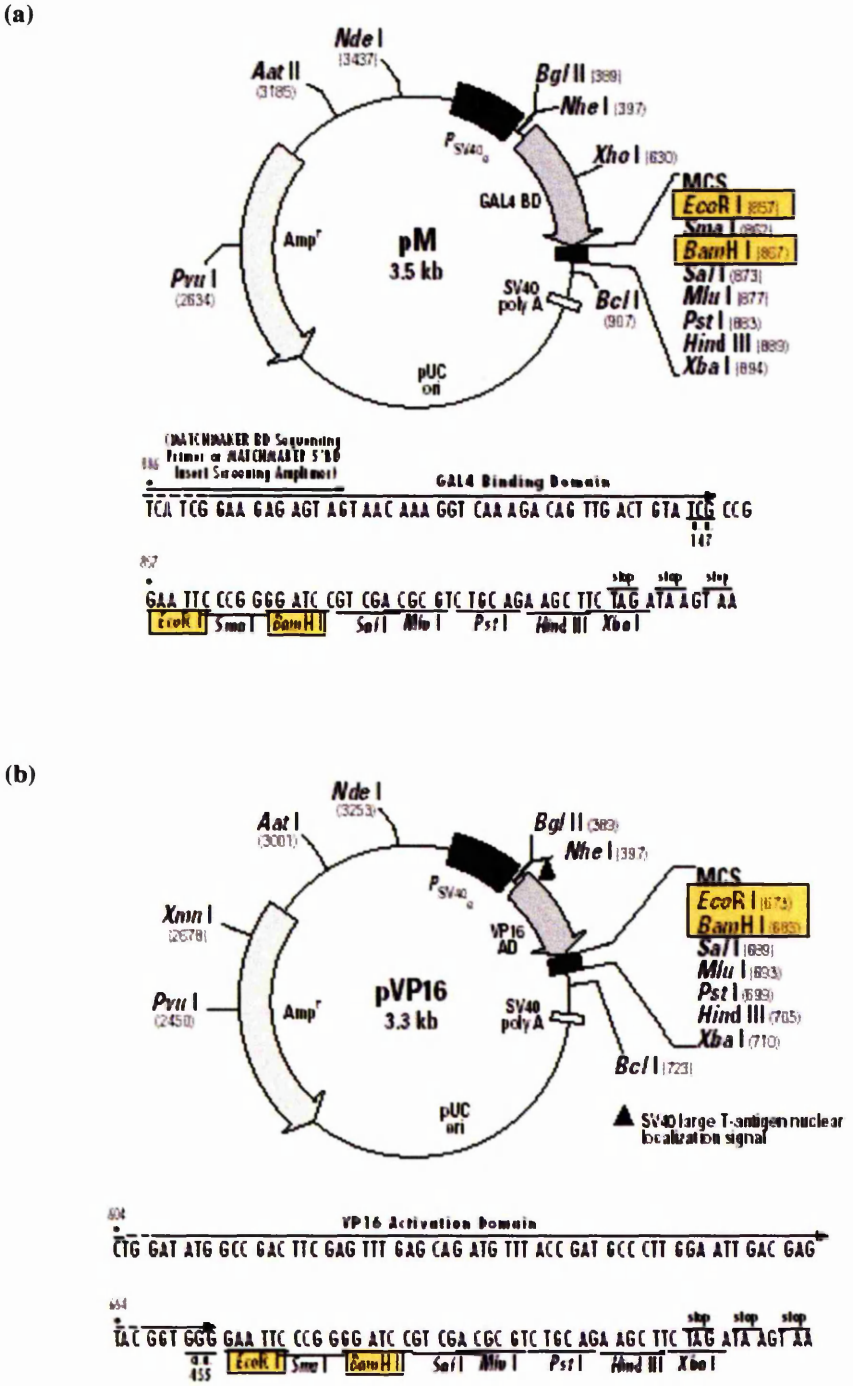

Figure 6.1. Vector map and MCS site of, (a) pM used to generate the BD-fusion proteins, and (b) pVP16 used to generate the AD-fusion proteins. The cDNA inserts were cloned into the MCS site of each vector using *Eco*RI/*Bam*HI restriction sites (yellow). The fusion proteins are expressed from a constitutive SV40 early promoter. Each vector contains an Amp^R marker for selection in *E. coli.*

6.3 Production of the mammalian two-hybrid constructs

To create both the mOGG1 and mDnaja3 mammalian two-hybrid constructs, the cDNA for each gene was excised from the respective pGBTK7 construct using *Eco*RI/*Bam*HI restriction sites and was religated into the MCS of the pM/VP16 vectors. The two cDNA sequences encoding mNTH1 and mDnaja1 were cloned by RT-PCR (as described in Section 2.5.3) and were also ligated into pM/VP16 using *Eco*RI/*Bam*HI restriction sites. Both the *Eco*RI and *Bam*HI restriction sites were engineered into the design of the 5′ and 3′ primers respectively. Correct fusion between the AD/BD and each of the cDNA inserts was confirmed by DNA sequencing, as was the fidelity of the sequences. The BD and AD mammalian two-hybrid expression vectors are shown in Figure 6.1.

In order to confirm that the fusion proteins were being expressed, each of the constructs described above was transfected into NIH 3T3 cells. After incubation at 37°C for 24 h, the cells were harvested, extracts prepared and proteins separated by SDS-PAGE. Expression of the fusion proteins was confirmed by wetsern blot analysis, using anti-GAL4 and anti-VP16 antibodies for the BD- and AD-fusion proteins, respectively (Clontech). The estimated molecular weight of each of the recombinant proteins is shown in Table 6.1. As predicted, each of the bands shown in Figure 6.2 corresponded to the correct molecular weight, confirming that each protein was being expressed as a fusion protein.

	BD	AD
mOGG1	53 kDa	43 kDa
mNTH1	48 kDa	39 kDa
mDnaja1	58 kDa	48 kDa
mDnaja3	67 kDa	57 kDa

Table 6.1. Table showing the predicted molecular weight of all BD/AD-fusion proteins used in the mammalian two-hybrid experiment.

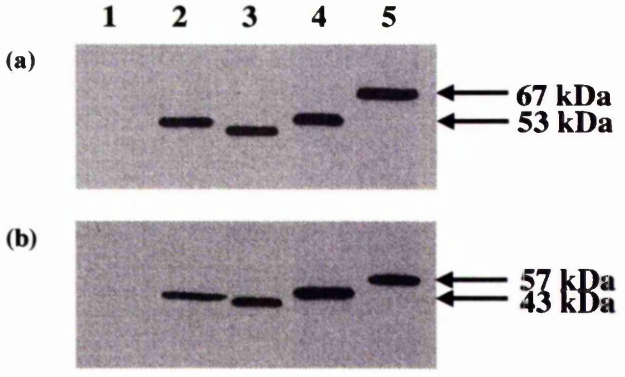

Figure 6.2. Western blot analysis of extracts from NIH 3T3 cells transfected with the mammalian two-hybrid expression constructs. (a) represents the pM constructs probed with an anti-GAL4 Ab, while (b) represents the pVP16 constructs probed with an anti-VP16 Ab. Lane 1, -ve control extract; lane 2, mOGG1; lane 3, mNTH1; lane 4, mDnaja1; lane 5, mDnaja3. The molecular weight of each protein was estimated by comparison with broad-range Kaleidoscope markers (BioRad).

6.4 Mammalian two-hybrid experiments

For each mammalian two-hybrid experiment, duplicate 6-well plates were seeded with 1.5 x 10^5 cells (NIH 3T3) per well and were incubated at 37°C for 24 h. The cells were then co-transfected with the relevant BD, AD and reporter constructs (pFR-luc and pRL-TK). After a further incubation for 24 h the cells were trypsinised, lysed and subjected to the dual luciferase reporter assay according to the manufacturer's instructions (Promega). Luciferase activity was detected using a Flash 'n' Glow luminometer (Berthold). A complete description of the mammalian two-hybrid protocol is given in Section 2.7.3.

The results of the mOGG1 and mNTH1 mammalian two-hybrid experiments are shown in Figure 6.3 and 6.4, respectively. Each of the interaction assays was performed using both the BD- and AD-fusion constructs of each protein (*i.e.* BD-mOGG1/AD-mDnaja1 and BD-mDnaja1/AD-mOGG1); a single set of control experiments was carried out for all the experiments. The relevant data sets for each interaction assay have been plotted on every graph. Furthermore, the luciferase activity readings have been corrected for the internal control.

The levels of luciferase activity observed in the mammalian two-hybrid experiments using both mOGG1 and mNTH1 indicated that neither of the DNA glycosylases interacted with either of the molecular chaperones *in vivo* under these experimental conditions. As shown by the positive control (Figures 6.3 and 6.4; lane g), a protein-protein interaction in the mammalian two-hybrid system generates a luciferase activity in excess of 100,000 fu (florescence units). However, each of the mOGG1 and mNTH1 interaction assays produced luciferase activity levels in line with the negative controls for each experiment. A similar outcome was gained when these experiments were repeated in HeLa cells, confirming that these results were reproducible in an alternative cell line (data not shown).

(a) *In vivo* interaction between mOGG1 and mDnaja1

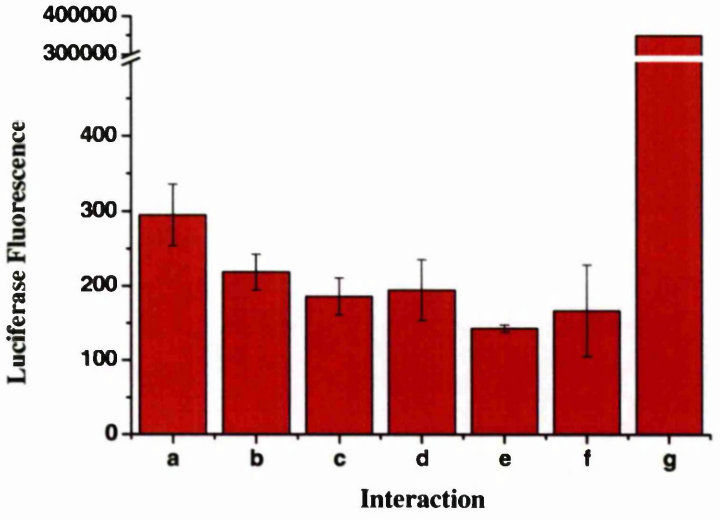

Key	BD	AD
a	mOGG1	mDnaja1
b	mDnaja1	mOGG1
c	mOGG1	AD
d	BD	mOGG1
e	mDnaja1	AD
f	BD	mDnaja1
g	p53	pT

(b) *In vivo* interaction between mOGG1 and mDnaja3

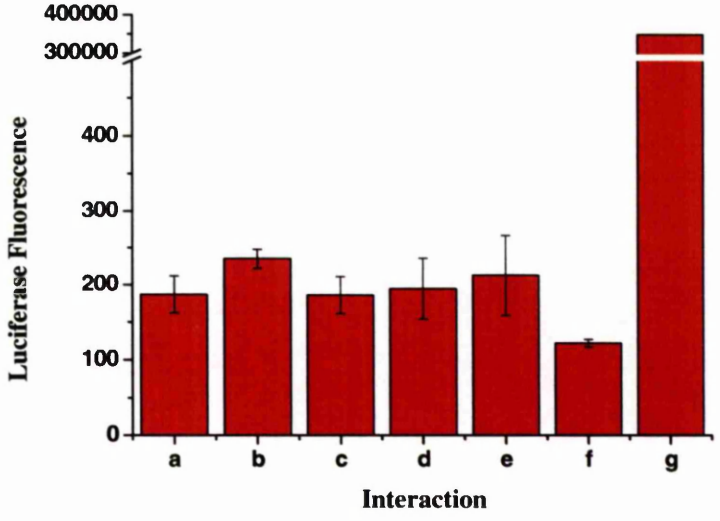

Key	BD	AD
a	mOGG1	mDnaja3
b	mDnaja3	mOGG1
c	mOGG1	AD
d	BD	mOGG1
e	mDnaja3	AD
f	BD	mDnaja3
g	p53	pT

Figure 6.3. Luciferase reporter activity determined in the mammalian two-hybrid experiments. (a) mOGG1 and mDnaja1, and (b) mOGG1 and mDnaja3.

(a) *In vivo* interaction between mNTH1 and mDnaja1

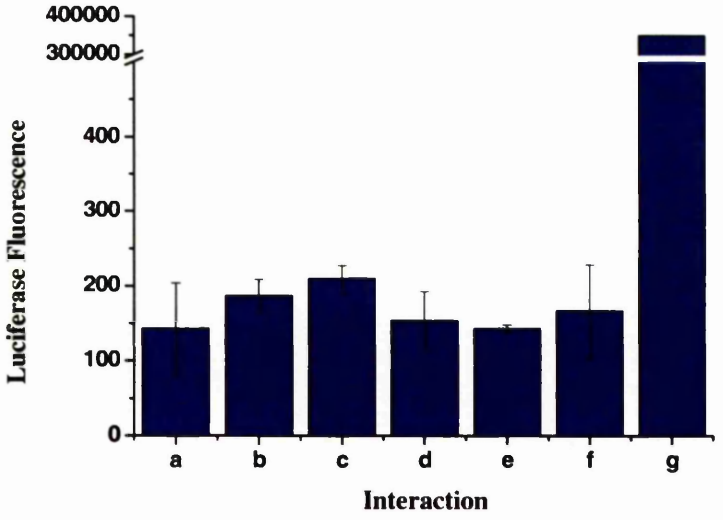

Key	BD	AD
a	mNTH1	mDnaja1
b	mDnaja1	mNTH1
c	mNTH1	AD
d	BD	mNTH1
e	mDnaja1	AD
f	BD	mDnaja1
g	p53	pT

(b) *In vivo* interaction between mNTH1 and mDnaja3

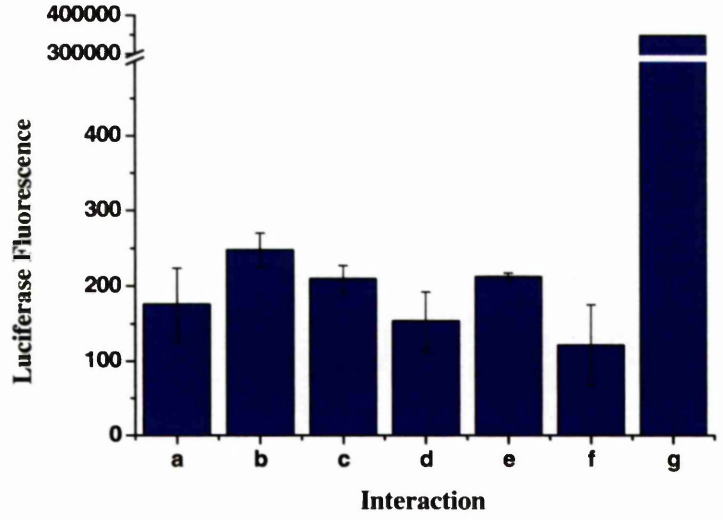

Key	BD	AD
a	mNTH1	mDnaja3
b	mDnaja3	mNTH1
c	mNTH1	AD
d	BD	mNTH1
e	mDnaja3	AD
f	BD	MDnaja3
g	p53	pT

Figure 6.4. Luciferase reporter activity determined in the mammalian two-hybrid experiments. (a) mNTH1 and mDnaja1, and (b) mNTH1 and mDnaja3.

6.5 Confirmation of mammalian two-hybrid results

The speculative nature of the experiments involving mNTH1 and mDnaja3 meant that the lack of protein-protein interactions was understandable, but the failure to detect a specific interaction between mOGG1 and mDnaja1 in this system was contrary to expectations and in contrast to the result of the yeast two-hybrid and IVTT pull-down experiments. However, DNA sequence analysis of the full-length mDnaja1 clone did leave some doubt as to the validity of the results involving this clone. While the cDNA sequences of the mOGG1, mNTH1 and mDnaja3 were all identical to the published data, the cDNA sequence of mDnaja1 did contain two point mutations (Figure 6.5). These mutations, as with those found in library clones 2 and 5, also altered the coding sequence of the gene. However, they did occur at different positions to the original mutations and therefore could have been responsible for disrupting the structure of the interacting domain of mDnaja1. A further consideration concerns the addition of the N-terminal region of mDnaja1 in these experiments, which may have altered the folding of the protein, enclosing a region of the protein that was previously involved in the protein-protein interaction.

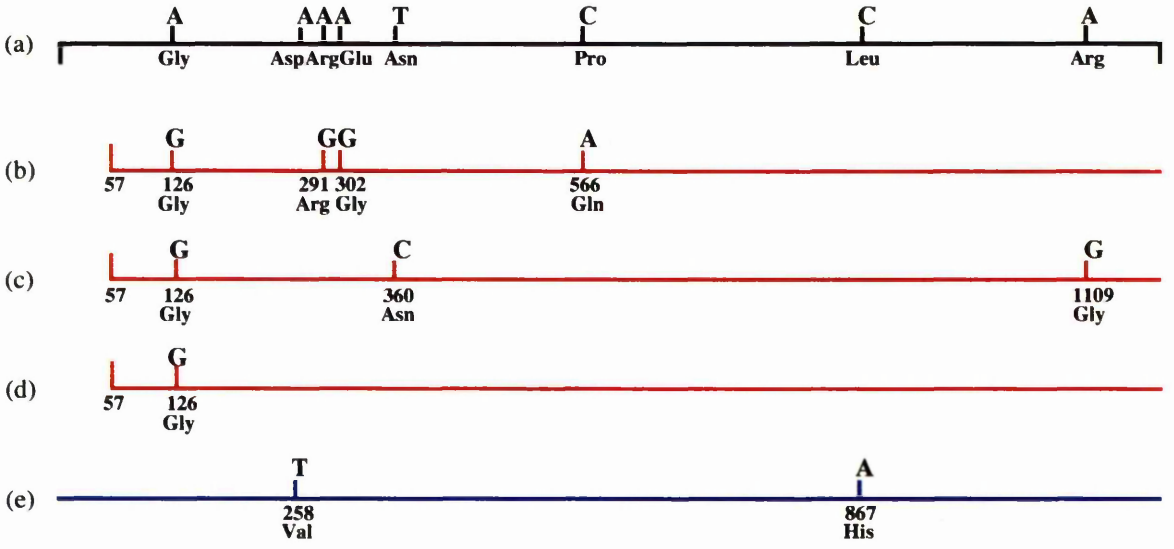

Figure 6.5. Illustration showing the position of the point mutations in each of the library cDNA clones and the mDnaja1 cDNA cloned by RT-PCR compared to the published full-length mDnaja1 sequence (Acc number: NM_008298). (a) published sequence, (b) clone 2 (c) clone 5, (d) clone 13 and (e) RT-PCR clone.

In order to explore whether the loss of interaction between mOGG1 and mDnaja1 was due to the presence of the point mutations, a cloning strategy was devised to generate a full-length mDnaja1 cDNA identical to the published sequence. This was achieved by replacing a section of the RT-PCR derived cDNA with that of the cDNA from clone 13 using an internal *Pme*I restriction site, together with the 3′ *Xho*I site (Figure 6.6). Furthermore, a second construct with a 57bp N-terminal truncation was also generated to test whether addition of the N-terminal region of the gene had disrupted the protein interaction. Each of these constructs, together with the mutated RT-PCR clone was re-tested in the mammalian two-hybrid system. However, once again the luciferase activity of the test clones was found to be in line with those of negative controls, indicating that mOGG1 and mDnaja1 did not interact *in vivo* under these experimental conditions (Figure 6.7).

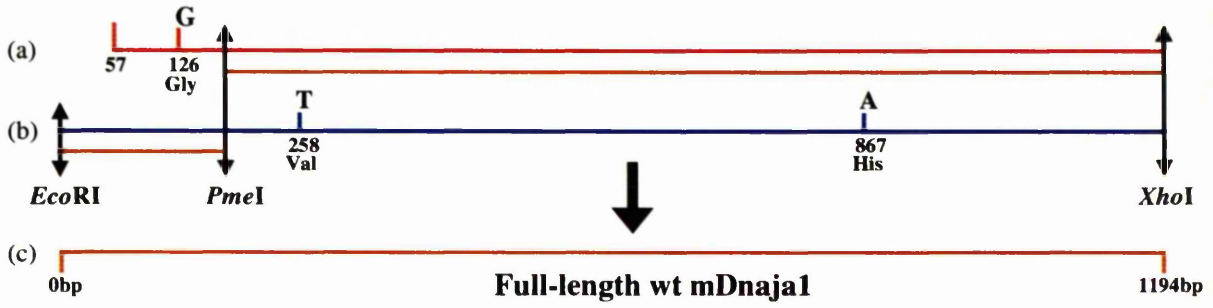

Figure 6.6. Illustration showing the cloning scheme used to create a full-length wild-type mDnaja1 cDNA clone. (a) represents the cDNA sequence of library clone 13, while (b) shows the RT-PCR clone and (c), the full-length mDnaja1 cDNA homologous to the published sequence (NM-008298).

In vivo interaction between mOGG1 and mDnaja1

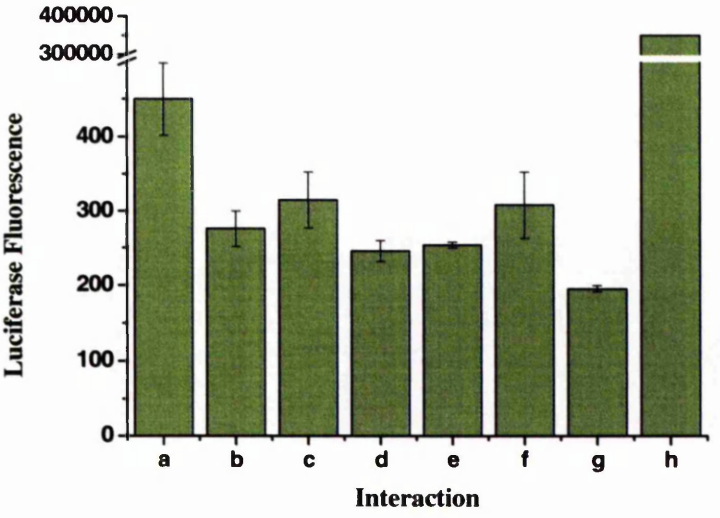

Key	BD	AD
a	mOGG1	mDnaja1 fl-Δ
b	mOGG1	mDnaja1 fl-wt
c	mOGG1	mDnaja1 trunc
d	BD	mOGG1
e	mDnaja1 fl-Δ	AD
f	mDnaja1 fl-wt	AD
g	mDnaja1 trunc	AD
h	p53	PT

Figure 6.7. Luciferase reporter activity determined in the mammalian two-hybrid experiment between mOGG1 and mDnaja1. Key: fl-Δ: full-length mDnaja1 clone containing two point mutations. fl-wt: full-length clone homologous to MN_008298. trunc: truncated version of the mDnaja1 clone.

As the *in vivo* results conflicted with the data obtained in the yeast two-hybrid and IVTT pull-down experiments, it was decided to repeat these early assays using both the N-terminal truncated, and full-length wt mDnaja1 cDNA sequences (Note: For the purpose of the following discussion, both the N-terminal truncated and full-length wt mDnaja1 cDNA sequences will be referred to as isoforms of the same sequence). To generate the yeast two-hybrid constructs, both isoforms of the mDnaja1 cDNA were excised from the respective pM constructs using *Eco*RI/*Bam*HI restriction sites and were religated into the MCSs of pGBTK7 and pGADT7 (the yeast two-hybrid BD and AD constructs, respectively).

For the yeast two-hybrid experiment, both the BD and AD constructs for both mDnaja1 isoforms were co-transformed into Y190 yeast with the corresponding mOGG1 construct. Each transformation mix was then plated onto SD-Leu-Trp-His and SD-Leu-Trp + X-gal selective media and incubated at 30°C for 10 days (complete protocol is described in Section 2.6.4). After this time, the plates were removed and the colonies examined. No colony growth was seen on the HIS selection plates and no blue colonies were formed on the X-gal plates in any of the experiments, indicating that no protein interactions had occurred (data not shown). Only the full-length wt mDnaja1 protein was tested against mOGG1 in the IVTT pull-down experiments. The expression of mDnaja1 was initiated from the T7 promoter region contained within the pGBTK7 vector. Once again the experimental procedure was carried out as described in Section 2.4.6. Figure 6.8 shows the phosphorimage of the IVTT pull-down experiment. While the mDnaja1 protein was efficiently expressed in the IVTT reaction the pull-down experiment showed no interactions with either the GST or the GST-mOGG1 protein (Figure 6.8).

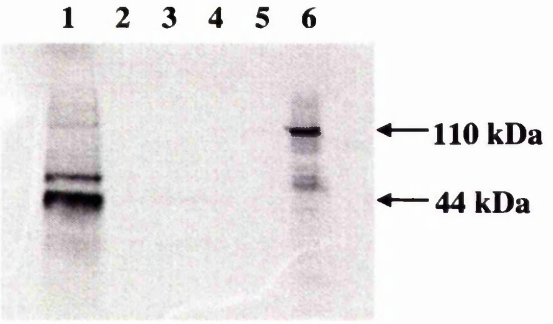

Figure 6.8. Phosphorimage of IVTT pull-down experiment for the full-length un-mutated mDnaja1 clone. Lane 1, IVTT-mDnaja1; Lane 2, IVTT-mDnaja1 incubated with beads (-ve con); Lane 3, IVTT-mDnaja1 incubated with pGST-beads (-ve con); Lane 4, IVTT-mDnaja1 incubated with pGST-mOGG1-beads; Lane 5, IVTT-pcDNA3 incubated with pGST-mOGG1-beads (-ve con); Lane 6, IVTT-hPMS2 incubated with pGST-hMLH1-beads (+ve con). Kaleidoscope broad-range protein markers (BioRad) were used to estimate the molecular weight of IVTT products.

6.6 Summary

The primary aim of the mammalian two-hybrid experiments was to further characterise, in an *in vivo* environment, the interaction between mOGG1 and mDnaja1. Prior to performing these experiments, a full-length version of the mDnaja1 cDNA was generated by RT-PCR to replace the missing 5′ region of the sequence. However, DNA sequence analysis of this clone showed that it contained two point mutations that altered the coding sequence of the gene. Therefore, a cloning strategy was devised and carried out to generate a full-length wt clone. Subsequently, both the mutant and wt mDnaja1 proteins were tested for an interaction with mOGG1 using the mammalian two-hybrid system. However, in contrast to the results of the yeast two-hybrid and IVTT pull-down experiments, no specific interaction was observed between these proteins. This result suggested that the addition of the N-terminal region of mDnaja1 might have altered the conformation of the protein such that the interaction with mOGG1 was abolished. In order to test this theory a third construct was generated that contained the N-terminal truncated version of the mDnaja1 cDNA and the experiments were repeated. However, once again no protein-protein interactions were observed using this construct.

In an attempt to clarify the effect of the N-terminal deletion, the full-length wt and truncated mDnaja1 cDNA's were re-cloned into the yeast two-hybrid vectors and both the yeast two-hybrid and IVTT pull-down experiments were repeated. However interestingly, no interactions were observed between mOGG1 and either of the mDnaja1 isoforms in the yeast two-hybrid or IVTT pull-down experiments.

In addition to the experiments involving mOGG1 and mDnaja1, the mammalian two-hybrid studies were expanded to include another DNA glycosylase, mNTH1, and the second molecular chaperone isolated from the yeast two-hybrid screens, mDnaja3. However similar to mOGG1 and mDnaja1, reciprocal experiments between each of the molecular chaperones and DNA glycosylases also failed to yield any protein-protein interactions.

Much of the data obtained in these experiments has produced conflicting results casting doubt as to the validity of the interaction between mOGG1 and mDnaja1. However, there are a series of considerations that need to be taken into account when explaining the results from each of these investigative techniques, since any number of factors may be involved in the generation or loss of protein-protein interactions. Furthermore, the cellular function of the interacting proteins must also be considered as this has an effect on how these proteins may react in various environments. These points will be elaborated in the final discussion in Chapter 8.

CHAPTER 7

7.0 Results: Analysis of mDnaja1 function in genome maintenance

7.1 Introduction

The DNA glycosylase, OGG1 has been well documented as playing an essential role in the maintenance of genomic integrity by the removal of the promutagenic lesion 8-oxodG from oxidatively damaged DNA. Cells that have loss, or have impaired function of OGG1 accumulate transversion mutations at a high frequency due to lack of repair of this lesion (Cabrera et al., 1988; Klungland et al., 1999b; Singh et al., 2001). Therefore, since the initial yeast two-hybrid and IVTT pull-down results indicated a physical and possibly functional interaction between mOGG1 and mDnaja1, it was decided to investigate if mDnaja1 also played a role in the maintenance of genomic integrity. These investigations were carried out using the *S. cerevisiae* (W303) mdj1 knockout (ko; yeast homolog of mDnaja1) and wild-type (wt) yeast strains, kindly donated by Dr E. Schwarz (University of Munich, Germany).

The mdj1 ko strain has been characterised as being temperature sensitive and exhibits a rapid loss of the mitochondrial genome at non-permissive temperatures. Furthermore, even at permissive temperatures, mitochondrial DNA may be lost (Rowley et al., 1994) (Duchniewicz et al., 1999). While respiratory activity is still maintained within these cells, the loss of mitochondrial DNA inevitably leads to compromised mitochondrial function and integrity, which in turn, leads to the release of increasing amounts of ROS (Tanaka et al., 1996). With this in mind it was decided initially to investigate the maintenance of cellular DNA integrity by comparing the frequency of spontaneous mutations generated in the mdj1 ko strain with that of the wt.

7.2 Principle of the yeast mutation analysis

Both the W303 wt and mdj1 ko yeast strains carried a single base mutation within the TRP1 gene (codon 67: TCA (Ser) to TAA (Stop). TRP1 gene is located in the nuclear genome) that prevented growth on media lacking in tryptophan. However, this codon may be restored to a serine codon by an A:T to C:G transversion mutation, initiated by the insertion of 8-oxodG opposite the central dA (Cheng et al., 1992). This property allowed the spontaneous mutation rate of each strain to be calculated in by assessing the number of Trp revertant colonies that formed from cells grown in media lacking Trp. To perform these experiments a single colony from each strain was grown in YPD to an OD_{600} of 0.6. These cells were harvested, washed in PBS and resuspended in 240 ml of SD-Trp media at a concentration of 4 x 10^5 cells/ml. The suspension was then distributed in 1 ml aliquots into each well of ten x 24 well plates and the plates were sealed and incubated at 22°C. The yeast cells settle on the bottom of each well and revertant colonies begin to appear after 6 days incubation. A cell count was taken from 3 representative wells 48 h after incubation to allow for any non-limiting residual growth in the final calculations. After 14 days incubation the wells containing Trp revertant colonies were counted (an example of a 24 well plate after 14 days incubation is shown in Figure 7.1), along with the total cell count from another 3 representative wells that did not contain any revertant colonies. The number of mutations/cell/generation was then calculated using an equation formulated by Von Borstel et al., (1971). A complete description of the protocols used in this experiment is given in Section 2.6.5.

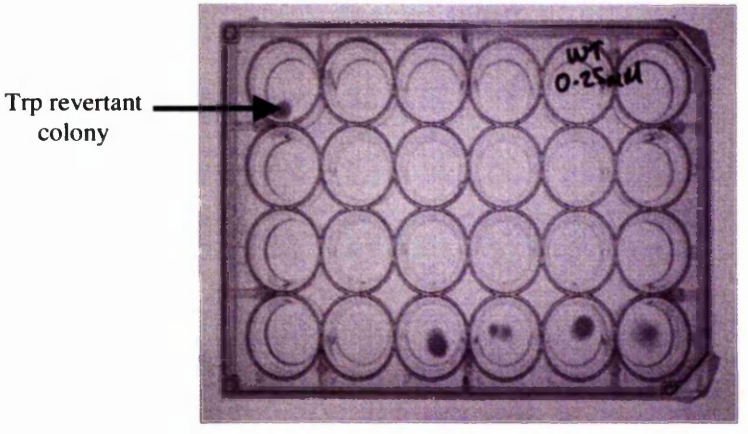

Figure 7.1. Photograph showing TRP revertant colonies formed in a 24 well plate containing W303 wt yeast after 14 days incubation at 22°C.

The following equations described by Von Borstel et al., (1971) were used to calculate the spontaneous mutation rate of each yeast strain. The results are displayed as the number of mutations/cell/generation.

Equations :

Equation (i), $e^{-m} = N_o / T$ which rearranges to $m = -\ln(N_o/T)$

Equation (ii), $M = m/2CW$

Key :

N = Number of wells with colonies after 14 days incubation.

N_o = Number of wells without colonies after 14 days incubation.

T = Total number of wells used in the experiment (240 wells).

W = Residual growth index (non-limiting residual growth after 48 hours incubation).

C = Cell count after 14 days incubation (taken from 3 representative wells that do not contain revertant yeast colonies) .

m = Average number of mutational events (taken from the total number of wells that contain mutant colonies, not the number of mutant colonies) per experiment.

M = Number of mutations/cell/generation (m/c/g).

The mutation analysis experiment was carried out in triplicate using 3 sets of 240 wells for each yeast strain. However, a single set of results from 240 wells is used in the sample calculation below. Initially, the number of wells containing Trp revertant colonies after 14 days incubation was recorded (Table 7.1). Next the non-limiting residual growth after 48 h incubation was calculated for each strain by dividing the growth after 48 h by the initial (0 h) growth (Table 7.2).

	Wt		ko	
	N	N_o	N	N_o
Expt.1	66	174	41	199

Table 7.1. Number of wells containing Trp revertant colonies from a total of 240 wells. The N_o values shown in red are used in the von Borstel calculation.

	wt	ko
0 h cell count	$4.0x10^5$ cells/ml	$4.0x10^5$ cells/ml
48 h cell count	$4.7x10^5$ cells/ml	$7.0x10^5$ cells/ml
Res. growth index (W)	1.17	1.75
14 Day cell count	$1.55x10^6$ cells/ml	$1x10^4$ cells/ml

Table 7.2. Table showing the cell counts for the 0, 48 h and 14 day time points. Each count was taken as an average from 3 representative wells that did not contain any Trp revertant colonies. The non-limiting residual growth is shown in green.

Equation (i) was then used to calculate the number of mutational events that occurred in the experiment. This was followed by the use of equation (ii) to calculate the number of mutations/cell/generation (m/c/g) for each strain. The factor of two in the denominator is necessary because the number of cell generations in the history of a culture is approximately twice the final number of cells. Finally, once the average m/c/g for all the experiments was calculated, the difference between the spontaneous mutation rates of each strain could be calculated (Equation (iii)).

Equation (i),

wt: $e^{-m} = N_o / T$ $m = -\ln(174/240)$ $\equiv m = 0.32$

ko: $e^{-m} = N_o / T$ $m = -\ln(199/240)$ $\equiv m = 0.187$

Equation (ii),

wt: $M = m/2CW = 0.32/(2 \times 1.55x10^6 \times 1.17) = 8.83x10^{-8}$ m/c/g

ko: $M = m/2CW = 0.187/(2 \times 1x10^4 \times 1.75) = 5.0x10^{-6}$ m/c/g

Equation (iii),

ko/wt $\equiv 5.0x10^{-6} / 8.83x10^{-8}$

= 57-fold increase in the mutation rate of

the mdj1 ko compared to the wt strain.

(The result shown here is one of the three experiments carried out)

7.3 Mutation analysis results.

The initial mutation analysis experiment, carried out during a visit to Dr L.J. Rasmussen's laboratory at Roskilde University, Denmark, showed an overall 65-fold increase in the spontaneous mutation rate of the mdj1 ko strain compared to the wt yeast (Figure 7.2a; The 57-fold increase shown in the example calculation was for one experiment only). However, this was unexpectedly reduced to a 1.5-fold difference on repeating the experiment in Manchester (Manchester data shown in Table 7.3). Interestingly, the change in the mutation rates was characterised by both a 5-fold increase in the wt mutation rate together with a 8-fold decrease in the ko mutation rate (Figure 7.2b). The reason behind the variation in results from Roskilde to Manchester has not been yet been elucidated as both the experimental procedure and media components used were the same. However, a further two experiments were carried out in Manchester producing similar results.

(a)

	Wt		ko	
	N	N_o	N	N_o
Expt.1	18	222	25	215

(b)

	wt	ko
0 h cell count	$4.0x10^5$ cells/ml	$4.0x10^5$ cells/ml
48 h cell count	$4.4x10^5$ cells/ml	$5.4x10^5$ cells/ml
Res. growth index (W)	1.1	1.35
14 Day cell count	$5.2x10^4$ cells/ml	$2.5x10^4$ cells/ml
m/c/g	$8.6x10^{-7}$ m/c/g	$1.17x10^{-6}$ m/c/g

Table 7.3. Mutation data from the Manchester experiments **(a)** Number of wells containing Trp revertant colonies from a total of 240 wells. **(b)** Table showing the cell counts for the 0, 48 h and 14 day time points. The non-limiting residual growth is shown in green.

In an attempt to develop a more robust assay, the 24 well plate method was replaced by plating known amounts of yeast ($1x10^8$ cells followed by a serial 10x dilution series to $1x10^3$ cells) prepared as previously described, onto SD-Trp agar plates. These plates were then incubated at 22°C and the number of revertant colonies was counted after 14 days. Furthermore, a set of cell survival plates was prepared (500 and 50 cells plated onto YPD agar) and the number of surviving colonies counted after 14 days incubation. This was used to correct the number colonies counted on the SD-Trp plates, thereby allowing the results to be calculated as the number of 'Trp revertants per 10^8 survivors' (see Section 2.6.5.2 for a complete description of this protocol). Using this method, 3 independent experiments produced a consistent 7-fold increase in the number of Trp revertants per 10^8 survivors in the mdj1 ko strain compared to the wt (Figure 7.2c).

Despite the variation in results, both the 24 well plate and SD-Trp agar plate assays showed a trend towards an increased spontaneous mutation frequency in the mdj1 ko strain compared to the wt. While these results show that the deletion of MDJ1 causes a direct increase in the number of DNA transversion mutations, it does not determine whether these mutations are generated by an increased amount of DNA lesions (generated by oxidative stress) or a reduced ability to process DNA lesions. Furthermore, while the cause of the mutagenic damage was not determined by this experiment, these results do compare favourably with the published data that shows the deletion of MDJ1 results in aberrant mitochondrial function and ultimately the generation of increasing amounts of ROS, which in turn, may cause mutagenic DNA damage.

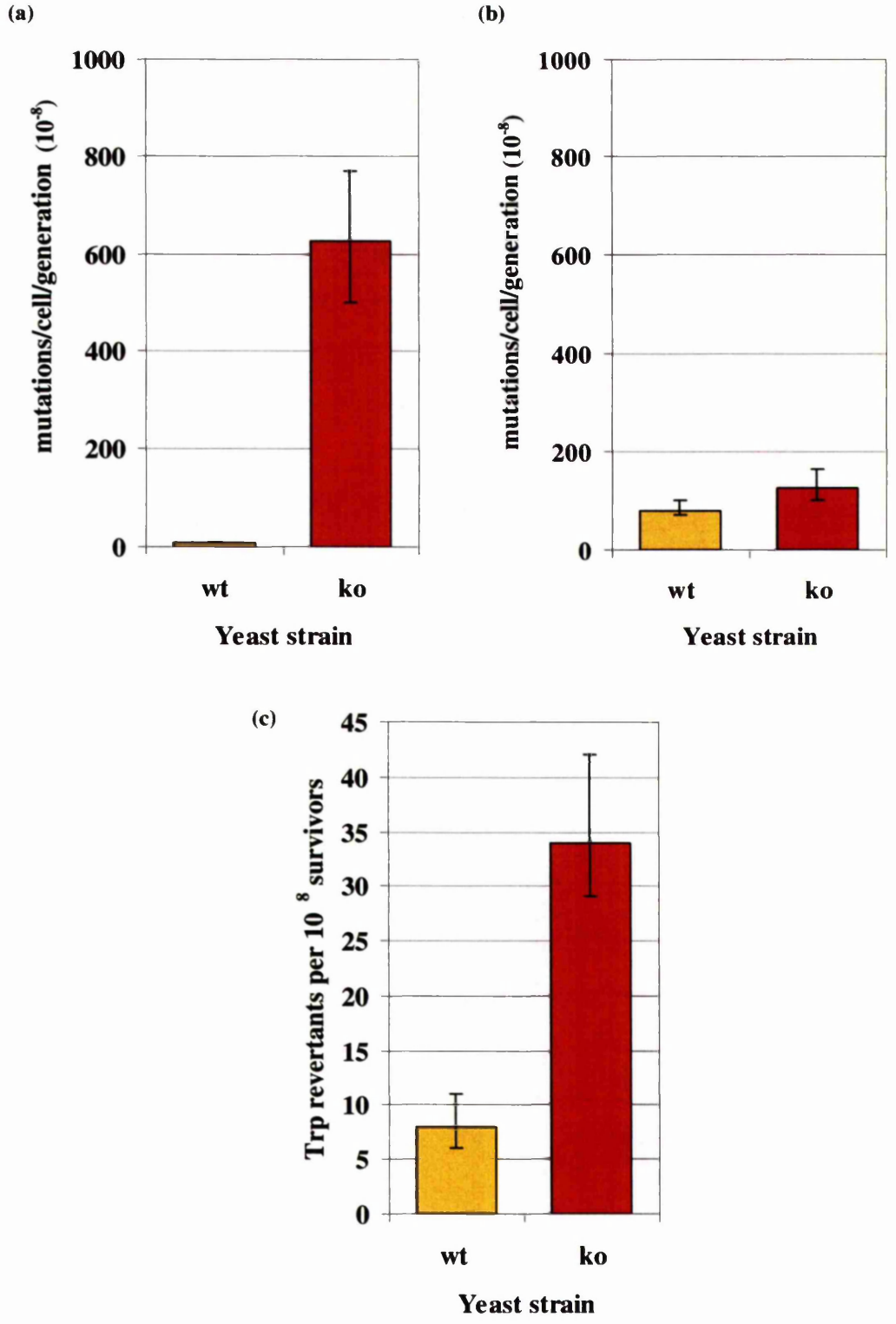

Figure 7.2. Analysis of spontaneous mutation frequency in W303 wt and mdj1 ko *S. cerevisiae* (a) Initial 24 well plate mutation analysis experiment carried out in Roskilde. (b) Repeat experiment carried out in Manchester. (c) SD-Trp agar plate assay.

7.4 Effect of oxidative DNA damage on mutation rates

As the role of MDJ1 in the maintenance of genomic stability is unclear, it was decided to investigate the effect of the MDJ1 deletion on the ability of cells to repair oxidative DNA damage. To this end, the two yeast strains (mdj1 ko and W303 wt) were treated with an oxidative DNA damaging agent (H_2O_2, 0-5 mM; see Section 2.6.5.3 for H_2O_2 treatment protocol), and the 24 well plate, and SD-Trp agar plate, mutation experiments were repeated. The results for the 24 well plate assay are shown in Figure 7.3a. The results showed a slight increase in the mutation rate of both strains up to a concentration of 0.5 mM H_2O_2, however, the difference in the mutation rates between the strains remained similar. This suggested that while the deletion of MDJ1 had increased the overall mutation rate, it had no marked affect on the ability of cells to repair induced oxidative DNA damage. However, once the H_2O_2 concentrations increased above 0.5 mM, the wt cells displayed a decrease in the mutation rate towards the base-line level, while the ko strain recovered less effectively (Figure 7.3a). While further experiments are needed to investigate this result, one explanation might be that the level of DNA damage occurring above 0.5 mM H_2O_2 became more significant, therefore inducing an upregulation of DNA repair activities, including oxidative scavengers. However, in the ko strain the loss of MDJ1 impaired the ability of these cells to cope with the increased damage indicating that MDJ1 might indeed play a role in the repair of oxidative DNA damage.

After treatment with 5 mM H_2O_2 no viable cells remained from either strain in the mutation analysis experiment. Furthermore, the cell survival data for this experiment showed that H_2O_2 treatment had a severe effect on the survival of both strains, with an initial drop to 20% (Figure 7.3b). Following the increase in H_2O_2 concentration, the wt yeast did show a marginal growth advantage up to 5 mM at which dose the survival for both strains dropped to less than 5 %.

Unfortunately it was not possible to repeat this experiment using the SD-Trp agar plate assay. After the yeast were treated with H_2O_2 the numbers of colonies counted on both the SD-Trp plates and the YPD control plates were erratic thus preventing any meaningful mutation rates to be calculated. This problem was not resolved and so no statistical calculations could be carried out.

(a)

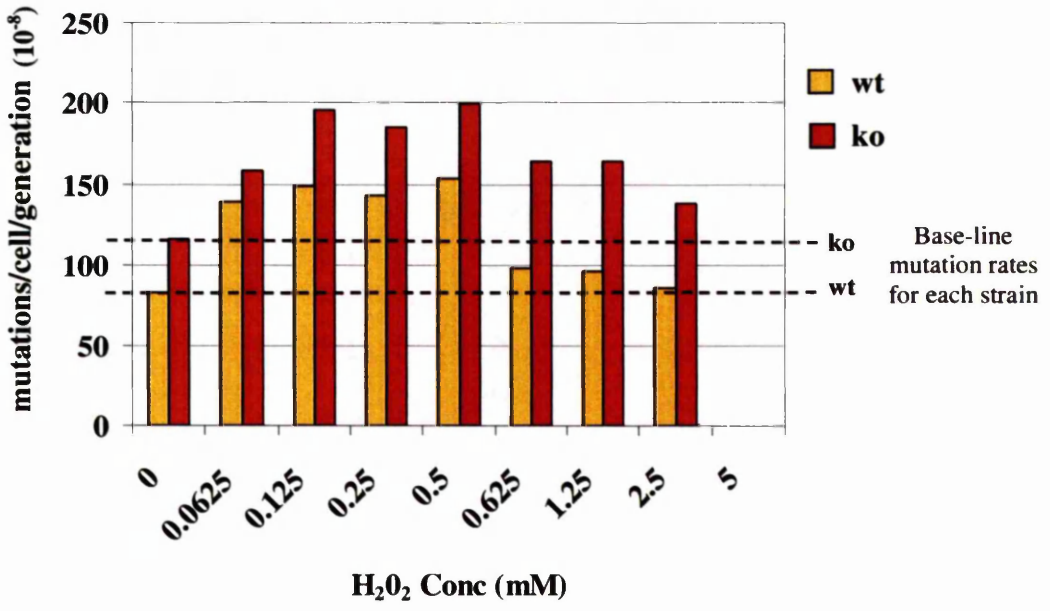

(b)

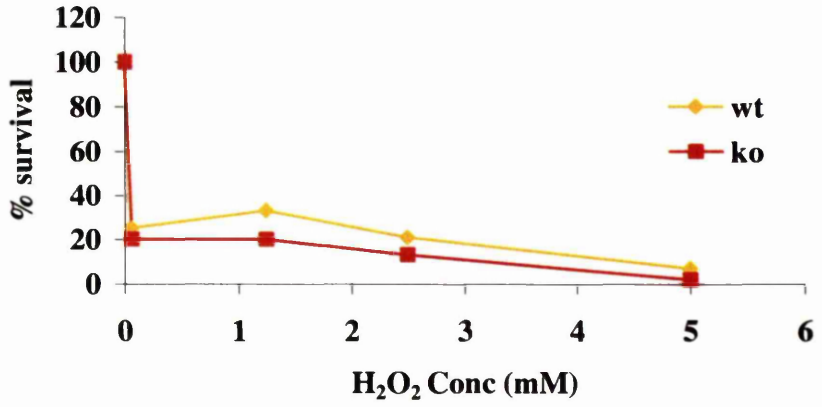

Figure 7.3. (a) 24 well plate mutation analysis experiment using W303 wt and mdj1 ko *S. cerevisiae* treated with H_2O_2 (0-5mM) (b) Cell survival assay of W303 wt and mdj1 ko *S. cerevisiae* following treatment with H_2O_2 (0-5mM).

7.5 Analysis of OGG1 activity

As the mutation analysis experiments suggested that the mdj1 ko yeast has a reduced ability to repair oxidative DNA damage, it was decided to determine the activity levels of yOGG1 in extracts prepared from each strain. To perform these experiments, a single colony from each strain was grown in YPD to an OD_{600} of 0.6. The cells were harvested, washed in PBS and cell extracts were prepared as described in Section 2.4.7. The 8-oxodG [^{32}P]-oligo substrate was then incubated at 30°C with either 20 μg or 40 μg of extract from each strain and aliquots were removed after 0, 1, 4 and 24 h. These samples were analysed by denaturing PAGE and the results are shown in Figure 7.4. Interestingly, the ko strain showed a 35% increase in cleavage activity over the wt strain indicating a significant upregulation of yOGG1 in these cells. This result suggested that the ko cells were experiencing an increased level of oxidative DNA damage under normal growth conditions than the wt. However, despite the increase in DNA repair activity the ko strain exhibited a higher mutation rate that the wt.

Indeed as previously discussed, the deletion of MDJ1 may well generate aberrant mitochondrial function resulting in an increase in the level of endogenous ROS being formed, which not only generates mutagenic DNA damage, but also raises the levels of oxidative stress and leads to an induction of DNA repair enzymes, including yOGG1. However, the mutation data also suggested an inability of these cells to deal with increasing oxidative damage efficiently and therefore the deletion of MDJ1 may also decrease the efficiency of the BER pathway directly via the loss of protein-protein interactions. This effect would not be shown in the OGG1 glycosylase assay as this system only shows the activity levels of yOGG1 rather than the efficiency of the whole BER pathway.

(a)

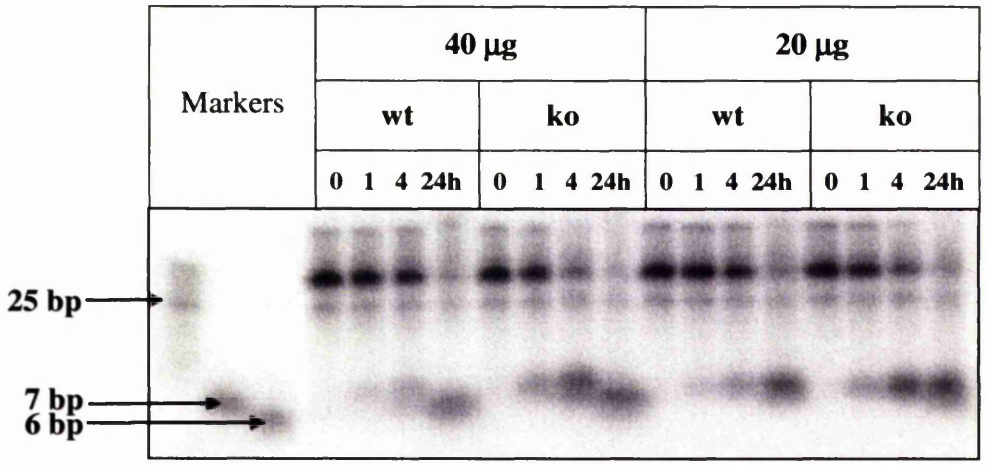

(b)

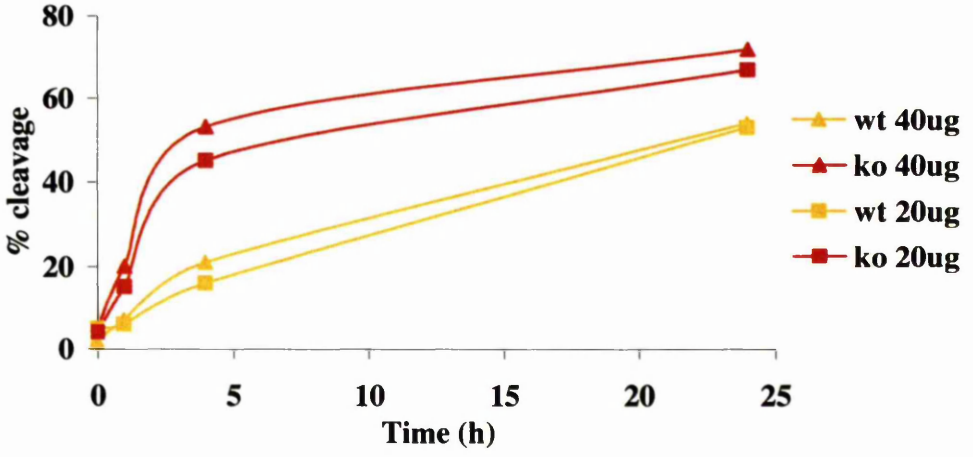

Figure 7.4. (a) Phosphorimage of OGG1 activity assay performed using 20 µg and 40 µg of yeast extract from W303 wt and mdj1 ko *S. cerevisiae*. (b) Cleavage activity of the extracts calculated by image analysis of the phosphorimage and expressed as % of substrate cleaved.

7.6 Summary

In summary, these experiments showed that the deletion of MDJ1 leads to an increase in the number of spontaneous mutations generated in nuclear DNA, indicating that MDJ1 is involved in the maintenance of genomic stability. However, this preliminary data does not allow any conclusions to be drawn regarding the exact role of MDJ1 in this respect, nor the cause of the increased mutation rate. From the literature, it is tempting to speculate that the deletion of MDJ1 and resulting mitochondrial DNA loss leads to an increase in the amount of ROS and thus mutagenic damage. However, an alternative explanantion could include an inability of the DNA repair mechanisms to effectively process base lesions without the presence of MDJ1. Indeed the upregulation of yOGG1 activity in this strain, which indicates an upregulation of the cellular defence pathways, in tandem with the inability of the ko strain to deal with increasing amounts of oxidative stress (by treatment with H_2O_2) tend towards the latter explanation. Despite these speculations, it is accepted that the data provided here is insufficient to draw any convincing conclusions and that any number of events could account for these results.

While time constraints did not allow the continuation of these experiments, a number of avenues are still open to investigation that could answer some of the questions described above. Analysis of the number of oxidative lesions contained within the genomes of the respective strains would provide an insight into the levels of cellular oxidative stress and may help to determine the source of the DNA mutations. Alternatively, repeating the mutation analysis experiments after treatment of the strains with a ROS scavenger (such as TEMPO) may provide similar information. With respect to mDnaja1 the mutation analysis experiments also need to be repeated in a mdj1 ko strain complemented with the mDnaja1 cDNA. Indeed the yeast constructs for this experiment have been made.

CHAPTER 8

8.0 Discussion

8.1 Introduction

While a significant amount of evidence has been gathered that indicates BER components interact to form a protein complex, these studies have only been carried out using BER proteins that are involved in the latter stages of repair (see Sections 1.7.1 and 1.9). Therefore, the aim of this study was to investigate whether BER DNA glycosylases, which act in the first step of the repair pathway, interact with any protein partners that may facilitate or regulate their activities to allow the efficient excision of base lesions, and/or promote the completion of the repair process.

A variety of methods are available to investigate protein-protein interactions, and it was decided to carry out these studies using the yeast-two hybrid system. This provides a simple method to both detect and identify novel proteins that might interact with the glycosylases. Furthermore, as a significant amount of DNA repair studies were being carried out using murine models within the department, these experiments were performed using murine homologs. Both the number and diversity of DNA glycosylases made it impossible to study all of these proteins, therefore two glycosylases, APNG and OGG1, were chosen to represent the mono-functional and bi-functional glycosylase families, respectively. OGG1 is involved in the repair of 8-oxodG:C, while APNG repairs various modifed purines (see Sections 1.8.1 and 1.8.4).

8.2 Summary of protein-protein interaction experiments

The cDNAs encoding murine OGG1 and APNG were used to screen a mouse testes cDNA library for novel protein partners. However, the co-expression of a library protein with APNG in yeast proved to be cytotoxic and consequently no two-hybrid interactions were observed. The reasons for this toxicity and possible solutions to the problem are discussed in detail in Section 3.7.1. In contrast, co-expression with mOGG1 did not result in the same toxicity and 24 two-hybrid interacting clones were obtained. Within these clones, two molecular chaperones, mDnaja1 (Section 3.7.2.1) and mDnaja3 (Section 3.7.2.3) were identified, with mDnaja1 being the most frequently occurring clone obtained from the library screen. DNA sequence analysis showed that each of the

cDNA clones encoding mDnaja1 and mDnaja3 contained N-terminal truncations. However, a subsequent literature search allowed the full-length mDnaja3 cDNA to be obtained from a collaborating laboratory. In addition to the molecular chaperones, a novel Ran binding protein, RanBP9 (Section 3.7.2.2), whose function has not yet been characterised, was also identified, as well as a number of novel or unknown cDNA sequences. Of these sequences, all but library clones 7 and 8 were predicted to encode short peptides in frame with the AD (a detailed discussion of these clones is given in Sections 3.7.2.4 and 3.7.2.5).

From the 24 two-hybrid clones, selected library cDNAs were re-cloned in order to further characterise the protein-protein interactions using IVTT pull-down experiments. These experiments confirmed the two-hybrid interaction between mOGG1 and mDnaja1 (N-ternimal truncated protein; Section 5.4.1). Similarly, an interaction was also observed between mOGG1 and mDnaja3 (full-length protein; Section 5.4.3), although the strength of this interaction was considerably weaker. A number of other two-hybrid clones were also tested using the IVTT pull-down method (see Sections 5.4.4-7). However, of these, only clone 18 produced a positive interaction with mOGG1 (Section 5.4.5). Furthermore, the IVTT pull-down interaction was generated from a novel protein expressed from an alternative ORF to that of the short AD fusion peptide. While time constraints did not allow this interaction to be characterised further, this experiment may be carried out in future studies. In addition, investigations should also be carried out to determine whether the presence of this novel protein, and subsequent interaction with mOGG1 in the IVTT pull-down experiment was fortuitous, or whether this protein was also responsible for the yeast two-hybrid interaction. Indeed, this might have occurred via a splicing event within the yeast that allowed the expression of this alternative ORF in fusion with the AD (see Section 3.7.2.5).

The IVTT pull-down experiments involving the remaining library clones did not produce any positive interactions (for a detailed description of these clones see Sections 5.4.4 and 5.4.6-7). However, these results should not necessarily be interpreted as suggesting that this set of clones represented false-positive two-hybrid interactions, since alternative cloning strategies and/or the use of a different metabolic label (for

example, [^{35}S]-Leu), might have produced results that differed to those observed in this study.

Following the yeast two-hybrid and IVTT pull-down experiments it was necessary to test the protein-protein interactions *in vivo*. These studies were conducted using the mammalian two-hybrid system. Included in this investigation was a second DNA glycosylase, mNTH1, and a full-length version of the mDnaja1 cDNA, both of which were cloned by RT-PCR. Reciprocal mammalian two-hybrid experiments were carried out between both DNA glycosylases and molecular chaperones, which included the use of both the N-terminal truncated and full-length mDnaja1 cDNA sequences. However, these experiments failed to produce a two-hybrid interaction between any of the test proteins. The speculative nature of the experiments involving mNTH1 and mDnaja3 meant that the lack of protein-protein interactions was understandable, but the failure to detect a specific interaction between mOGG1 and mDnaja1 was contrary to expectations and in contrast to the results obtained in the yeast two-hybrid and IVTT pull-down experiments. Therefore, it was decided to repeat these early experiments using the newly cloned full-length mDnaja1 cDNA. However, neither the yeast two-hybrid, nor IVTT pull-down experiments showed any protein-protein interactions between mOGG1 and mDnaja1.

In summary, while mOGG1 was found to interact with a variety of polypeptides and short peptides in the yeast two-hybrid screens, the subsequent confirmation of these interactions has proved difficult to obtain. Interestingly, a yeast two-hybrid analysis using the human homolog of OGG1 has produced a similar situation (Radicella J.P, personal communication), raising the possibility that either OGG1 does not interact with any other proteins, or alternatively, that the yeast two-hybrid system is unsuitable for the investigation of weak or transient protein interactions between OGG1 and other targets.

In particular, the observed interaction between mOGG1 and mDnaja1 is open to speculation. To date, the yeast-two hybrid and IVTT pull-down results suggest that the N-terminal truncation of mDnaja1 facilitated the interaction with mOGG1, as no interaction was observed when using the full-length protein. Indeed, it is possible that

an internalised hydrophobic region of mDnaja1 was exposed by the truncation, which allowed this interaction to occur. Alternatively, the truncation may have generated a conformational change in mDnaja1 that produced a similar effect. If this were the case, the interaction between mOGG1 and mDnaja1 would be non-specific and classed as a false-positive interaction. Similarly, this argument could be used explain the loss of protein-protein interactions observed between mOGG1 and mDnaja3 in the mammalian two-hybrid experiment.

Interestingly, neither the full-length, nor truncated mDnaja1 proteins interacted with mOGG1 in the mammalian two-hybrid experiments. This result is not easily explained. However, the contrived detection methods used by the two-hybrid and IVTT pull-down experiments to identify protein-protein interactions, leaves the possibility that some interactions may not be detectable using all of these techniques. Indeed, as previously alluded to in Sections 3.6 and 6.1, a consideration for each of these experiments is the effects of steric hindrance generated by the various fusion domains. As the fusion domains differ in each of the experiments, so will the effect this has on the protein-protein interactions. The problems described above and others associated with using both the two-hybrid and *in vitro* pull-down methods have been reviewed by Guarente (1993) and Fields and Sternglanz (1994).

A further consideration in the interpretation of the results involves the biochemical function of the molecular chaperones. Both mDnaja1 and mDnaja3 belong to the HSP40 family of proteins. In concert with HSP70 and HSP90, the HSP40 chaperones assist newly synthesised proteins to fold or to translocate through membranes, stabilise certain protein conformations and help to eliminate denatured proteins by targeting them for degradation. In addition, the HSP40 proteins have also been shown to prevent the aggregation of denatured and/or mis-folded proteins (Helmbrecht et al., 2000; Jolly and Morimoto, 2000). Therefore, as the yeast two-hybrid and IVTT pull-down experiments involve either the expression or presence of significant amounts of mOGG1 in a "foreign" environment, a potential exists for the molecular chaperones to bind any aggregated or mis-folded protein, thus generating a positive protein-protein interaction. Furthermore, as the proteins expressed in the mammalian two-hybrid experiments are of murine origin, there is a greater likelyhood that all of the protein was folded correctly

and therefore, no interactions were observed using this technique (Guarente., 1993; Fields and Sternglanz., 1994). Alternatively, the interaction might have occurred as a consequence of the molecular chaperone role of mDnaja1 in transporting newly synthesised proteins across the mitochondrial membrane. While such interactions hold little relevance for the functional activity of mOGG1, it would represent a functional property of the molecular chaperones.

In addition to the yeast two-hybrid investigations, recombinant mOGG1 was purified to provide protein for use in the IVTT pull-down experiments, OGG1 glycosylase activity assays, and for the production of anti-mOGG1 antibodies. While the initial effort to purify this protein using a His-tag system resulted in low protein yields, recombinant mOGG1 (and subsequently hOGG1a) was eventually purified using a GST-tag system. Furthermore, the subsequent functional assay of GST-mOGG1 gave rise to the discovery of a novel δ-elimination activity for this protein, currently under investigation within the department (Elder R.H., Parsons. J.P., personal communication). Intriguingly, this activity was not observed in the human homolog. Unfortunately, the cleavage of the GST-tag by thrombin digestion resulted in the partial degradation of both the mOGG1 and hOGG1a proteins, while the engineered thrombin site was found to be resistant to cleavage. Although the fusion with the GST-tag was convenient for the IVTT pull-down experiment, it was not ideal as an immunogen for obtaining specific anti-m/hOGG1 antibodies (see Section 4.4). Therefore, this line of investigation was not pursued further at this time. If anti-m/hOGG1 antibodies had been available, these would have been used to perform co-immunoprecipitation (see Scetion 8.5) and co-localisation experiments using endogenous mOGG1 in an attempt to confirm the yeast two-hybrid and IVTT pull-down results.

While investigating the physical interactions between mOGG1 and mDnaja1, a set of preliminary investigations was undertaken to examine whether mDnaja1 played a role in genomic integrity. These studies were carried out by investigating differences in the spontaneous mutation rates between the *S. cerevisiae* W303 MDJ1 knockout (yeast homolog of mDnaja1) and wild-type strains. The deletion of MDJ1 had previously been shown to result in aberrant mitochondrial function, and ultimately led to an increased generation of ROS (Duchniewicz et al., 1999; Tanaka et al., 1996). The mutation

analysis experiments showed that the deletion of MDJ1 also resulted in a direct increase in the number of transversion mutations over the wild-type, indicating that MDJ1 is involved in the maintenance of genomic stability. However, these initial experiments did not allow any conclusions to be drawn regarding the exact role of MDJ1 in this respect, nor the cause of the increased mutation rate. Although this may have occurred as a result of aberrant mitochondrial function leading to an increase in the amount of ROS and thus DNA lesions, or a reduced ability of the DNA repair mechanisms to process DNA lesions. To investigate the effects of the deletion on DNA repair, the yeast strains were treated with an oxidising agent (H_2O_2). The results indicated that the ko strain exhibited a reduced DNA repair capacity at higher levels of oxidative stress (above 0.5 mM H_2O_2). However, this result was made more interesting by the finding that the ko strain exhibited an up regulation of yOGG1 activity in cell extracts, indicating an up regulation of DNA repair pathways. In order to draw any meaningful conclusions from this preliminary study, a series of experiments would have to be performed. These are described in Section 7.6.

8.3 DNA repair and Heat-shock proteins

While the results obtained for the interaction between mOGG1 and the molecular chaperones, mDnaja1 and mDnaja3, are still open to interpretation, there is accumulating evidence indicating an involvement of molecular chaperones in DNA repair. Indeed, a number of studies have linked an up-regulation in the levels of HSPs (via the heat shock response) with a resistance to oxidative stress. Heat shock proteins have been shown to confer protection in a global manner by the prevention of protein denaturation, the subsequent renaturation of stress damaged proteins, and the ubiquitination of proteins that are toxic to cells (Finley and Chau, 1991). Furthermore, the induction of HSPs, prior to inducing oxidative damage has been shown not only to increase cell survival, but also to increase the level of DNA repair activity (Keszenman et al., 2000; Mitchel and Morrison, 1982; Mitchel and Morrison, 1983). Following these findings, subsequent studies have identified a direct association between HSPs and both the NER and BER pathways. In *E. coli*, these investigations demonstrated that the conformation of heat-labile NER proteins was stabilised by the presence of HSPs. Furthermore, after heat-denaturation these proteins could be refolded, restoring complete function. Interestingly, under non-stressful conditions the addition of HSPs

was also found to increase the efficiency of NER *in vitro*, while in contrast, a DnaK (HSP70 homolog) deletion strain showed a significant decrease in survival following treatment with UV, as well as a reduced level of photoproduct removal (Zou et al., 1998). These results suggest that while HSPs are essential to protect against cellular stress, they also provide a useful role in the maintenance of normal DNA repair. The relationship between HSPs and DNA repair is further supported by the finding that HSPs directly co-immunoprecipitate with components of the BER pathway. Both HSP27 and HSP70 were found to interact with UDG and HAP1, respectively (Kenny et al., 2001; Mendez et al., 2000). Furthermore, the interaction between HSP70 and HAP1 was shown to significantly increase the rate of strand incision at AP sties (Kenny et al., 2001).

The results of these studies provide evidence for a role of HSPs in DNA repair and as such support the further investigation of the interaction between mOGG1 and mDnaja1. Furthermore, the chaperone function of the HSPs might indicate that they could provide a scaffold for both the NER and BER pathways, possibly maintaining the structure of a multi-protein complex. Indeed, the chaperones, HSP90 and HSP70, have been well characterised as forming interactions with many cell-cycle proteins, protein kinases and transcription factors, to either stabilise protein conformations or act as structural proteins to promote the formation of protein complexes. HSP70 family members and/or HSP90, transiently associate with key molecules of the cell cycle control systems, including p53, Cdk4, Wee-1, c-Myc, pRb and p27/Kip1 (for reviews see; Helmbrecht et al., 2000; Jolly and Morimoto, 2000). Furthermore, Hsp70 and/or Hsp90 also interact with important kinases of the mitogen-activated signal cascades, such as Src kinases, tyrosine receptor kinases, Raf and MAP-kinases (for reviews see; Gabai et al., 2000; Helmbrecht et al., 2000).

8.4 Protein interactions with BER DNA glycosylases

Although the yeast two-hybrid analysis carried out in this study has produced mixed results, this technique has been used successfully to identify protein partners for two other DNA glycosylases. The human homologs of APNG and NTH1 have been shown to interact with the hHR23 and YB-1 proteins, respectively (Miao et al., 2000; Marenstein et al., 2001). The interaction between hAPNG and hHR23 was shown to

increase both the substrate binding affinity and glycosylase activity of hAPNG for alkylated bases (Miao et al., 2000). Interestingly, as the hHR23-XPC protein complex is known to recognise and bind damaged bases in the initial stages of global NER (see Section 1.7.2), the hHR23 protein might provide a similar role in BER by recruiting APNG to the site of base damage. Indeed, the ability of APNG to remove normal purines as well as damaged purines could indicate the requirement for such a protein to provide substrate specificity.

The interaction between hNTH1 and YB-1 was shown to increase both the glycosylase and AP-lyase activities of hNTH1 on thymine glycols (Marenstein et al., 2001). YB-1 is a multifunctional DNA binding protein belonging to the *E. coli* cold-shock family of proteins (Jones and Laird, 1999). This protein undergoes a translocation from the cytoplasm to the nucleus upon exposure of cells to UV irradiation or genotoxic anti-cancer agents, suggesting a stress inducible response (Koike et al., 1997). Furthermore, YB-1 has also been shown to bind structurally modified DNA and physically interact with PCNA, providing a link to both the BER and NER pathways (Ise et al., 1999). It is interesting that despite the structural similarity between the NTH1-like family of DNA glycosylases, none of the yeast two-hybrid screens has identified a protein partner common to all of the glycosylases. This suggests that these factors provide specific roles in BER. Furthermore, while all of the factors have been found to provide a stimulatory role in glycosylase activity they have not been found to be essential components of the BER pathway.

In addition to the yeast two-hybrid screens, a number of studies have investigated protein interactions with DNA glycosylases using a more intuitive approach. An observation that Cockayne syndrome patients, with mutations in the XPG gene, displayed an inability to remove thymine glycol led to an investigation into the role of XPG in the repair of this lesion (Bessho, 1999; Cooper et al., 1997). These studies showed that XPG was able to stimulate the binding affinity and glycosylase activity of hNTH1 for thymine glycol (Klungland et al., 1999a). However, these proteins did not co-immunoprecipitate from cellular extracts (Bessho, 1999; Klungland et al., 1999a). Furthermore, these effects were shown to be specific for hNTH1, as XPG did not affect the activities of hOGG1, hUDG, HAP1 or DNA polβ (Klungland et al., 1999a).

A similar observation has been reported between HAP1 and hOGG1, whereby HAP1 appears to stimulate the release of 8-oxodG by OGG1. However, as with hNTH1 and hXPG, no physical interactions can be detected between the respective proteins. The explanation for this finding is related to the poor AP-lyase activity of OGG1 (Zharkov et al., 2000). Once the damaged base has been removed by the glycosylase activity of OGG1 (generating an abasic site), the rate of incision by the associated AP-lyase becomes the rate-limiting step in the repair pathway. However, the rate of repair is increased by the presence of HAP1, which has a higher binding affinity for abasic sites and appears to displace the glycosylase. HAP1 is able to incise the DNA more efficiently than OGG1 and thus the repair process is completed more efficiently. Furthermore, the displaced glycosylase is also free to bind and remove another lesion, therefore, increasing the overall rate of repair. The inefficiency of the AP-lyase activity of OGG1 might be related to the danger this activity could pose when cells are place under severe oxidative stress. In this instance, the repair of multiple oxidative lesions by OGG1 could result in the formation of multiple DNA strand breaks that could be lethal to cells. Therefore, the delayed AP-lyase activity and strong binding affinity of OGG1 to abasic sites may safeguard the abasic site until other components required for the subsequent steps of BER are recruited.

8.5 Future perspective

Both the amount and nature of the results obtained from the yeast two-hybrid screens means that despite a significant amount of work, the findings of this study remain at a preliminary stage. Indeed, a number of the yeast two-hybrid library clones require further investigation, specifically the RanBP9 and clone 18 cDNA products. However, the majority of this discussion will concentrate on the continued investigation of the interaction between mOGG1 and the molecular chaperone, mDnaja1.

As the experiments carried out in this study produced inconclusive evidence for the interaction between mOGG1 and mDnaja1, the primary aim of any future investigations should be to determine if a physical interaction exists between these proteins *in vivo*. Furthermore, these investigations should take into account the issues raised in Section 8.2, regarding the effects of steric hindrance and the environment in which the protein-

protein interactions are tested. Ideally, these interactions would be investigated by co-immunoprecipitation of the endogenous proteins from murine cell extracts. However, as no specific antibodies are available against mOGG1 or mDnaja1, an alternative option involves the co-expression of epitope-tagged proteins in a murine cell line, and subsequent co-immunoprecipitation using antibodies against the epitope-tags (as discussed in Section 6.1). While mOGG1 and mDnaja1 would still be expressed as fusion proteins, the small size of the peptide tags should generate less steric intereference. Furthermore, these tags could also be used for immunohistochemistry experiments, to assess whether the proteins co-localise within the cell.

In addition to these studies, the OGG1 glycosylase assay provides a further two lines of investigation. The addition of both purified mOGG1 and mDnaja1 to the assay would allow the assessment of any functional effects this interaction might have on the glycosylase activity of mOGG1. Furthermore, the addition of DNA-protein and protein-protein cross-linking reagents would allow the formation of any complexes to be assessed in a super-shift assay while bound to the 8-oxodG lesion.

While yeast two-hybrid analysis provides a useful method to screen a large number of proteins for potential interactions the system possesses a number of limitations that might prevent the detection of many transient protein-protein interactions. The inconclusive results obtained in this study means that the fundamental question posed in this study, "Do BER DNA glycosylases interact with any protein partners?" remains unanswered. Therefore, in parallel with the continued two-hybrid investigations a significant effort should be made to confirm the rationale of this project by determining whether OGG1 does indeed interact with any other endogenous proteins. The recent availability of commercial anti-hOGG1 antibodies will allow co-immunoprecipiation experiments to be performed investigating this area. While the identity of any proteins precipitated with hOGG1 would be unknown, the presence of any proteins precipitated with hOGG1 could be confirmed either by silver staining or, if present in low concentrations, by the metabolic labelling of cells prior to performing the co-immunoprecipitation. This initial step would determine the presence of potential interacting factors, providing a strong basis for further investigation. However, in addition this experiment could be modified to assess whether oxidative DNA damage

(specifically 8-oxodG) alters the appearance and/or number of proteins that bind hOGG1 while repairing 8-oxodG. The generation of 8-oxodG lesions could be carried out by treatment of the cells with methylene blue and white light, while subsequent treatment with a DNA-protein cross-linking agent such as UV light would then cross-link any hOGG1 in complex with the 8-oxodG lesion. If the presence of interacting proteins was confirmed from these experiments, the identity of these factors would then be determined by probing for known BER components with antibodies, or if unsuccessful, the isolation of protein bands and subsequent analysis by proteomics (2D-gel analysis and protein sequencing).

REFERENCES

Aburatani, H., Hippo, Y., Ishida, T., Takashima, R., Matsuba, C., Kodama, T., Takao, M., Yasui, A., Yamamoto, K., and Asano, M. (1997). Cloning and characterization of mammalian 8-hydroxyguanine-specific DNA glycosylase/apurinic, apyrimidinic lyase, a functional mutM homologue, Cancer Res *57*, 2151-6.

Arai, K., Morishita, K., Shinmura, K., Kohno, T., Kim, S. R., Nohmi, T., Taniwaki, M., Ohwada, S., and Yokota, J. (1997). Cloning of a human homolog of the yeast OGG1 gene that is involved in the repair of oxidative DNA damage, Oncogene *14*, 2857-61.

Araujo, S. J., and Wood, R. D. (1999). Protein complexes in nucleotide excision repair, Mutat Res *435*, 23-33.

Aruoma, O. I., Halliwell, B., and Dizdaroglu, M. (1989). Iron ion-dependent modification of bases in DNA by the superoxide radical-generating system hypoxanthine/xanthine oxidase, J Biol Chem *264*, 13024-8.

Asami, S., Hirano, T., Yamaguchi, R., Tomioka, Y., Itoh, H., and Kasai, H. (1996). Increase of a type of oxidative DNA damage, 8-hydroxyguanine, and its repair activity in human leukocytes by cigarette smoking, Cancer Res *56*, 2546-9.

Aspinwall, R., Rothwell, D. G., Roldan-Arjona, T., Anselmino, C., Ward, C. J., Cheadle, J. P., Sampson, J. R., Lindahl, T., Harris, P. C., and Hickson, I. D. (1997). Cloning and characterization of a functional human homolog of Escherichia coli endonuclease III, Proc Natl Acad Sci U S A *94*, 109-14.

Au, K. G., Cabrera, M., Miller, J. H., and Modrich, P. (1988). Escherichia coli mutY gene product is required for specific A-G----C.G mismatch correction, Proc Natl Acad Sci U S A *85*, 9163-6.

Baldwin, A. S. (2001). Control of oncogenesis and cancer therapy resistance by the transcription factor NF-kappaB, J Clin Invest *107*, 241-6.

Beckman, K. B., and Ames, B. N. (1998). The free radical theory of aging matures, Physiol Rev *78*, 547-81.

Beehler, B. C., Przybyszewski, J., Box, H. B., and Kulesz-Martin, M. F. (1992). Formation of 8-hydroxydeoxyguanosine within DNA of mouse keratinocytes exposed in culture to UVB and H2O2, Carcinogenesis *13*, 2003-7.

Bennett, R. A., Wilson, D. M., 3rd, Wong, D., and Demple, B. (1997). Interaction of human apurinic endonuclease and DNA polymerase beta in the base excision repair pathway, Proc Natl Acad Sci U S A *94*, 7166-9.

Ben-Zvi, A. P., and Goloubinoff, P. (2001). Review: mechanisms of disaggregation and refolding of stable protein aggregates by molecular chaperones, J Struct Biol *135*, 84-93.

Bessho, T. (1999). Nucleotide excision repair 3' endonuclease XPG stimulates the activity of base excision repairenzyme thymine glycol DNA glycosylase, Nucleic Acids Res *27*, 979-83.

Bessho, T., Roy, R., Yamamoto, K., Kasai, H., Nishimura, S., Tano, K., and Mitra, S. (1993). Repair of 8-hydroxyguanine in DNA by mammalian N-methylpurine-DNA glycosylase, Proc Natl Acad Sci U S A *90*, 8901-4.

Bhagwat, M., and Gerlt, J. A. (1996). 3'- and 5'-strand cleavage reactions catalyzed by the Fpg protein from Escherichia coli occur via successive beta- and delta-elimination mechanisms, respectively, Biochemistry *35*, 659-65.

Bishop, J. M. (1991). Molecular themes in oncogenesis, Cell *64*, 235-48.

Bjoras, M., Luna, L., Johnsen, B., Hoff, E., Haug, T., Rognes, T., and Seeberg, E. (1997). Opposite base-dependent reactions of a human base excision repair enzyme on DNA containing 7,8-dihydro-8-oxoguanine and abasic sites, Embo J *16*, 6314-22.

Blakely, W. F., Fuciarelli, A. F., Wegher, B. J., and Dizdaroglu, M. (1990). Hydrogen peroxide-induced base damage in deoxyribonucleic acid, Radiat Res *121*, 338-43.

Boiteux, S., and Radicella, J. P. (2000). The human OGG1 gene: structure, functions, and its implication in the process of carcinogenesis, Arch Biochem Biophys *377*, 1-8.

Boldogh, I., Milligan, D., Lee, M. S., Bassett, H., Lloyd, R. S., and McCullough, A. K. (2001). hMYH cell cycle-dependent expression, subcellular localization and association with replication foci: evidence suggesting replication-coupled repair of adenine:8-oxoguanine mispairs, Nucleic Acids Res *29*, 2802-9.

Bonicel, A., Mariaggi, N., Hughes, E., and Teoule, R. (1980). In vitro gamma irradiation of DNA: identification of radioinduced chemical modifications of the adenine moiety, Radiat Res *83*, 19-26.

Boveris, A. (1977). Mitochondrial production of superoxide radical and hydrogen peroxide, Adv Exp Med Biol *78*, 67-82.

Breen, A. P., and Murphy, J. A. (1995). Reactions of oxyl radicals with DNA, Free Radic Biol Med *18*, 1033-77.

Breimer, L. H., and Lindahl, T. (1984). DNA glycosylase activities for thymine residues damaged by ring saturation, fragmentation, or ring contraction are functions of endonuclease III in Escherichia coli, J Biol Chem *259*, 5543-8.

Breimer, L. H., and Lindahl, T. (1985). Thymine lesions produced by ionizing radiation in double-stranded DNA, Biochemistry *24*, 4018-22.

Burney, S., Niles, J. C., Dedon, P. C., and Tannenbaum, S. R. (1999). DNA damage in deoxynucleosides and oligonucleotides treated with peroxynitrite, Chem Res Toxicol *12*, 513-20.

Cabrera, M., Nghiem, Y., and Miller, J. H. (1988). mutM, a second mutator locus in Escherichia coli that generates G.C----T.A transversions, J Bacteriol *170*, 5405-7.

Cadet, J., Bourdat, A. G., D'Ham, C., Duarte, V., Gasparutto, D., Romieu, A., and Ravanat, J. L. (2000). Oxidative base damage to DNA: specificity of base excision repair enzymes, Mutat Res *462*, 121-8.

Cadet, J., Delatour, T., Douki, T., Gasparutto, D., Pouget, J. P., Ravanat, J. L., and Sauvaigo, S. (1999). Hydroxyl radicals and DNA base damage, Mutat Res *424*, 9-21.

Caldecott, K. W., Aoufouchi, S., Johnson, P., and Shall, S. (1996). XRCC1 polypeptide interacts with DNA polymerase beta and possibly poly (ADP-ribose) polymerase, and DNA ligase III is a novel molecular 'nick-sensor' in vitro, Nucleic Acids Res *24*, 4387-94.

Cappelli, E., Taylor, R., Cevasco, M., Abbondandolo, A., Caldecott, K., and Frosina, G. (1997). Involvement of XRCC1 and DNA ligase III gene products in DNA base excision repair, J Biol Chem *272*, 23970-5.

Castaing, B., Geiger, A., Seliger, H., Nehls, P., Laval, J., Zelwer, C., and Boiteux, S. (1993). Cleavage and binding of a DNA fragment containing a single 8-oxoguanine by wild type and mutant FPG proteins, Nucleic Acids Res *21*, 2899-905.

Chada, S., Le Beau, M. M., Casey, L., and Newburger, P. E. (1990). Isolation and chromosomal localization of the human glutathione peroxidase gene, Genomics *6*, 268-71.

Chen, Q., Marsh, J., Ames, B., and Mossman, B. (1996). Detection of 8-oxo-2'-deoxyguanosine, a marker of oxidative DNA damage, in culture medium from human mesothelial cells exposed to crocidolite asbestos, Carcinogenesis *17*, 2525-7.

Cheng, K. C., Cahill, D. S., Kasai, H., Nishimura, S., and Loeb, L. A. (1992). 8-Hydroxyguanine, an abundant form of oxidative DNA damage, causes G----T and A----C substitutions, J Biol Chem *267*, 166-72.

Chiba, I., Takahashi, T., Nau, M. M., D'Amico, D., Curiel, D. T., Mitsudomi, T., Buchhagen, D. L., Carbone, D., Piantadosi, S., Koga, H., and et al. (1990). Mutations in the p53 gene are frequent in primary, resected non-small cell lung cancer. Lung Cancer Study Group, Oncogene *5*, 1603-10.

Colman, M. S., Afshari, C. A., and Barrett, J. C. (2000). Regulation of p53 stability and activity in response to genotoxic stress, Mutat Res *462*, 179-88.

Cooper, P. K., Nouspikel, T., Clarkson, S. G., and Leadon, S. A. (1997). Defective transcription-coupled repair of oxidative base damage in Cockayne syndrome patients from XP group G, Science *275*, 990-3.

Cunningham, R. P. (1997). DNA glycosylases, Mutat Res *383*, 189-96.

David-Cordonnier, M. H., Boiteux, S., and O'Neill, P. (2001). Excision of 8-oxoguanine within clustered damage by the yeast OGG1 protein, Nucleic Acids Res *29*, 1107-13.

Davis, R. J. (2000). Signal transduction by the JNK group of MAP kinases, Cell *103*, 239-52.

Daya-Grosjean, L., Dumaz, N., and Sarasin, A. (1995). The specificity of p53 mutation spectra in sunlight induced human cancers, J Photochem Photobiol B *28*, 115-24.

de Boer, J., and Hoeijmakers, J. H. (1999). Cancer from the outside, aging from the inside: mouse models to study the consequences of defective nucleotide excision repair, Biochimie *81*, 127-37.

de Rijke, J. M., Schouten, L. J., Hillen, H. F., Kiemeney, L. A., Coebergh, J. W., and van den Brandt, P. A. (2000). Cancer in the very elderly Dutch population, Cancer *89*, 1121-33.

Dhenaut, A., Boiteux, S., Radicella, J. P. (2000). Characterisation of the hOGG1 promoter and its expression during the cell cycle, Mutat Res *461(2)*, 109-18.

Dimitriadis, E. K., Prasad, R., Vaske, M. K., Chen, L., Tomkinson, A. E., Lewis, M. S., and Wilson, S. H. (1998). Thermodynamics of human DNA ligase I trimerization and association with DNA polymerase beta, J Biol Chem *273*, 20540-50.

Doherty, A. J., Serpell, L. C., and Ponting, C. P. (1996). The helix-hairpin-helix DNA-binding motif: a structural basis for non-sequence-specific recognition of DNA, Nucleic Acids Res *24*, 2488-97.

Doll, R., and Peto, R. (1981). The causes of cancer: quantitative estimates of avoidable risks of cancer in the United States today, J Natl Cancer Inst *66*, 1191-308.

Duchniewicz, M., Germaniuk, A., Westermann, B., Neupert, W., Schwarz, E., and Marszalek, J. (1999). Dual role of the mitochondrial chaperone Mdj1p in inheritance of mitochondrial DNA in yeast, Mol Cell Biol *19*, 8201-10.

Durocher, D., and Jackson, S. P. (2001). DNA-PK, ATM and ATR as sensors of DNA damage: variations on a theme?, Curr Opin Cell Biol *13*, 225-31.

Eide, L., Bjoras, M., Pirovano, M., Alseth, I., Berdal, K. G., and Seeberg, E. (1996). Base excision of oxidative purine and pyrimidine DNA damage in Saccharomyces cerevisiae by a DNA glycosylase with sequence similarity to endonuclease III from Escherichia coli, Proc Natl Acad Sci U S A *93*, 10735-40.

Elder, R. H., Jansen, J. G., Weeks, R. J., Willington, M. A., Deans, B., Watson, A. J., Mynett, K. J., Bailey, J. A., Cooper, D. P., Rafferty, J. A., *et al.* (1998). Alkylpurine-DNA-N-glycosylase knockout mice show increased susceptibility to induction of mutations by methyl methanesulfonate, Mol Cell Biol *18*, 5828-37.

Evans, J., Maccabee, M., Hatahet, Z., Courcelle, J., Bockrath, R., Ide, H., and Wallace, S. (1993). Thymine ring saturation and fragmentation products: lesion bypass, misinsertion and implications for mutagenesis, Mutat Res *299*, 147-56.

Feig, D. I., Sowers, L. C., and Loeb, L. A. (1994). Reverse chemical mutagenesis: identification of the mutagenic lesions resulting from reactive oxygen species-mediated damage to DNA, Proc Natl Acad Sci U S A *91*, 6609-13.

Fields, S., and Sternglanz, R. (1994). The two-hybrid system: an assay for protein-protein interactions, Trends Genet *10*, 286-92.

Finley, D., and Chau, V. (1991). Ubiquitination, Annu Rev Cell Biol *7*, 25-69.

Fowlis, D. J., and Balmain, A. (1993). Oncogenes and tumour suppressor genes in transgenic mouse models of neoplasia, Eur J Cancer *29A*, 638-45.

Gabai, V. L., Yaglom, J. A., Volloch, V., Meriin, A. B., Force, T., Koutroumanis, M., Massie, B., Mosser, D. D., and Sherman, M. Y. (2000). Hsp72-mediated suppression of c-Jun N-terminal kinase is implicated in development of tolerance to caspase-independent cell death, Mol Cell Biol *20*, 6826-36.

Gill, R. D., Cussac, C., Souhami, R. L., and Laval, F. (1996). Increased resistance to N,N',N''-triethylenethiophosphoramide (thiotepa) in cells expressing the Escherichia coli formamidopyrimidine-DNA glycosylase, Cancer Res *56*, 3721-4.

Girard, P. M., Guibourt, N., and Boiteux, S. (1997). The Ogg1 protein of Saccharomyces cerevisiae: a 7,8-dihydro-8-oxoguanine DNA glycosylase/AP lyase whose lysine 241 is a critical residue for catalytic activity, Nucleic Acids Res *25*, 3204-11.

Graves, R. J., Felzenszwalb, I., Laval, J., and O'Connor, T. R. (1992). Excision of 5'-terminal deoxyribose phosphate from damaged DNA is catalyzed by the Fpg protein of Escherichia coli, J Biol Chem *267*, 14429-35.

Guarente, L. (1993). Strategies for the identification of interacting proteins, Proc Natl Acad Sci U S A *90*, 1639-41.

Gupta, R. C., and Lutz, W. K. (1999). Background DNA damage for endogenous and unavoidable exogenous carcinogens: a basis for spontaneous cancer incidence?, Mutat Res *424*, 1-8.

Guschlbauer, W., Duplaa, A. M., Guy, A., Teoule, R., and Fazakerley, G. V. (1991). Structure and in vitro replication of DNA templates containing 7,8-dihydro-8-oxoadenine, Nucleic Acids Res *19*, 1753-8.

Hanahan, D., and Weinberg, R. A. (2000). The hallmarks of cancer, Cell *100*, 57-70.

Hang, B., Singer, B., Margison, G. P., and Elder, R. H. (1997). Targeted deletion of alkylpurine-DNA-N-glycosylase in mice eliminates repair of 1,N6-ethenoadenine and hypoxanthine but not of 3,N4-ethenocytosine or 8-oxoguanine, Proc Natl Acad Sci U S A *94*, 12869-74.

Hartl, F. U. (1996). Molecular chaperones in cellular protein folding, Nature *381*, 571-9.

Hastie, N. D., Dempster, M., Dunlop, M. G., Thompson, A. M., Green, D. K., and Allshire, R. C. (1990). Telomere reduction in human colorectal carcinoma and with ageing, Nature *346*, 866-8.

Hata, M., and Ohtsuka, K. (2000). Murine cDNA encoding a novel type I HSP40/DNAJ homolog, mmDjA4(1), Biochim Biophys Acta *1493*, 208-10.

Hatahet, Z., Zhou, M., Reha-Krantz, L. J., Morrical, S. W., and Wallace, S. S. (1998). In search of a mutational hotspot, Proc Natl Acad Sci U S A *95*, 8556-61.

Hazra, T. K., Izumi, T., Maidt, L., Floyd, R. A., and Mitra, S. (1998). The presence of two distinct 8-oxoguanine repair enzymes in human cells: their potential complementary roles in preventing mutation, Nucleic Acids Res *26*, 5116-22.

Helmbrecht, K., Zeise, E., and Rensing, L. (2000). Chaperones in cell cycle regulation and mitogenic signal transduction: a review, Cell Prolif *33*, 341-65.

Henle, E. S., and Linn, S. (1997). Formation, prevention, and repair of DNA damage by iron/hydrogen peroxide, J Biol Chem *272*, 19095-8.

Hoeijmakers, J. H. (2001). Genome maintenance mechanisms for preventing cancer, Nature *411*, 366-74.

Hollenbach, S., Dhenaut, A., Eckert, I., Radicella, J. P., and Epe, B. (1999). Overexpression of Ogg1 in mammalian cells: effects on induced and spontaneous oxidative DNA damage and mutagenesis, Carcinogenesis *20*, 1863-8.

Houlston, R. S., and Peto, J. (1996). Genetic predisposition to cancer, Chapman & Hall, London).

Hsieh, P. (2001). Molecular mechanisms of DNA mismatch repair, Mutat Res *486*, 71-87.

Ikeda, S., Biswas, T., Roy, R., Izumi, T., Boldogh, I., Kurosky, A., Sarker, A. H., Seki, S., and Mitra, S. (1998). Purification and characterization of human NTH1, a homolog of Escherichia coli endonuclease III. Direct identification of Lys-212 as the active nucleophilic residue, J Biol Chem *273*, 21585-93.

Inoue, S., and Kawanishi, S. (1995). Oxidative DNA damage induced by simultaneous generation of nitric oxide and superoxide, FEBS Lett *371*, 86-8.

Ise, T., Nagatani, G., Imamura, T., Kato, K., Takano, H., Nomoto, M., Izumi, H., Ohmori, H., Okamoto, T., Ohga, T., *et al.* (1999). Transcription factor Y-box binding protein 1 binds preferentially to cisplatin-modified DNA and interacts with proliferating cell nuclear antigen, Cancer Res *59*, 342-6.

Jiricny, J. (1998). Eukaryotic mismatch repair: an update, Mutat Res *409*, 107-21.

Jiricny, J., and Nystrom-Lahti, M. (2000). Mismatch repair defects in cancer, Curr Opin Genet Dev *10*, 157-61.

Jolly, C., and Morimoto, R. I. (2000). Role of the heat shock response and molecular chaperones in oncogenesis and cell death, J Natl Cancer Inst *92*, 1564-72.

Jones, P. A., and Laird, P. W. (1999). Cancer epigenetics comes of age, Nat Genet *21*, 163-7.

Kamiya, H., Miura, H., Murata-Kamiya, N., Ishikawa, H., Sakaguchi, T., Inoue, H., Sasaki, T., Masutani, C., Hanaoka, F., Nishimura, S., and et al. (1995). 8-Hydroxyadenine (7,8-dihydro-8-oxoadenine) induces misincorporation in in vitro DNA synthesis and mutations in NIH 3T3 cells, Nucleic Acids Res *23*, 2893-9.

Karin, M., and Lin, A. (2002). NF-kappaB at the crossroads of life and death, Nat Immunol *3*, 221-7.

Kasai, H., Nishimura, S., Kurokawa, Y., and Hayashi, Y. (1987). Oral administration of the renal carcinogen, potassium bromate, specifically produces 8-hydroxydeoxyguanosine in rat target organ DNA, Carcinogenesis *8*, 1959-61.

Kastan, M. B., and Lim, D. S. (2000). The many substrates and functions of ATM, Nat Rev Mol Cell Biol *1*, 179-86.

Kennedy, B. J. (1998). Cancer death and older age, Cancer *83*, 1066-8.

Kenny, M. K., Mendez, F., Sandigursky, M., Kureekattil, R. P., Goldman, J. D., Franklin, W. A., and Bases, R. (2001). Heat shock protein 70 binds to human apurinic/apyrimidinic endonuclease and stimulates endonuclease activity at abasic sites, J Biol Chem *276*, 9532-6.

Keszenman, D. J., Carmen Candreva, E., and Nunes, E. (2000). Cellular and molecular effects of bleomycin are modulated by heat shock in Saccharomyces cerevisiae, Mutat Res *459*, 29-41.

Klungland, A., Hoss, M., Gunz, D., Constantinou, A., Clarkson, S. G., Doetsch, P. W., Bolton, P. H., Wood, R. D., and Lindahl, T. (1999a). Base excision repair of oxidative DNA damage activated by XPG protein, Mol Cell *3*, 33-42.

Klungland, A., Rosewell, I., Hollenbach, S., Larsen, E., Daly, G., Epe, B., Seeberg, E., Lindahl, T., and Barnes, D. E. (1999b). Accumulation of premutagenic DNA lesions in mice defective in removal of oxidative base damage, Proc Natl Acad Sci U S A *96*, 13300-5.

Koike, K., Uchiumi, T., Ohga, T., Toh, S., Wada, M., Kohno, K., and Kuwano, M. (1997). Nuclear translocation of the Y-box binding protein by ultraviolet irradiation, FEBS Lett *417*, 390-4.

Koppenol, W. H., Moreno, J. J., Pryor, W. A., Ischiropoulos, H., and Beckman, J. S. (1992). Peroxynitrite, a cloaked oxidant formed by nitric oxide and superoxide, Chem Res Toxicol *5*, 834-42.

Ku, H. H., Brunk, U. T., and Sohal, R. S. (1993). Relationship between mitochondrial superoxide and hydrogen peroxide production and longevity of mammalian species, Free Radic Biol Med *15*, 621-7.

Kubota, Y., Nash, R. A., Klungland, A., Schar, P., Barnes, D. E., and Lindahl, T. (1996). Reconstitution of DNA base excision-repair with purified human proteins: interaction between DNA polymerase beta and the XRCC1 protein, Embo J *15*, 6662-70.

Kunzler, M., and Hurt, E. (2001). Targeting of Ran: variation on a common theme?, J Cell Sci *114*, 3233-41.

Kvam, E., and Tyrrell, R. M. (1997). Induction of oxidative DNA base damage in human skin cells by UV and near visible radiation, Carcinogenesis *18*, 2379-84.

Langer, T., Lu, C., Echols, H., Flanagan, J., Hayer, M. K., and Hartl, F. U. (1992). Successive action of DnaK, DnaJ and GroEL along the pathway of chaperone-mediated protein folding, Nature *356*, 683-9.

Laval, F. (1994). Expression of the E. coli fpg gene in mammalian cells reduces the mutagenicity of gamma-rays, Nucleic Acids Res *22*, 4943-6.

Le Page, F., Margot, A., Grollman, A. P., Sarasin, A., and Gentil, A. (1995). Mutagenicity of a unique 8-oxoguanine in a human Ha-ras sequence in mammalian cells, Carcinogenesis *16*, 2779-84.

Lehmann, A. R. (2001). The xeroderma pigmentosum group D (XPD) gene: one gene, two functions, three diseases, Genes Dev *15*, 15-23.

Leonard, G. A., Guy, A., Brown, T., Teoule, R., and Hunter, W. N. (1992). Conformation of guanine-8-oxoadenine base pairs in the crystal structure of d(CGCGAATT(O8A)GCG), Biochemistry *31*, 8415-20.

Lesko, S. A., Lorentzen, R. J., and Ts'o, P. O. (1980). Role of superoxide in deoxyribonucleic acid strand scission, Biochemistry *19*, 3023-8.

Lindahl, T. (1976). New class of enzymes acting on damaged DNA, Nature *259*, 64-6.

Lindahl, T., and Wood, R. D. (1999). Quality control by DNA repair, Science *286*, 1897-905.

Lu, R., Nash, H. M., and Verdine, G. L. (1997). A mammalian DNA repair enzyme that excises oxidatively damaged guanines maps to a locus frequently lost in lung cancer, Curr Biol *7*, 397-407.

Marenstein, D. R., Ocampo, M. T., Chan, M. K., Altamirano, A., Basu, A. K., Boorstein, R. J., Cunningham, R. P., and Teebor, G. W. (2001). Stimulation of human endonuclease III by Y box-binding protein 1 (DNA-binding protein B). Interaction between a base excision repair enzyme and a transcription factor, J Biol Chem *276*, 21242-9.

Marnett, L. J. (2000). Oxyradicals and DNA damage, Carcinogenesis *21*, 361-70.

Masson, M., Niedergang, C., Schreiber, V., Muller, S., Menissier-de Murcia, J., and de Murcia, G. (1998). XRCC1 is specifically associated with poly(ADP-ribose) polymerase and negatively regulates its activity following DNA damage, Mol Cell Biol *18*, 3563-71.

Melov, S., Coskun, P., Patel, M., Tuinstra, R., Cottrell, B., Jun, A. S., Zastawny, T. H., Dizdaroglu, M., Goodman, S. I., Huang, T. T., *et al.* (1999). Mitochondrial disease in superoxide dismutase 2 mutant mice, Proc Natl Acad Sci U S A *96*, 846-51.

Mendez, F., Sandigursky, M., Franklin, W. A., Kenny, M. K., Kureekattil, R., and Bases, R. (2000). Heat-shock proteins associated with base excision repair enzymes in HeLa cells, Radiat Res *153*, 186-95.

Miao, F., Bouziane, M., Dammann, R., Masutani, C., Hanaoka, F., Pfeifer, G., and O'Connor, T. R. (2000). 3-Methyladenine-DNA glycosylase (MPG protein) interacts with human RAD23 proteins, J Biol Chem *275*, 28433-8.

Michaels, M. L., Cruz, C., Grollman, A. P., and Miller, J. H. (1992). Evidence that MutY and MutM combine to prevent mutations by an oxidatively damaged form of guanine in DNA, Proc Natl Acad Sci U S A *89*, 7022-5.

Michaels, M. L., Pham, L., Cruz, C., and Miller, J. H. (1991). MutM, a protein that prevents G.C----T.A transversions, is formamidopyrimidine-DNA glycosylase, Nucleic Acids Res *19*, 3629-32.

Minowa, O., Arai, T., Hirano, M., Monden, Y., Nakai, S., Fukuda, M., Itoh, M., Takano, H., Hippou, Y., Aburatani, H., *et al.* (2000). Mmh/Ogg1 gene inactivation results in accumulation of 8-hydroxyguanine in mice, Proc Natl Acad Sci U S A *97*, 4156-61.

Mitchel, R. E., and Morrison, D. P. (1982). Heat-shock induction of ionizing radiation resistance in Saccharomyces cerevisiae. Transient changes in growth cycle distribution and recombinational ability, Radiat Res *92*, 182-7.

Mitchel, R. E., and Morrison, D. P. (1983). Heat-shock induction of ultraviolet light resistance in Saccharomyces cerevisiae, Radiat Res *96*, 95-9.

Mo, J. Y., Maki, H., and Sekiguchi, M. (1992). Hydrolytic elimination of a mutagenic nucleotide, 8-oxodGTP, by human 18-kilodalton protein: sanitization of nucleotide pool, Proc Natl Acad Sci U S A *89*, 11021-5.

Monden, Y., Arai, T., Asano, M., Ohtsuka, E., Aburatani, H., and Nishimura, S. (1999). Human MMH (OGG1) type 1a protein is a major enzyme for repair of 8-hydroxyguanine lesions in human cells, Biochem Biophys Res Commun *258*, 605-10.

Mori, M., Toyokuni, S., Kondo, S., Kasai, H., Naiki, H., Toichi, E., Hosokawa, M., and Higuchi, K. (2001). Spontaneous loss-of-function mutations of the 8-oxoguanine DNA glycosylase gene in mice and exploration of the possible implication of the gene in senescence, Free Radic Biol Med *30*, 1130-6.

Moriya, M., and Grollman, A. P. (1993). Mutations in the mutY gene of Escherichia coli enhance the frequency of targeted G:C-->T:a transversions induced by a single 8-oxoguanine residue in single-stranded DNA, Mol Gen Genet *239*, 72-6.

Nagashima, M., Kasai, H., Yokota, J., Nagamachi, Y., Ichinose, T., and Sagai, M. (1995). Formation of an oxidative DNA damage, 8-hydroxydeoxyguanosine, in mouse lung DNA after intratracheal instillation of diesel exhaust particles and effects of high dietary fat and beta-carotene on this process, Carcinogenesis *16*, 1441-5.

Nakamura, M., Masuda, H., Horii, J., Kuma, K., Yokoyama, N., Ohba, T., Nishitani, H., Miyata, T., Tanaka, M., and Nishimoto, T. (1998). When overexpressed, a novel centrosomal protein, RanBPM, causes ectopic microtubule nucleation similar to gamma-tubulin, J Cell Biol *143*, 1041-52.

Nash, H. M., Bruner, S. D., Scharer, O. D., Kawate, T., Addona, T. A., Spooner, E., Lane, W. S., and Verdine, G. L. (1996). Cloning of a yeast 8-oxoguanine DNA glycosylase reveals the existence of a base-excision DNA-repair protein superfamily, Curr Biol *6*, 968-80.

Nash, H. M., Lu, R., Lane, W. S., and Verdine, G. L. (1997). The critical active-site amine of the human 8-oxoguanine DNA glycosylase, hOgg1: direct identification, ablation and chemical reconstitution, Chem Biol *4*, 693-702.

Nebreda, A. R., and Porras, A. (2000). p38 MAP kinases: beyond the stress response, Trends Biochem Sci *25*, 257-60.

Nghiem, Y., Cabrera, M., Cupples, C. G., and Miller, J. H. (1988). The mutY gene: a mutator locus in Escherichia coli that generates G.C----T.A transversions, Proc Natl Acad Sci U S A *85*, 2709-13.

Nilsen, H., and Krokan, H. E. (2001). Base excision repair in a network of defence and tolerance, Carcinogenesis *22*, 987-98.

Nishioka, K., Ohtsubo, T., Oda, H., Fujiwara, T., Kang, D., Sugimachi, K., and Nakabeppu, Y. (1999). Expression and differential intracellular localization of two major forms of human 8-oxoguanine DNA glycosylase encoded by alternatively spliced OGG1 mRNAs, Mol Biol Cell *10*, 1637-52.

Nishitani, H., Hirose, E., Uchimura, Y., Nakamura, M., Umeda, M., Nishii, K., Mori, N., and Nishimoto, T. (2001). Full-sized RanBPM cDNA encodes a protein possessing a long stretch of proline and glutamine within the N-terminal region, comprising a large protein complex, Gene *272*, 25-33.

Norbury, C. J., and Hickson, I. D. (2001). Cellular responses to DNA damage, Annu Rev Pharmacol Toxicol *41*, 367-401.

Nowell, P. C. (1976). The clonal evolution of tomour progression, Science *194*, 23-28.
O'Connor, T. R., Boiteux, S., and Laval, J. (1988). Ring-opened 7-methylguanine residues in DNA are a block to in vitro DNA synthesis, Nucleic Acids Res *16*, 5879-94.

O'Connor, T. R., Graves, R. J., de Murcia, G., Castaing, B., and Laval, J. (1993). Fpg protein of Escherichia coli is a zinc finger protein whose cysteine residues have a structural and/or functional role, J Biol Chem *268*, 9063-70.

Olden, K., and Wilson, S. (2000). Environmental health and genomics: visions and implications, Nat Rev Genet *1*, 149-53.

Olinski, R., Zastawny, T., Budzbon, J., Skokowski, J., Zegarski, W., and Dizdaroglu, M. (1992). DNA base modifications in chromatin of human cancerous tissues, FEBS Lett *309*, 193-8.

Otteneder, M., and Lutz, W. K. (1999). Correlation of DNA adduct levels with tumor incidence: carcinogenic potency of DNA adducts, Mutat Res *424*, 237-47.

Pandya, G. A., and Moriya, M. (1996). 1,N6-ethenodeoxyadenosine, a DNA adduct highly mutagenic in mammalian cells, Biochemistry *35*, 11487-92.

Park, S. G., Cha, M. K., Jeong, W., and Kim, I. H. (2000). Distinct physiological functions of thiol peroxidase isoenzymes in Saccharomyces cerevisiae, J Biol Chem *275*, 5723-32.

Peto, R., Parish, S. E., and Gray, R. G. (1986). Age-related factors in carcinogenesis, IARC Sci Publ. 58).

Pflaum, M., Will, O., and Epe, B. (1997). Determination of steady-state levels of oxidative DNA base modifications in mammalian cells by means of repair endonucleases, Carcinogenesis *18*, 2225-31.

Piret, B., Schoonbroodt, S., and Piette, J. (1999). The ATM protein is required for sustained activation of NF-kappaB following DNA damage, Oncogene *18*, 2261-71.

Pisani, P., Parkin, D. M., Bray, F., and Ferlay, J. (1999). Estimates of the worldwide mortality from 25 cancers in 1990, Int J Cancer *83*, 18-29.

Pisani, P., Parkin, D. M., Munoz, N., and Ferlay, J. (1997). Cancer and infection: estimates of the attributable fraction in 1990, Cancer Epidemiol Biomarkers Prev *6*, 387-400.

Prasad, R., Singhal, R. K., Srivastava, D. K., Molina, J. T., Tomkinson, A. E., and Wilson, S. H. (1996). Specific interaction of DNA polymerase beta and DNA ligase I in a multiprotein base excision repair complex from bovine testis, J Biol Chem *271*, 16000-7.

Purmal, A. A., Kow, Y. W., and Wallace, S. S. (1994). Major oxidative products of cytosine, 5-hydroxycytosine and 5-hydroxyuracil, exhibit sequence context-dependent mispairing in vitro, Nucleic Acids Res *22*, 72-8.

Quan, F., Korneluk, R. G., Tropak, M. B., and Gravel, R. A. (1986). Isolation and characterization of the human catalase gene, Nucleic Acids Res *14*, 5321-35.

Rabow, L. E., and Kow, Y. W. (1997). Mechanism of action of base release by Escherichia coli Fpg protein: role of lysine 155 in catalysis, Biochemistry *36*, 5084-96.

Radicella, J. P., Dherin, C., Desmaze, C., Fox, M. S., and Boiteux, S. (1997). Cloning and characterization of hOGG1, a human homolog of the OGG1 gene of Saccharomyces cerevisiae, Proc Natl Acad Sci U S A *94*, 8010-5.

Rosenquist, T. A., Zharkov, D. O., and Grollman, A. P. (1997). Cloning and characterization of a mammalian 8-oxoguanine DNA glycosylase, Proc Natl Acad Sci U S A *94*, 7429-34.

Rowley, N., Prip-Buus, C., Westermann, B., Brown, C., Schwarz, E., Barrell, B., and Neupert, W. (1994). Mdj1p, a novel chaperone of the DnaJ family, is involved in mitochondrial biogenesis and protein folding, Cell *77*, 249-59.

Royaux, I., Minner, F., Goffinet, A. M., and de Rouvroit, C. L. (1998). A DnaJ-like gene, Hsj2, maps to mouse chromosome 5, at approximately 24 cM from the centromere, Genomics *53*, 415.

Sandigursky, M., Yacoub, A., Kelley, M. R., Xu, Y., Franklin, W. A., and Deutsch, W. A. (1997). The yeast 8-oxoguanine DNA glycosylase (Ogg1) contains a DNA deoxyribophosphodiesterase (dRpase) activity, Nucleic Acids Res *25*, 4557-61.

Saparbaev, M., and Laval, J. (1994). Excision of hypoxanthine from DNA containing dIMP residues by the Escherichia coli, yeast, rat, and human alkylpurine DNA glycosylases, Proc Natl Acad Sci U S A *91*, 5873-7.

Sarker, A. H., Ikeda, S., Nakano, H., Terato, H., Ide, H., Imai, K., Akiyama, K., Tsutsui, K., Bo, Z., Kubo, K., *et al.* (1998). Cloning and characterization of a mouse homologue (mNthl1) of Escherichia coli endonuclease III, J Mol Biol *282*, 761-74.

Schulz, I., Mahler, H. C., Boiteux, S., and Epe, B. (2000). Oxidative DNA base damage induced by singlet oxygen and photosensitization: recognition by repair endonucleases and mutagenicity, Mutat Res *461*, 145-56.

Seiler, F., Rehn, B., Rehn, S., Hermann, M., and Bruch, J. (2001). Quartz exposure of the rat lung leads to a linear dose response in inflammation but not in oxidative DNA damage and mutagenicity, Am J Respir Cell Mol Biol *24*, 492-8.

Shibutani, S., Bodepudi, V., Johnson, F., and Grollman, A. P. (1993). Translesional synthesis on DNA templates containing 8-oxo-7,8-dihydrodeoxyadenosine, Biochemistry *32*, 4615-21.

Shibutani, S., Takeshita, M., and Grollman, A. P. (1991). Insertion of specific bases during DNA synthesis past the oxidation-damaged base 8-oxodG, Nature *349*, 431-4.

Shiloh, Y. (2001). ATM and ATR: networking cellular responses to DNA damage, Curr Opin Genet Dev *11*, 71-7.

Sidorkina, O. M., and Laval, J. (1998). Role of lysine-57 in the catalytic activities of Escherichia coli formamidopyrimidine-DNA glycosylase (Fpg protein), Nucleic Acids Res *26*, 5351-7.

Sidorkina, O. M., and Laval, J. (2000). Role of the N-terminal proline residue in the catalytic activities of the Escherichia coli Fpg protein, J Biol Chem *275*, 9924-9.

Singer, B., and Hang, B. (1997). What structural features determine repair enzyme specificity and mechanism in chemically modified DNA?, Chem Res Toxicol *10*, 713-32.

Singh, K. K., Sigala, B., Sikder, H. A., and Schwimmer, C. (2001). Inactivation of Saccharomyces cerevisiae OGG1 DNA repair gene leads to an increased frequency of mitochondrial mutants, Nucleic Acids Res *29*, 1381-8.

Steenken, S. (1997). Electron transfer in DNA? Competition by ultra-fast proton transfer?, Biol Chem *378*, 1293-7.

Suzuki, H., Takahashi, T., Kuroishi, T., Suyama, M., Ariyoshi, Y., and Ueda, R. (1992). p53 mutations in non-small cell lung cancer in Japan: association between mutations and smoking, Cancer Res *52*, 734-6.

Tainer, J. A., Getzoff, E. D., Richardson, J. S., and Richardson, D. C. (1983). Structure and mechanism of copper, zinc superoxide dismutase, Nature *306*, 284-7.

Takao, M., Aburatani, H., Kobayashi, K., and Yasui, A. (1998). Mitochondrial targeting of human DNA glycosylases for repair of oxidative DNA damage, Nucleic Acids Res *26*, 2917-22.

Tanaka, M., Kovalenko, S. A., Gong, J. S., Borgeld, H. J., Katsumata, K., Hayakawa, M., Yoneda, M., and Ozawa, T. (1996). Accumulation of deletions and point mutations in mitochondrial genome in degenerative diseases, Ann N Y Acad Sci *786*, 102-11.

Tani, M., Shinmura, K., Kohno, T., Shiroishi, T., Wakana, S., Kim, S. R., Nohmi, T., Kasai, H., Takenoshita, S., Nagamachi, Y., and Yokota, J. (1998). Genomic structure and chromosomal localization of the mouse Ogg1 gene that is involved in the repair of 8-hydroxyguanine in DNA damage, Mamm Genome *9*, 32-7.

Tchou, J., Bodepudi, V., Shibutani, S., Antoshechkin, I., Miller, J., Grollman, A. P., and Johnson, F. (1994). Substrate specificity of Fpg protein. Recognition and cleavage of oxidatively damaged DNA, J Biol Chem *269*, 15318-24.

Tchou, J., Kasai, H., Shibutani, S., Chung, M. H., Laval, J., Grollman, A. P., and Nishimura, S. (1991). 8-oxoguanine (8-hydroxyguanine) DNA glycosylase and its substrate specificity, Proc Natl Acad Sci U S A *88*, 4690-4.

Tebbs, R. S., Flannery, M. L., Meneses, J. J., Hartmann, A., Tucker, J. D., Thompson, L. H., Cleaver, J. E., and Pedersen, R. A. (1999). Requirement for the Xrcc1 DNA base excision repair gene during early mouse development, Dev Biol *208*, 513-29.

Teoule, R., Bert, C., and Bonicel, A. (1977). Thymine fragment damage retained in the DNA polynucleotide chain after gamma irradiation in aerated solutions. II, Radiat Res *72*, 190-200.

Tsurudome, Y., Hirano, T., Yamato, H., Tanaka, I., Sagai, M., Hirano, H., Nagata, N., Itoh, H., and Kasai, H. (1999). Changes in levels of 8-hydroxyguanine in DNA, its repair and OGG1 mRNA in rat lungs after intratracheal administration of diesel exhaust particles, Carcinogenesis *20*, 1573-6.

Tudek, B., Boiteux, S., and Laval, J. (1992). Biological properties of imidazole ring-opened N7-methylguanine in M13mp18 phage DNA, Nucleic Acids Res *20*, 3079-84.

Umemura, T., Sai, K., Takagi, A., Hasegawa, R., and Kurokawa, Y. (1990). Formation of 8-hydroxydeoxyguanosine (8-OH-dG) in rat kidney DNA after intraperitoneal administration of ferric nitrilotriacetate (Fe-NTA), Carcinogenesis *11*, 345-7.

van der Kemp, P. A., Thomas, D., Barbey, R., de Oliveira, R., and Boiteux, S. (1996). Cloning and expression in Escherichia coli of the OGG1 gene of Saccharomyces cerevisiae, which codes for a DNA glycosylase that excises 7,8-dihydro-8-oxoguanine and 2,6-diamino-4-hydroxy-5-N-methylformamidopyrimidine, Proc Natl Acad Sci U S A *93*, 5197-202.

Verdine, G. L., and Bruner, S. D. (1997). How do DNA repair proteins locate damaged bases in the genome?, Chem Biol *4*, 329-34.

Viswanathan, A., and Doetsch, P. W. (1998). Effects of nonbulky DNA base damages on Escherichia coli RNA polymerase-mediated elongation and promoter clearance, J Biol Chem *273*, 21276-81.

von Borstel, R. C., Cain, K. T., Steinberg, C. M. (1971). Inheritance of spontaneous mutability in yeast, Genetics *69(1)*, 17-27.

Wahl, G. M., and Carr, A. M. (2001). The evolution of diverse biological responses to DNA damage: insights from yeast and p53, Nat Cell Biol *3*, E277-86.

Wang, D., Kreutzer, D. A., and Essigmann, J. M. (1998). Mutagenicity and repair of oxidative DNA damage: insights from studies using defined lesions, Mutat Res *400*, 99-115.

Waskiewicz, A. J., and Cooper, J. A. (1995). Mitogen and stress response pathways: MAP kinase cascades and phosphatase regulation in mammals and yeast, Curr Opin Cell Biol *7*, 798-805.

Wei, Q., Gu, J., Cheng, L., Bondy, M. L., Jiang, H., Hong, W. K., and Spitz, M. R. (1996). Benzo(a)pyrene diol epoxide-induced chromosomal aberrations and risk of lung cancer, Cancer Res *56*, 3975-9.

Weitzman, S. A., Turk, P. W., Milkowski, D. H., and Kozlowski, K. (1994). Free radical adducts induce alterations in DNA cytosine methylation, Proc Natl Acad Sci U S A *91*, 1261-4.

Whitehouse, C. J., Taylor, R. M., Thistlethwaite, A., Zhang, H., Karimi-Busheri, F., Lasko, D. D., Weinfeld, M., and Caldecott, K. W. (2001). XRCC1 stimulates human polynucleotide kinase activity at damaged DNA termini and accelerates DNA single-strand break repair, Cell *104*, 107-17.

Wilson, D. M., 3rd, and Thompson, L. H. (1997). Life without DNA repair, Proc Natl Acad Sci U S A *94*, 12754-7.

Wilson, S. H. (1998). Mammalian base excision repair and DNA polymerase beta, Mutat Res *407*, 203-15.

Wood, R. D. (1996). DNA repair in eukaryotes, Annu Rev Biochem *65*, 135-67.

Wood, R. D. (1999). DNA damage recognition during nucleotide excision repair in mammalian cells, Biochimie *81*, 39-44.

Yanofsky, C., Cox, E. C., and Horn, V. (1966). The unusual mutagenic specificity of an E. Coli mutator gene, Proc Natl Acad Sci U S A *55*, 274-81.

Zharkov, D. O., Rieger, R. A., Iden, C. R., and Grollman, A. P. (1997). NH2-terminal proline acts as a nucleophile in the glycosylase/AP-lyase reaction catalyzed by Escherichia coli formamidopyrimidine-DNA glycosylase (Fpg) protein, J Biol Chem *272*, 5335-41.

Zharkov, D. O., Rosenquist, T. A., Gerchman, S. E., and Grollman, A. P. (2000). Substrate specificity and reaction mechanism of murine 8-oxoguanine-DNA glycosylase, J Biol Chem *275*, 28607-17.

Zou, Y., Crowley, D. J., and Van Houten, B. (1998). Involvement of molecular chaperonins in nucleotide excision repair. Dnak leads to increased thermal stability of UvrA, catalytic UvrB loading, enhanced repair, and increased UV resistance, J Biol Chem *273*, 12887-92.